24118

NATIONAL LIBRARY
OTTAWA

CANADA

BIBLIOTHÈQUE NATIONALE
OTTAWA

NAME OF AUTHOR..BRIAN...DOUGLAS...READ.....

TITLE OF THESIS...THE..EFFECTS..OF..MEMBRANE
..LIPID..FLUIDITY..ON..MEDIATED..
..MEMBRANE...TRANSPORT...PROCESSES

UNIVERSITY...THE..UNIVERSITY..OF..ALBERTA.....

DEGREE FOR WHICH THESIS WAS PRESENTED....PH.D.....

YEAR THIS DEGREE GRANTED....1975....SPRING.....

Permission is hereby granted to THE NATIONAL LIBRARY OF CANADA to microfilm this thesis and to lend or sell copies of the film.

The author reserves other publication rights, and neither the thesis nor extensive extracts from it may be printed or otherwise reproduced without the author's written permission.

(Signed)...Brian Read.....

PERMANENT ADDRESS:

Dept. of Chemistry
Chelsea College
The University of London
London, U.K.

DATED. November 20...1974

NL-91 (10-68)

THE UNIVERSITY OF ALBERTA

THE EFFECTS OF MEMBRANE LIPID FLUIDITY ON MEDIATED MEMBRANE TRANSPORT PROCESSES

by

© BRIAN DOUGLAS READ

A THESIS

SUBMITTED TO THE FACULTY OF GRADUATE STUDIES AND RESEARCH

IN PARTIAL FULFILMENT OF THE REQUIREMENTS FOR THE DEGREE

OF DOCTOR OF PHILOSOPHY

DEPARTMENT OF BIOCHEMISTRY

EDMONTON, ALBERTA

SPRING, 1975

THE UNIVERSITY OF ALBERTA

FACULTY OF GRADUATE STUDIES AND RESEARCH

The undersigned certify that they have read, and recommend to the Faculty of Graduate Studies and Research, for acceptance a thesis entitled "THE EFFECTS OF MEMBRANE LIPID FLUIDITY ON MEDIATED MEMBRANE TRANSPORT PROCESSES" submitted by BRIAN DOUGLAS READ in partial fulfilment of the requirements for the degree of Doctor of Philosophy.

Ronald N. McElhaney
Supervisor

W.H. Evans

Werner Puetkau

A.R. Patton

Cyril M. Kay

Mark E. Tanteletta
External Examiner

Date November 13, 1974

To my son, Justin

ABSTRACT

A structural feature which seems to be common to all biomembranes is a lipid bilayer with a hydrophobic interior. This bilayer is usually interrupted by membrane proteins, either partially embedded in the lipid, or traversing the entire bilayer. Lipids arranged in such a way can undergo phase transitions from a crystalline gel to a liquid-crystalline state, while remaining in the lamellar bilayer configuration. The importance of the physical state and properties of the membrane lipid to many biomembrane functions, including passive permeability and active transport, membrane enzyme activities, response to antigens and overall cell viability has recently been recognized. The purpose of the project undertaken here was to investigate the relationship of facilitated diffusion rates to bilayer lipid fluidity in order to gain some information about the nature of the transport proteins and their spatial relationships to the lipid bilayer.

The first system investigated was the glucose transport system in Acholeplasma laidlawii B. This system had not been described, so its characterization was undertaken. The uptake of glucose, as measured by swelling rates of cells in isotonic glucose solutions, or by radioactive tracer uptake, is much faster than would be predicted for passive diffusion. It is inhibited by phlorizin, tannic acid and phloretin, and by high temperature. Under the conditions

employed, metabolism of the glucose has a significant effect on the apparent uptake seen, so it was not possible to obtain values for Vm or Km, or to determine whether or not accumulation against a concentration gradient occurs. 2-Deoxyglucose, but not 3-O-methyl glucose, competes with glucose for uptake.

When the fluidity of the membrane lipid was altered by varying the exogenous fatty acids supplied to A. laidlawii, or by culturing the cells in the presence or absence of cholesterol, a striking dependence of glucose transport rate on fluidity was noted. In all cases the cells with the more fluid membranes showed a more rapid glucose flux.

The glucose and uridine facilitated diffusion systems of human erythrocytes were also investigated. Here, the lipid fluidity was altered either by treating the cells with anesthetics or by exchanging cholest-4-en-3-one for membrane cholesterol. The alteration of the fluidity obtained was monitored by measuring the passive permeation of the cells by uridine in the presence of a potent inhibitor of its facilitated diffusion system, or the efflux of glucose from spherical vesicles formed from the total erythrocyte membrane lipid. Neither facilitated diffusion system appeared to show a dependence of rate on lipid fluidity.

The third system studied was the rat erythrocyte. The fatty acid composition of the membrane was altered by

fatty acid-deficient diets, and the effects on the 3-O-methyl glucose and uridine transport systems observed. It appeared that compensatory metabolic mechanisms prevented the alteration of either the lipid fluidity, or the transport rates, even though a change in the types of fatty acids present was seen.

ACKNOWLEDGEMENTS

I would like to express my gratitude to my supervisor, Dr. R. N. McElhaney for his guidance and encouragement and for the congenial relationship which contributed greatly to my productivity, as well as making the execution of this research a pleasurable and stimulating experience.

I am also indebted to Dr. A. R. P. Paterson and Dr. Carol Cass for their discussions with me of the uridine transport system in erythrocytes and gift of 6-[(2-hydroxy-5-nitrobenzyl)thio]guanosine.

I would like to thank Mr. Yuji Saito, Mr. Michael Eze, and Mr. John Silvius for their helpful discussions and co-operation during the course of this work. I am also grateful to Mr. Neil Bell for his invaluble assistance with many of the experiments, and to Mr. V. Ledsham for drawing the figures for this thesis.

The kindness and cooperation of the many other members of this department who shared their ideas and expertise and their equipment with me, who translated materials from German and Russian, and who helped in many other ways is greatly appreciated.

Financial support from the University of Alberta in the form of Graduate Teaching Assistantships and a Dissertation Fellowship is gratefully acknowledged.

TABLE OF CONTENTS

	Page
LIST OF TABLES	xiii
LIST OF FIGURES	xiv
LIST OF ABBREVIATIONS	xix
CHAPTER I - INTRODUCTION	1
I. Review of the Literature	1
II. Objective of this Study	21
CHAPTER II - GENERAL MATERIALS AND METHODS	25
I. Materials	25
Chemicals	25
Biological materials	27
II. Methods	29
Lipid extraction and purification	29
Fatty acid analysis	29
Radioactivity counting	30
Paper chromatography	31
Conditioning of dialysis tubing	31
CHAPTER III - STUDIES WITH *ACHOLEPLASMA LAIDLAWII* B	33
I. Introduction	33
II. Methods	35
Growth of *Acholeplasma laidlawii*	35
Liposome formation	36

TABLE OF CONTENTS (Continued)

		Page
	Swelling rates	37
	Photomicrography	39
	Differential thermal analysis	40
	Radioisotope tracer flux experiments	41
	Binding measurements	42
	Analytical procedures	44
III.	Results	48
	Relationship of absorbance to cell volume	48
	Effects of inhibitors on swelling rates	48
	Effect of pH on swelling rates	59
	Effect of glucose concentration on swelling rates	63
	Effect of high temperature on swelling rates	63
	Passive permeation of liposomes by glucose	64
	Effect of fatty acid composition on swelling rates	66
	Differential thermal analysis	74
	Effect of fatty acid composition on cell size	75
	Metabolic fates of permeants	77
	Kinetics of radioactive sugar accumulation	90
IV.	Discussion	109

TABLE OF CONTENTS (Continued)

	Page
CHAPTER IV - URIDINE AND GLUCOSE TRANSPORT IN HUMAN ERYTHROCYTES	114
I. Introduction	114
II. Methods	121
Buffer systems	121
Preparation of egg yolk lecithin ...	123
Sterol exchange	125
Determination of intracellular volumes	125
Transport measurements	126
Uridine passive flux	130
Glucose efflux from liposomes	131
Analytical procedures	133
III. Results	136
Effect of HTG on saturability	136
Mixing efficiency in syringe reaction vessel	136
Effects of anesthetics on permeabilities	139
Effects of sterol exchange on permeabilities	146
IV. Discussion	156
CHAPTER V - URIDINE AND 3-O-METHYL GLUCOSE TRANSPORT IN RAT ERYTHROCYTES	160
I. Introduction	160

TABLE OF CONTENTS (Continued)

	Page
II. Methods	163
Diet formulation	163
Metabolism of permeants	164
Transport measurements	165
Swelling rates in glycerol	167
Analytical procedures	167
III. Results	168
Metabolism of permeants	168
Efflux of glucose from liposomes	172
Swelling rates in glycerol	175
Facilitated diffusion rates	175
Effect of HTG on uridine uptake	176
IV. Discussion	180
CHAPTER VI - CONCLUSION	184
I. Discussion of Results	184
II. Suggestions for Further Research	190
BIBLIOGRAPHY	196
APPENDIX 1.	210
APPENDIX 2.	213
APPENDIX 3.	216

LIST OF TABLES

Table		Page
I	Effects of Inhibitors on Swelling Rates ..	51
II	Effects of Protein Modification on Swelling Rates	58
III	Fatty Acid Composition of *Acholeplasma laidlawii* Lipids	69
IV	Effects of Lipid Composition on Heats of Activation	74
V	Effect of Membrane Lipid Composition on Cell Size	77
VI	Reproducibility of Volume Dispensed by Syringe	138
VII	Homogeneity of Contents of Syringe after Mixing	138
VIII	Effects of Incubation with Sterols on Km and Vm of Uridine Equilibrium Exchange Efflux	155
IX	Fatty Acid Composition of Rat Erythrocyte Membranes	173
X	Fatty Acid Nomenclature and Melting Points	217

LIST OF FIGURES

Figure		Page
1	Effect of Osmolarity on Absorbance	49
2	Chemical Structures of Transport Inhibitors and of Permeants	50
3	Inhibition of Swelling of A. laidlawii in D- or L-Glucose by Phloretin	53
4	Effect of 0.001mM Phloretin on Uptake of [^{14}C]-D-Glucose	55
5	Scatchard Plot of Phloretin Binding to Acholeplasma laidlawii	56
6	Swelling Rates vs pH	60
7	Swelling Rates vs pH	62
8	Swelling Rate vs Glucose Concentration ...	64
9	Inactivation of Glucose Transport by High Temperature	65
10	Swelling Rates of Acholeplasma laidlawii and Derived Liposomes in Glucose and Erythritol	68
11	Effect of Membrane Lipid Composition on Swelling Rates	72
12	Arrhenius Plots of Swelling of 16:0/18:1t-Grown Cells	73

LIST OF FIGURES (Continued)

Figure		Page
13	Differential Thermal Analysis of Membranes and Lipids from Cells Grown in the Presence of Palmitic plus Elaidic Acids	76
14	Effect of Inhibitors on D-Glucose Metabolism	80
15	Metabolism of 0.02mM D-Glucose by Acholeplasma laidlawii	82
16	Metabolism of 200mM D-Glucose by Acholeplasma laidlawii	83
17	Metabolism of L-Glucose and 2-Deoxyglucose by A. laidlawii	85
18	Metabolism of L-Glucose and 2-Deoxyglucose by A. laidlawii	86
19	Metabolism of 3-O-Methyl Glucose by Acholeplasma laidlawii	87
20	Metabolism of Maltose by Acholeplasma laidlawii	89
21	Saturability of [^{14}C]-D-Glucose Uptake by A. laidlawii in the Presence of 10mM IAA	91
22	Competition by D-Glucose and 3-O-Methyl Glucose for [^{14}C]-D-Glucose Uptake by A. laidlawii with 10mM IAA	92

LIST OF FIGURES (Continued)

Figure		Page
23	Competition by D-Glucose and 3-O-Methyl Glucose for [^{14}C]-3-O-Methyl Glucose Uptake by *Acholeplasma Laidlawii*.....	94
24	Effect of Glucose Concentration on Uptake by *Acholeplasma laidlawii*.....	96
25	Effect of Glucose Concentration on Uptake by *Acholeplasma laidlawii*.....	98
26	Effect of Glucose Concentration and of IAA on Glucose Uptake by *Acholeplasma laidlawii*.....	99
27	Chromatography of Cell Extract after 10 min Incubation with [^{14}C]-D-Glucose	101
28	Effect of Fatty Acid Composition on Uptake of 0.1mM [^{14}C]-D-Glucose	102
29	Effect of Fatty Acid Composition on Uptake of 1.0mM [^{14}C]-D-Glucose	103
30	Effect of Fatty Acid Composition on Uptake of 10.0mM [^{14}C]-D-Glucose	104
31	Inhibition of [^{14}C]-2-Deoxyglucose Uptake by Glucose and Glucose Analogs	108
32	Passive Efflux of Uridine from Erythrocytes	137
33	Effect of 100mM Ether and of 50mM Procaine-HCl on Glucose Efflux	141

LIST OF FIGURES (Continued)

Figure		Page
34	Effects of Ether and Procaine-HCl on Passive [^{14}C]-Uridine Uptake by Erythrocytes	142
35	Effects of Ether and Procaine-HCl on D-Glucose Equilibrium Exchange Efflux .	144
36	Effects of Ether and Procaine-HCl on [^{14}C]-Uridine Efflux from Erythrocytes	145
37	Effects of Sterol Exchange on Passive Fluxes	149
38	Effect of Sterol Exchange on Passive Flux	150
39	Effect of Sterol Exchange on Glucose Efflux	151
40	Effect of Sterol Exchange on Passive Uridine Flux	153
41	Effect of Sterol Exchange on Uridine Equilibrium Exchange Efflux. Lineweaver-Burk Plot.	154
42	Metabolism of [^{14}C]-Uridine by Rat Erythrocytes	170
43	Metabolism of [^{14}C]-3-O-Methyl Glucose by Rat Erythrocytes	171
44	Efflux of Glucose from Rat Erythrocyte Liposomes	174
45	3-O-Methyl Glucose Uptake by Rat Erythrocytes	177

LIST OF FIGURES (Continued)

Figure		Page
46	Uridine Exchange Efflux from Rat Erythrocytes	178
47	Effect of HTG on Uridine Flux in Rat Erythrocytes	179
48	Biosynthetic Relationships Between Unsaturated Fatty Acids	182

LIST OF ABBREVIATIONS

ADP	adenosine-5'-diphosphate
ATP	adenosine-5'-triphosphate
BSA	bovine serum albumin
°C	degrees centigrade
cm	centimeters
CPM	counts per minute
DNFB	1-fluoro-2,4-dinitrobenzene
DSC	differential scanning calorimetry
DTA	differential thermal analysis
EDTA	ethylenediaminetetraacetate
ESR	electron spin resonance
et al.	et alii (and others)
g	grams or gravitational acceleration
GLC	gas-liquid chromatography
hsec	hecto-seconds (1 hsec = 100 sec)
HTG	6-[(2-hydroxy-5-nitrobenzyl)thio]guanosine
IAA	iodoacetic acid
l	liter
M	molar
mg	milligram
min	minute
ml	milliliter
mm	millimeter
mM	millimolar
mosM	milliosmolar

LIST OF ABBREVIATIONS (Continued)

mV	millivolt
NADP	nicotinamide adenine dinucleotide phosphate
NEM	N-ethylmaleimide
nm	nanometer
NMR	nuclear magnetic resonance
PCMB	para-chloromercuribenzoate
PEP	phosphoenol pyruvate
psi	pounds per square inch
S.D.	standard deviation
sec	second
Tc	transition temperature
TCA	trichloroacetic acid
TLC	thin-layer chromatography
tris	2-amino-2-hydroxymethyl-1,3-propanediol
UV	ultra-violet
μM	micro-molar

CHAPTER I

INTRODUCTION

I Review of the Literature

A feature which seems to be shared by all biomembranes is a structure based on a lipid bilayer, comprised of polar lipids oriented with their hydrophobic "tail" portions projecting inward approximately perpendicular to the bilayer plane and their polar "heads" located at the two outer surfaces. This structure was proposed in 1925 by Gorter and Grendel, based on their calculation that the lipid extracted from erythrocyte membranes could be spread on a monolayer which occupied twice as much area as did the cell membranes (1). In 1935, this feature was incorporated into the classic Danielli-Davson model, which also postulated the existence of protein layers at the polar surfaces (2). For the next three decades, evidence from electron microscopy, X-ray diffraction, and chemical analyses, largely with the myelin sheath of Schwann cells, gradually accumulated in support of this proposal (For review, see Hendler (3)). During this time various proposals regarding the position, configuration, and mode of binding of membrane proteins were made, but no further quantum jumps in the knowledge of biomembrane structure occurred until relatively recently, when a large number of new physical and chemical techniques became available for the study of membrane architecture.

Two of these techniques are differential thermal

analysis and differential scanning calorimetry, which have become available for organic chemistry and biological studies in the last 15 years as sensitive instruments requiring only milligram quantities of materials have been developed (4). In differential thermal analysis, a sample and an inert reference material are heated or cooled at the same rate of energy flux and the difference in temperature between them is recorded. Any endothermic or exothermic transition occurring in the sample will produce a peak or trough in the plot of differential temperature vs time or vs temperature of the sample or reference material. The alternate technique of differential scanning calorimetry maintains the reference material and the sample at the same temperature, while recording the differential heat input required to do this as temperature increases or decreases. The heat of transition can be obtained from the area under the peak in the DSC trace.

Many substances, such as phospholipids, do not undergo a direct thermal transition from crystal to liquid, but rather have one or more intervening "liquid-crystalline" or "mesomorphic" states. With phospholipid bilayers, the solid-->liquid-crystalline transition corresponds to a fluidization of the hydrocarbon chains with retention of the overall bilayer structure. Transitions between crystalline, liquid-crystalline, and isotropic liquid states can be detected by DTA or DSC. The nature of the liquid-crystalline

states of some phospholipids representative of those found in biomembranes has been investigated by Phillips et al., using DSC (5). By comparing the heat per methylene group of the alpha-crystalline gel-->liquid-crystal transition in lecithins to that required for complete melting of the corresponding hydrocarbons, they were able to obtain an estimate of the configurational entropy of the hydrocarbon chains in the liquid-crystalline state. The increase in entropy in going from the gel, which is a lamellar arrangement, with hydrocarbon chains in each layer in the extended, trans configuration and packed in a hexagonal lattice, to the lamellar liquid-crystalline state is about 2/3 as great as that which would occur with complete fluidization of hydrocarbon chains which are not joined to a polar headgroup. This is compatible with a structure of the liquid-crystalline state in which the hydrocarbon chains undergo hindered rotation about C-C bonds, and show some degree of average orientation perpendicular to the bilayer plane.

Such crystalline-->liquid-crystalline phase transitions have also been detected in biological membranes by DSC and DTA. Acholeplasma laidlawii B is an organism whose membrane fatty acid composition can be varied over a wide range by supplying the appropriate fatty acids in the growth medium (6). Differential scanning calorimetry of intact membranes of this organism showed a reversible thermotropic phase

transition which occurred at the same temperatures as in extracted membrane lipids dispersed in water, and had an enthalpy about 75% as great as seen with the extracted lipids (7). The transition temperature (Tc) decreased with increasing unsaturation of the membrane lipids, as is predicted from studies with synthetic lecithins (8,9). Cells grown at temperatures below their transition temperature became osmotically unstable, suggesting that viability is dependent on the presence of some liquid-crystalline lipid in the membrane. It has subsequently been verified that about 10% of the membrane lipid of this organism must be in the liquid-crystalline state for cell viability (10). Similar thermotropic phase transitions have been detected by DSC in intact cells, membranes, and aqueous dispersions of membrane lipids from Micrococcus lysodeikticus (11), and rat liver mitochondria and microsomes, and aqueous dispersions of their isolated lipids (12). In both cases, the lipids were found to be in the liquid-crystalline state at physiological temperatures.

The existence of a lipid bilayer in A. laidlawii membranes, and the involvement of at least 80% of the lipids in a thermotropic phase transition have been supported by X-ray diffraction studies (13). The transition in intact organisms, isolated membranes, or dispersions of isolated lipids is manifested as a gradual disappearance of a broad 4.6 Angstrom reflection and appearance of a sharp 4.15

Angstrom reflection as the temperature is lowered.

Nuclear magnetic resonance (NMR) and electron spin resonance (ESR) are two related spectroscopic techniques which have recently been used in several ways to yield a wealth of information about the orientation, motion, environment, and phase state of biomembrane lipids. In both techniques, a strong magnetic field is applied to the sample to cause a splitting of two degenerate energy levels of a nucleus or electron (14). These degenerate energy levels have the opposite magnetic spin quantum numbers, but have the same energies in the absence of an applied field. Transition between the split levels can occur by absorbtion of radio frequency or microwave radiation, and this absorbtion is measured. NMR spectra may be obtained from the hydrogen nucleus, so this technique has the advantage of not requiring the addition of any foreign molecule which may perturb the structure being investigated. It is, however, less sensitive and less specific than ESR. ESR requires the addition of a "probe" molecule having an unpaired electron. While this introduces uncertainty about the effect of the probe on the features being investigated, it can be an advantage in that ESR is more specific than NMR, since only the specific molecule and position occupied by the probe is seen.

In NMR, the magnetic field experienced by a particle is influenced by the fields of adjacent electrons. This effect

depends upon orientation of the orbitals in space, so that different particles in the sample may experience slightly different resultant local magnetic fields, producing broadening of the spectral absorbtion band because there are many different resonant conditions present close together in frequency rather than just one. Molecular motion can narrow the bands to produce a high resolution spectrum if thermal motion is much faster than the resonant frequency so that a time average of all orientations is seen for each particle (15). For this reason, information about the mobility of groups can be obtained from the linewidths of NMR spectra. By this method, phase transitions in anhydrous phosphatidylethanolamine were readily detected by a sharp decrease in linewidth of the –CH2– absorbtion band at the transition temperature as samples were heated (16). Phase transitions in hydrated dipalmitoyl phosphatidylcholine (17) and in sonicated dimyristoyl phosphatidylcholine dispersions (18) were alsc detected by NMR. The addition of cholesterol to liquid–crystalline lecithin dispersions up to a 1:1 mole ratio causes selective immobilization of the first 10 methylene groups in each hydrocarbon chain, resulting in an overall fluidity which is intermediate between the gel and liquid–crystalline states, and abolishes the thermotropic phase transition (19,20). Cerebroside and sphingomyelin, the major components of the myelin membrane, show a phase transition occurring above physiological temperatures (21). In the presence of cholesterol, a –CH2– peak of intermediate

mobility is present in the NMR spectrum, both above and below Tm. Studies of ^{13}C-nuclear magnetic resonance in sonicated egg yolk phosphatidylcholine bilayer vesicles have revealed a gradient of increasing mobility of methylene groups along the hydrocarbon chains from the glycerol backbone toward the terminal methyl groups (22). The extension of this methodology to natural membranes is complicated by the fact that there are many other compounds present besides lipid which contribute to the spectra. The spectra of myelin (23), erythrocyte membranes (17), and sarcoplasmic reticulum membranes (24), however, are consistent with the lipid being present in a bilayer. The hydrocarbon chains in erythrocyte membranes seem rather rigid, perhaps due to interaction with cholesterol or proteins. On the other hand, the $\pm N-(CH3)3$ groups of phosphatidylcholine and sphingomyelin in erythrocyte membranes are rather free to move (18). About 80% of the fatty acid chains in rabbit sarcoplasmic reticulum membranes undergo only limited motion(24), and a large fraction of the hydrocarbon chains of A. laidlawii can be in a state of mobility similar to the gel state of dimyristoyl phosphatidylcholine without loss of viability (25).

The technique of electron spin resonance spectroscopy requires a probe containing an unpaired electron. The nitroxide free radical is very stable and has been incorporated into various types of molecules which serve as

probes of membrane and bilayer structure. Because of the anisotropy of the resonance, this technique can also provide information about orientation of the probe, provided that the geometry of the N-O bond relative to the probe molecule is fixed.

Three types of paramagnetic probes have been used extensively in the study of membranes. One type consists of various derivatives of sterols, having a 5-membered ring containing the nitroxyl group attached to the sterol. In these derivatives the orientation of the N-O bond with respect to the rest of the molecule is fixed. It was shown, using the spin probe 3-spiro-[2'-(N-oxyl-4',4'-dimethyl-oxazolidine)]-cholestane, that the sterol long axis is oriented essentially perpendicular to the plane of the film when it is incorporated into dipalmitoyl-PC or egg yolk-PC lamellar bilayers (26). Increasing saturation of the hydrocarbon chains, or the addition of cholesterol, increased the orientation and decreased the mobility of the probe. A thermotropic gel-->liquid-crystalline phase transition, and the fluidizing effect of cholesterol on the gel state can be detected in sphingomyelin bilayers (27). This type of spin label study has also indicated that the lipids of erythrocyte ghosts and of influenza virus are arranged in a partially fluid bilayer (28).

The second type of spin probe has the nitroxide-containing ring attached to various positions on the

hydrocarbon chain of a fatty acid, which may be esterified to a glycerol backbone. Studies with these types of spin labels have shcwn a gradient of increasing mobility along the hydrocarbcn chains of the probes from the polar to the terminal methyl group in lecithin multibilayers (29), extracted lipids from Halobacterium cutirubrum (30), membranes from A. laidlawii and Mycoplasma hominis (31), and yeast membranes (32). Phase transitions occurring near physiological temperatures could be detected in many biomembranes (33–36). The fluidization of the hydrocarbon region by the presence of unsaturation in fatty acid chains (32), and the induction by cholesterol of a state of fluidity intermediate between the gel and liquid–crystalline states, were confirmed (37–39). In some membranes, evidence of immobilizatien of lipid by binding to protein is seen. Cytochrome oxidase isolated from beef heart mitochondria along with associated phospholipids spontaneously forms closed vesicular membranes. These contain a fixed amount of immobilized bound lipid, sufficient to form a single layer surrounding the protein complex (boundary lipid), and variable amounts of fluid lipid (40–42). The boundary lipid is necessary for maximal activity of this enzyme, but additional fluid lipid has no further effect once all the binding sites are filled. In Halobacterium cutirubrum, which has a low membrane lipid content (lipid:protein ratio < 0.2), the membrane proteins seem to impose a significant ordering on nearly all the lipid, and to abolish the

fluidity gradient along the hydrocarbon chains (30).

In sonicated phospholipid vesicles, spin labels on the inside surface can be distinguished from those on the outside by differences in packing caused by the curvature of the surface. Using ascorbate to destroy the paramagnetism of the label on the outside surface by reduction, it has been shown that exchange of lipid molecules between the two sides of the bilayer is very slow (asymmetry of the membrane decays with a half-life of 6.5 hr at 30°C) (43). On the other hand, lateral diffusion of individual phospholipid molecules within the plane of the bilayer in membranes of rabbit sarcoplasmic reticulum (44) or A. laidlawii (45) is very rapid.

The third class of spin labels is represented by the compound 2,2,6,6-Tetramethylpiperidine-1-oxyl (TEMPO). Since this compound exhibits a different ESR spectrum in water than in a hydrophobic environment, and since its solubility in a lipid bilayer depends on the bilayer fluidity, the state of fluidity can be determined from the TEMPO spectrum (46). This probe has been used to detect phase transitions in E. coli membrane lipids at physiological temperatures (47). It has also been shown using TEMPO that 84% of the membrane lipid of rabbit sarcoplasmic reticulum is in the fluid state at 25°C (46). The discrepancy between this result and the NMR data showing largely immobilized lipid in sarcoplasmic reticulum membranes (24) may be due to

perturbation of the environment by the spin label, so some caution is necessary in evaluating ESR data (48,49).

The techniques of freeze-fracturing and freeze-etching, developed in 1963 (50), have been combined with electron microscopy to give information about the structure of the surface and interior of cell membranes. The sample is deep frozen and splintered by a crude microtome at about -200°C. Water can be sublimed from the surface by cooling the microtome knife to liquid nitrogen temperatures under high vacuum . The etched specimen is then "shadowed" by applying platinum vapor at a small angle to the surface to reveal textural detail, and a "replica" made by applying a thicker layer of carbon. This carbon-platinum replica is examined in the electron microscope. It has been shown that one of the fracture planes is through the center of the hydrocarbon region of the bilayer (51-53), so that the internal organization of the bilayer can be seen. Freeze-etching has revealed the presence of small (80-200 Angstrom diameter) globular particles and depressions in the interiors of many membranes. These are seen randomly arranged in onion root tip cells (51), red blood cells (52-55), Tetrahymena pyriformis (56), and A. laidlawii (57,58). That these particles are proteins is shown by their removal from red blood cell membranes by pronase digestion (59), their depletion in A. laidlawii membranes by incubation of the cells in the absence of amino acids or the presence of

puromycin (58), and their distribution in erythrocyte membranes in the same pattern as glycoprotein phytohemagglutinin (PHA) receptors on the cell surface. Cooling of A. laidlawii (57) or Tetrahymena pyriformis (56) membranes below their Tc results in aggregation of the particles and the appearance of large bare patches, presumably due to exclusion of the proteins from areas of lipid which is in the gel state. Exposure of erythrocyte ghosts to pH=5.5 at low ionic strength also produces a reversible aggregation of particles within 2–4 minutes, which indicates that the ghost membrane is a planar fluid domain, interrupted by mobile protein intercalations (55).

Additional evidence for protein located within the interior of the bilayer has been obtained from studies involving chemical modification of human erythrocyte membrane proteins. These techniques require reagents which will not penetrate intact membranes, and which can react with exposed proteins, detectably altering them. Intact cells, sealed or leaky ghosts, membrane vesicles, or solubilized membranes are treated with the reagent, then proteins are separated by SDS–polyacrylamide electrophoresis, and the fractions which have been attacked by the reagent determined. When membrane proteins were digested with proteolytic enzymes, the results indicated an asymmetric distribution of proteins on the two sides of the membrane, and the existence of one or two proteins which

span the membrane (60–64). It was found that only one to three proteins in intact membranes or resealed ghosts are susceptible to attack, while a large number of proteins are attacked in leaky ghosts. Attack at one side only of the membrane was also achieved by forming inside-out or right-side-out sealed membrane vesicles, separating them by centrifugation, then treating with enzymes (64). Evidence for a protein which spans the membrane comes from the existence of different proteolysis products of a certain protein, depending upon which side of the membrane is attacked.

Labelling of tyrosines and histidines with ^{125}I, using lactoperoxidase (65), labelling of tyrosines with ^{35}S–sulfanilic acid diazonium salt (60,66), and labelling of glycoprotein carbohydrate with ^{35}S–formyl–methionyl sulphone methyl phosphate (FMMP) (61) have all supported the conclusion from proteolytic enzyme digestion that only a few proteins are exposed at the outside surface, but most are exposed at the inside. All of these interpretations, however, are subject to uncertainty regarding the effect of ghost formation on the native structure of membrane proteins. More conclusive evidence for the existence of three proteins which span the membrane was obtained by iodinating erythrocyte ghost proteins from either the outside or the inside with lactoperoxidase (67). Iodination at the inside surface only was achieved by sealing

lactoperoxidase or lactoperoxidase plus glucose oxidase inside ghosts, then washing to remove the enzymes from the outside. Hydrogen peroxide for the iodination was either added directly to the ghosts, or generated on the inside by the action of glucose oxidase on glucose added to the mixture. The presence of catalase in the solution added to the exterior of the ghosts assured that no hydrogen peroxide was present outside the ghosts. This procedure eliminates the possibility that the labelling of more proteins in leaky ghosts could result from exposure of more proteins at the outside surface by the opening up of the ghosts, rather than from attack of the enzyme at the inside surface. Three glycoproteins were found which could be labelled from both the inside and the outside of the ghosts.

The lateral mobility of membrane proteins has been demonstrated by the intermixing of surface antigens after cell fusion (68). Different colored fluorescent antibodies to surface antigens of human and mouse tissue culture cells were prepared, then the two cell types were fused by Sendai virus. At 37°C, fused cells showed the antibodies segregated into the two halves of the cell after 5 minutes, but completely intermixed after 40 minutes. Low temperature prevented this mixing, presumably by decreasing the membrane fluidity.

Singer and Nicolson have proposed a model for biomembrane structure, based on much of the preceding data,

which they call the "Fluid Mosaic Model" (69,70). In this model they distinguish between peripheral and integral membrane proteins. Peripheral proteins, which can be dissociated from the membrane free of lipid and in a soluble form by relatively mild treatments, are not essential to the basic membrane structure. Integral proteins require detergents or organic solvents to dissociate them from membranes; they often contain bound lipid when isolated, and they are insoluble or highly aggregated if the lipid is all removed. These are postulated to be amphipathic, largely globular, proteins which are partially buried within the hydrocarbon lipid core and interact hydrophobically with their lipid environment. They may have their polar regions exposed at only one membrane surface, or may span the bilayer, being exposed at both sides. These proteins, singly or in small aggregates, are free to diffuse laterally through the viscous two-dimensional fluid domain formed by the membrane lipids. These lipids are largely in the form of a fluid bilayer, although some may be bound to protein. Rotational transitions of proteins from the outer to inner membrane surfaces, or vice versa, would occur at only negligibly slow rates, allowing the maintenance of transmembrane asymmetry.

The phase transitions and degree of fluidity of biomembrane lipids have been shown to affect many biological functions asscciated with membranes. When the passive

permeabilities of A. laidlawii cells and derived liposomes (closed spherical lipid bilayer vesicles) to ethylene glycol, glycerol, and erythritol were studied as a function of temperature and of fatty acid composition, the activation energies for passive permeation were found to be independent of fatty acid composition (71,72). The energies were the same in cells as in liposomes and were consistent with the calculated energy required to completely dehydrate the permeant molecules. The incorporation of methyl-branched, unsaturated, or shorter chain fatty acids reduced the transition temperatures and presumably increased the fluidity of the hydrocarbon region at any given temperature above the phase transition. The permeabilities of both cells and liposomes increased in the order of increasing lipid fluidity. The incorporation of cholesterol, which produces more ordered packing of fatty acid hydrocarbon chains, decreased permeability.

A comparison has been made of the temperature dependence of physiological parameters, mitochondrial enzyme activities, and lipid phase transitions in two types of plants and two types of animals (33,73). Tissues from the rat, a homeothermic animal, and the sweet potato, a chilling-sensitive plant, are injured by exposure to temperatures below 23°C and 12°C respectively. Intact mitochondrial membranes from rat liver or from sweet potato, or lipids extracted from these membranes exhibit phase

transitions at these temperatures, which can be detected by electron spin resonance spectroscopy. Furthermore, the membrane-bound mitcchondrial enzymes succinate oxidase, succinate dehydrogenase, and cytochrome c oxidase exhibit discontinuities in their Arrhenius plots at these temperatures. These discontinuities are abolished by treatment with detergent, which disrupts the packing of the lipid into a bilayer, but not by fragmentetion of the membranes and destruction of the permeability barrier by sonication, hypctonic swelling, or freezing and thawing. The poikilothermic animal, the rainbow trout, and the chilling-resistant plant, the potato, do not show physiological damage when ccoled from 36°C to 1°C, nor do the mitochondrial membranes or lipids show phase transitions, nor do the mitcchondrial enzymes studied show discontinuities in their Arrhenius plots over this temperature range.

Many other membrane enzymes have been shown to exhibit lipid-dependent discontinuities in Arrhenius plots of their activities. In an unsaturated fatty acid auxotroph of *E. coli*, glycerol 3-phosphate acyltransferase activity showed a continuous decrease in the slope of its Arrhenius plot above 15°C (74). Growth on the less fluid *trans*-unsaturated fatty acids increased this temperature to 20°C. Both 1-acylglycerol-3-phosphate acyltransferase and glycerol-3-phosphate dehydrogenase showed linear Arrhenius

plots but, with the first enzyme, the slope was steeper in membranes containing trans-unsaturated fatty acids. Manipulation of the fatty acid composition of membranes of Saccharomyces cerevisiae, either by switching from aerobic to anaerobic growth conditions or vice versa (75), or by supplementing the medium with fatty acids (76) shifts discontinuities in the Arrhenius plots of cytochrome c oxidase (75), and kynurenine hydroxylase and oligomycin-sensitive ATPase (76) in the directions expected from the effects of the fatty acids incorporated on membrane fluidity. Lamb kidney outer medulla $(Na^+ + K^+)$-ATPase shows a discontinuity in the Arrhenius plot at 20°C, which coincides with the lipid phase transition, as detected by ESR spectroscopy (35). A similar effect is seen in A. laidlawii with Mg^{2+}-dependent ATPase, but not with NADH-oxidase or p-nitrophenylphosphatase (77). The discontinuities in the Arrhenius plots of ATPase activity correlated with the low temperature end of the lipid phase transition, as detected by differential scanning calorimetry. Inhibition by F^- of $(Na^+ + K^+)$-ATPase and of acetylcholinesterase of rat erythrocytes (78) and by Na^+ of (Ca^{2+})-ATPase of E. coli (79) is also dependent on the fluidity of the membrane lipids. Using mutants of E. coli which are unable to synthesize unsaturated fatty acids, or to beta-oxidize fatty acids, it is possible to effect alterations in the membrane lipid fluidity by varying the unsaturated fatty acids supplied in the growth medium. A dependence of

beta-galactoside and beta-glucoside transport on membrane lipid fluidity has been shown in these mutants. Using three different fatty acid supplements, breaks in Arrhenius plots of beta-galactoside transport occurred at three different temperatures (80). These temperatures lie at or near the liquid-crystalline-->crystalline phase transitions of whole cells, membranes, or phospholipids, as determined by dilatometry, light scattering, monolayer force-area isotherms, or fluorescence probing. Other workers have examined beta-galactoside and beta-glucoside transport in these mutants over a wider temperature range, and have found two or three discontinuities in the Arrhenius plots (81-83). The lower discontinuity corresponds to the appearance of liquid-crystalline lipid, and the upper one to the disappearance of the last of the crystalline lipid, as detected by solubility of the spin label TEMPO in the lipid phase. Between these two temperatures lateral phase separations of crystalline and liquid-crystalline lipid were postulated to occur. The exact nature of the intermediate transition was not clear, but its effects are seen in both transport systems, as well as in spin-labelling experiments. At the high-temperature discontinuity, lowering of the temperature by 1° caused a dramatic increase in transport rates in some cells. It was suggested that this is due to an increased isothermal lateral compressibility of the membrane lipids at the point where crystalline lipid first appears. A maximum in the rate of Na^+ diffusion through phospholipid

bilayers has been observed at the midpoint of their phase transition detected by fluorescence (84). This was interpreted as being due to an increased Na^+ permeability at boundary regions between liquid and solid domains rather than a high lateral compressibility with lateral phase separations. Additional support for the concept of lateral phase separations in membranes has come from the observation that the rate of intermixing of antigens in newly-formed human-mouse heterokaryons increased as temperature was lowered from 21° tc 15°C (85). This could be due either to the lower area available for diffusion as islands of solid lipid form, or to the remaining fluid lipid having a lower viscosity than the total membrane lipid at a slightly higher temperature.

The biological importance of the physical properties of membrane lipid to the organism is illustrated by the fact that a large number of organisms have been shown to alter their fatty acid compositions as a response to a change in growth temperature in such a manner as to compensate for the change in fluidity that would be produced by the temperature shift (86-90).

II Objective of this Study

Four mechanisms by which substances cross cell membranes can be defined, two of which do not require metabolic energy, and two of which are metabolism-dependent (91). Passive diffusion is an unmediated process whereby the permeant crosses the membrane as a result of random molecular motion without interacting specifically with any molecular species in the membrane. Facilitated diffusion is a saturable process, involving some type of stereospecific combination with a membrane component. Like passive diffusion, this process cannot produce accumulation against a gradient of electrochemical potential and is not linked to metabolic energy. Active transport uses metabolic energy to effect a change in the affinity of a specific membrane carrier molecule for the permeant, thereby causing its accumulation against a gradient. This affinity change must be somehow linked to the orientation of the carrier, either through a conformational change which translocates the permeant, or through a vectorial effect showing transmembrane asymmetry on a "shuttle-type" mobile carrier. In group translocation a covalent change is exerted on the transported molecule such that the reaction itself results in the passage of the molecule through the diffusion barrier. It seems quite clear that most, if not all, mediated transport processes involve membrane proteins. A central question which must be resolved before acceptable

molecular descriptions of these phenomena can be provided is the nature of the functional and spatial relationships between the transport proteins and the membrane lipids. After this project was begun, data were published showing a dependence of active transport of sugars in E. coli on lipid fluidity (92,93). This implies that some component of the transport system undergoing a movement or conformational change is in direct contact with membrane lipid.

The dependence of the rate of facilitated diffusion on lipid fluidity had never been examined. Three characteristics which must be accounted for by any mechanism postulated for this phenomenon are enhancement of flux rate, saturability, and specificity. These criteria may be satisfied by mobile carrier molecules embedded in the membrane which bind permeant at one face, diffuse through or rotate in the membrane, then release it at the other side, by proteins spanning the membrane which translocate their permeant binding sites through the membrane by a conformational change, or by specialized regions of the membrane which provide aqueous channels through the lipid. These channels could still conceivably exhibit permeant specificity if they were lined with fixed substrate binding sites (94). A transport site like this, or one involving conformational changes, but which is embedded in a specialized region removed from the membrane lipid or surrounded by some specialized lipid species may not show a

dependence of transpcrt rate on the bulk properties of the membrane lipids.

In this regard, it is informative to compare the effects of lipid fluidity on two types of ion-transporting antibiotics, whose effects on the K^+ conductance of planar bilayer membranes were studied (95). Gramicidin is a hollow cylindrical mclecule which acts by embedding itself within the membrane lipid tc form a channel through the bilayer (96). Gramicidin-mediated potassium flux through a planar bilayer membrane decreases with decreasing temperature below the lipid phase transition temperature (Tc), but shows no temperature dependence (and therefore no dependence on lipid fluidity) above Tc. No discontinuous change in K^+ conductance is seen at Tc (95). Nonactin and valinomycin act by binding cations to form a complex which then diffuses through the lipid bilayer (96-99). These antibiotics show an increase in K^+ conductance with increasing temperature above Tc, and a discontinuous decrease to essentially zero at the phase transitiон point (95). Adding cholesterol to bilayer lipid membranes (99), or decreasing the fluidity of A. laidlawii membranes by adding cholesterol or by altering the fatty acid compositicn (100) also decreases the nonactin and valinomycin-mediated monovalent cation fluxes.

The objective of this study was to determine the effect of membrane lipid fluidity on rates of facilitated diffusion. The systems used were A. laidlawii B, human

erythrocytes, and rat erythrocytes. With A. laidlawi, the fluidity could be readily altered by changing the supplemented fatty acids in the growth medium, or by adding cholesterol. Since no facilitated diffusion system had been defined in this organism, it was necessary to characterize some system. The glucose and maltose uptake systems were investigated.

The human erythrocyte membrane has fairly well-defined facilitated diffusicn systems for glucose (101-104) and for uridine (105-107). The fluidity of the lipid region of human erythrocyte membranes was altered by the addition of anaesthetics and by exchanging other sterols for membrane cholesterol, and the effects on these transport systems determined. With rat erythrocytes it was necessary to partially characterize the uridine and 3-O-methyl-D-glucose facilitated diffusicn systems. Then an attempt was made to modify the lipid fluidity by feeding the animals a defined diet with various fatty acid supplements added, and the effects of the modifications on transport determined.

CHAPTER II

GENERAL MATERIALS AND METHODS

I Materials

Chemicals

Growth medium for Acholeplasma laidlawii was prepared from Difco Bacto-Tryptose (Difco Laboratories, Detroit, Michigan). Large quantities having the same lot number were purchased at a time, as it was found that the organism frequently required several weeks to attain optimal growth after changing to a different lot of tryptose.

Fatty acids were obtained from Analabs, New Haven, Connecticut, U. S. A., or from Nu-Chek-Prep, Elysian, Minnesota, U. S. A. The fatty acid methyl esters used as standards for GLC were also from Nu-Chek-Prep. Cholest-4-en-3-one was obtained from Fluka AG, Chemische Fabrik, Switzerland.

Tripalmitin, tristearin, and safflower oil were from the Nutritional Biochemicals Corporation, Cleveland, Ohio, U. S. A.

Pyruvic acid, ADP, NADP, and PEP were purchased from the Sigma Chemical Company, St. Louis, Missouri. ATP, inosine, and uridine were from Raylo Chemicals Limited, Edmonton, Alberta, Canada. L-glucose and 3-O-methyl glucose

were from Calbiochem, San Diego, California, U. S. A.

Radioactive sugars and nucleosides were purchased from either New England Nuclear, Dorval, Quebec, Canada, or ICN, Irvine, California, U. S. A. [^{3}H]-Phlorizin was from New England Nuclear, and [^{3}H]-phloretin was a gift from Dr. I. Benes, Czechoslovak Academy of Sciences, Prague, Czechoslovakia. [^{14}C]-Uridine was labelled in the 2 position, 2-deoxyglucose in the 1 position, 3-O-methyl glucose on the methyl group, L-glucose in the 1 position, and maltose, sucrose, and D-glucose were uniformly labelled. [^{3}H]-Phlorizin was generally labelled at exchangeable hydrogens.

Unlabelled phloretin and phlorizin were both obtained from K&K Chemicals (now a subsidiary of ICN), and procaine-HCl was from Matheson Coleman and Bell, Norwood, Ohio, U. S. A.

6-[(2-Hydroxy-5-nitrobenzyl)thio]guanosine (HTG) was a gift from Dr. A. R. P. Paterson, Cancer Research Unit, The University of Alberta, Edmonton, Alberta, Canada. Methylarsine oxide was a gift from the Vineland Chemical Sales Corporation, Vineland, New Jersey, U. S. A.

Alumina (Woelm Alumina Neutral TLC) was from Waters Associates Inc., Framingham, Massachusetts, U. S. A., Unisil (250-325 mesh) from the Clarkson Chemical Company, Inc., Williamsport, Pennsylvania, U. S. A., Biosil HA (200-325

mesh) from Bio•Rad Laboratories, Richmond, California, U. S. A., and silica gel G from Brinkmann Instruments Ltd., Toronto, Ontario, Canada.

Organic solvents were reagent grade, obtained from Baker Chemicals through Canlab, Edmonton, Alberta, Canada. Contaminants in excess of the specifications were occasionally seen, so spot checks on the purity of solvents were run by GLC.

All other chemicals used were reagent grade, obtained from Canlab or from Fisher Scientific, Edmonton, Alberta, Canada.

Biological materials

Enzymes: Hexokinase (Sigma type F-300 Sulfate-free) and glucose-6-phosphate dehydrogenase (Sigma type XV) were purchased from the Sigma Chemical Company. Pronase was from Calbiochem, and trypsin from Mann Research Laboratories Inc., New York, New York, U. S. A.

Blood: Fresh (less than 1 week old) human blood was obtained from the Red Cross Society Blood Transfusion Service, Edmonton, Alberta. 450 ml of blood were collected in 63 ml of CPD (citrate-phosphate-dextrose) solution containing 0.206 g of anhydrous citric acid, 1.66 g of trisodium citrate dihydrate, 0.14 g of sodium biphosphate and 1.61 g

of dextrose.

Organism: A. laidlawii, strain B (formerly Mycoplasma laidlawii) has been continuously cultured in this laboratory for several years by daily transfer of small innocula to fresh growth medium. The organism was originally obtained from G. ff. Edward (Wellcome Research Laboratories, Beckenham, Kent, England).

Rats: Female Sprague-Dawley rats were obtained from the Health Sciences Animal Center at the University of Alberta, immediatly after weaning (age = 3 weeks). Blood was collected in 20 ml of buffer (150mM NaCl, 5mM sodium phosphate, pH=7.4, 0.8% trisodium citrate dihydrate) after decapitating the animals. To obtain as much blood as possible, 15 psi of negative pressure was applied to the neck of the decapitated rat's body, using a funnel and suction filtration flask, while continuously washing the blood down into the flask with blood collection buffer from a wash bottle and stirring.

II Methods

Lipid extraction and purification

Lipids were extracted from A. laidlawii suspensions or from erythrocyte ghosts by the method of Bligh and Dyer (108). The material was extracted twice with chloroform:methanol:water 1:2:0.8 (v:v:v), centrifuging each time for 15 min at 13,000Xg and retaining the supernatants. To 380 ml of pooled supernatants were added 100 ml of chloroform, 100 ml of water, then 200 ml more of chloroform, shaking after each addition. This mixture was centrifuged for 15 min at 13,000Xg, producing two liquid phases with denatured protein at the interface. The upper phase and the protein material were aspirated and discarded, and the lower chloroform layer was evaporated to a small volume. This was then applied to a column of 5-10 g of Biosil-HA silicic acid in chloroform, and the column eluted with 100 ml of methanol. This elution recovered all the lipid material, while protein and other non-lipid contaminants were retained on the column.

Fatty acid analysis

Fatty acids present in the extracted lipids were converted to their methyl esters by acid-catalyzed transesterification. The lipid extract was taken to dryness in a screw-cap glass tube with a teflon cap liner under a stream

of nitrogen, then 10 ml of methanol and 5 drops of concentrated sulfuric acid were added. These tubes were tightly capped and incubated at 70°C for 2 hr, then the contents were added to 20 ml of water in a 125 ml separatory funnel. This mixture was extracted twice with 10 ml of hexane and these extracts dried by passage through anhydrous sodium sulfate. After evaporating the solvent under nitrogen to a very small volume, the fatty acid analysis was performed by GLC (gas-liquid chromatography) on a 6 ft by 1/4 in column of 10% diethyleneglycol succinate on Anakrom 60/70 AS mesh. Conditions for individual analyses are described with the results.

Radioactivity counting

Radioactivity was determined by liquid scintillation counting, using a Beckman LS-200B counter. Samples were counted either as a 1 ml aqueous solution in 10 ml of Aquasol, or were dried on 2.3 cm Whatman No. 3 filter papers and counted in 10 ml of toluene containing 4 g/l of Omnifluor (New England Nuclear). After applying 0.2 ml of sample to the filters, supported by straight pins, they were dried overnight at room temperature, then at 110°C for 30 min before counting. Aqueous samples were corrected for quenching by the external standard ratio. Curves of counting efficiency *vs* external standard ratio were constructed by counting a series of vials containing the same amount of

radioactive material and varying amounts of the quenching material (hemoglobin or TCA).

Paper chromatography

Chromatography was carried out at room temperature in the descending mode on 18 in X 22 in sheets of Whatman No. 1 paper. Samples were applied 3.5 in from one end, at least 2 in apart. For radioactive materials, profiles of the distribution of counts on the paper were obtained by cutting a 4 cm wide strip from the paper centered at the applied spot, then cutting this strip into 2 X 2 cm squares and counting each two adjacent squares together in 10 ml of toluene-Omnifluor. Reducing sugars were stained by spraying with saturated silver nitrate in aqueous acetone (Mix 0.5 ml sat. aq. $AgNO_3$ with 100 ml acetone, then add water dropwise until clear.), then with 2 g of NaOH in 100 ml of 90% aqueous ethanol. 2-Deoxyglucose was visualized by spraying with 1% boric acid in 90% aqueous methanol containing 1% HCl, then heating 1-3 min at 100°-105°C. After this treatment, the 2-deoxyglucose spots exhibited a purple fluorescence when viewed under short-wave UV light (109).

Conditioning of dialysis tubing

Dialysis tubing (Arthur H. Thomas Co., Philadelphia, Pennsylvania) was conditioned before use by boiling for 5 min in 5% sodium carbonate, containing 50mM disodium EDTA,

then stretched by pulling longitudinally while applying pressure with the tap (110). After thorough washing, the tubing was stored in 50% aqueous ethanol at 4°C until used.

CHAPTER III

STUDIES WITH ACHOLEPLASMA LAIDLAWII B

I Introduction

Acholeplasma laidlawii B is an organism which is uniquely suited to the study of biomembrane structure and function. It has no cell wall and only one type of membrane—the plasma membrane (111). The fatty acid composition and thus the phase transition temperature of the membrane lipids can be significantly and reproducibly altered by varying the fatty acids added to the growth medium (10). When grown in the absence of sterols, the membrane contains no cholesterol, but cholesterol can be incorporated to a level of up to 8% (by wt.) of the membrane lipids by adding up to 25 mg of cholesterol per 1 of culture to the growth medium (112). Because of the absence of a cell wall, the cells can swell and shrink as a response to the osmotic pressure of their environment. This allows transport by a suspension of cells in an isotonic solution of permeant to be followed by monitoring the changes in light absorbance produced by swelling of the cells as they are penetrated by permeant (71).

The passive permeability of this organism to ethylene glycol, glycerol, and erythritol has been studied as a function of fatty acid composition and cholesterol content of the membrane (71,72). Significant differences were seen in these passive permeabilities with different growth

conditions. An increase in fatty acid chain length, an increase in membrane cholesterol, a decrease in unsaturation or the substitution of *trans* for *cis* double bonds all had the effect of reducing permeability. This is as would be expected from the physical properties of these lipids, and the data verify the contention that significant alterations in membrane fluidity occur in a predictable manner with variations of the lipid composition of the membranes.

The mediated transport systems in *A. laidlawii* have not been as extensively characterized as in some other organisms for a variety of reasons. This organism is more difficult to culture than more extensively studied organisms like *E. coli*. The lack of a cell wall, while advantageous for assaying permeability by swelling rates, also makes it more difficult to separate cells from medium by Millipore filtration in order to carry out radioisotope tracer studies. The small size of the cells (500nm diameter (113)) results in a large surface area/volume ratio and a small intracellular volume. This makes preloading of the cells with a significant amount of radioactive compound more difficult and increases the significance of binding of permeant to the cell surface. It also creates problems in sampling at early enough times because of the limited capacity of the intracellular compartment compared to the surface over which transport occurs. Osmotic lysis of *A. laidlawii* cells results in the formation of very leaky

structures (114), so it has not been possible to use sealed membrane vesicles which have been very useful in the study of transport in E. coli and other bacteria because of the absence of cytoplasmic enzymes from these vesicles (91).

An accumulation of K^+ by active transport has been shown in A. laidlawii (115,116). Cirillo and Razin refer to unpublished evidence for glucose uptake by facilitated diffusion in A. laidlawii, but the nature of the evidence is not described (117). Tarshis and co-workers have reported that glucose, fructose, and maltose are taken up by A. laidlawii by active transport systems having rather high affinities for these sugars (118-120). Their interpretations of the data, however, are subject to several criticisms, particularily in light of some of the results to be presented here (See appendix 1 for discussion).

It was necessary to find a facilitated diffusion system, so that the effect of lipid fluidity on it could be determined. We decided to look at the uptake of glucose and of maltose, since these two sugars can serve as energy sources for the organism (113).

II Methods

Growth of Acholeplasma laidlawii

A. laidlawii B cells were grown at 35°C in a fatty acid-supplemented, lipid-poor growth medium as described by

McElhaney and Tourtellotte (121). For 6 l of media, 120 g of Difco Bacto-Tryptose were dissolved by heating in 1.2 l of water, then cooled, acidified with 48 ml of concentrated HCl, and extracted twice with 300 ml of chloroform to remove most of the lipid. After adding water to 6 l, 22.2g tris, and 16.8g NaOH, and adjusting the pH to 8.0-8.2, the medium was autoclaved to drive off the dissolved chloroform. Before innoculating, 10 ml of sterile 25% glucose solution, 500,000 units of penicillin, 40 ml of 10% fatty acid-poor BSA, sterilized by filtration through a Seitz filter, and a total of 0.12 mmoles of fatty acid supplement[1] dissolved in 2.4 ml of ethanol were added per l of medium. A mixture of palmitic acid (16:0) plus an unsaturated fatty acid was used in proportions such that the unsaturate was approximately 50% of the total fatty acids and the palmitate was approximately 40%. When cholesterol was present it was added as a 1% ethanolic solution containing the fatty acids to the level of 24 mg of cholesterol per l of medium.

Liposome formation

After extraction and purification by column chromatography on silicic acid of lipids from cells, liposomes were prepared by a modification of the method outlined by De Gier *et al.* (122). Lipid extract in

[1]See appendix 3 for fatty acid nomenclature and physical properties.

chloroform was added to a tared culture tube and the solvent removed under a stream of nitrogen. The lipid was dried overnight *in vacuo*, then the tube was reweighed. A 1 cm diameter glass bead and 0.05 ml each of 100mM KCl and 100mM $MgSO_4$ per mg of lipid were added and the lipid was dispersed by vortex mixing, keeping the temperature between 30° and 40°C. For swelling experiments, the liposome suspensions were diluted, if necessary, with 50mM KCl + 50mM $MgSO_4$ to obtain the desired optical density.

Swelling rates

Swelling of cells induced by uptake of permeant was followed by monitoring the absorbance at 450nm of a cell suspension (71). The validity of reciprocal absorbance as a measure of cell volume was determined by plotting this parameter *vs* the reciprocal of the concentration of sucrose in which cells are suspended. These cells have been shown to behave as ideal osmometers, that is, to show an inverse dependence of cell volume on the osmolarity of the suspending medium (R. N. McElhaney, personal communication). Since sucrose is a non-permeating substance (123), a linear relationship would verify the validity of the swelling rate assay of permeation. For measuring absorbance, a Zeiss PM QII spectrophotometer and M4 QIII monochrometer equipped with a thermostatted cell compartment and built-in magnetic stirrer was used with a 2 cm path length cell. For some

determinations a water-jacketed cuvette was used, which was custom built by Acadian Instruments Ltd., Don Mills, Ontario, Canada. Cells were suspended in 200mM sucrose, and the swelling was initiated by rapidly adding 0.05 or 0.1 ml of this suspension to 4.5 ml or 7.5 ml of a 200mM solution of permeant in the cuvette while stirring. The transmittance of light was continuously recorded on a Beckman model 1005 10 inch recorder, connected to the spectrophotemeter through an adjustable ballast potential which allowed a 1mV input to the recorder to be matched to a 10mV output so that the full-scale chart deflection read from 50% to 60% transmittance. Initial slopes of the curves of % transmittance *vs* time and initial values of % transmittance were obtained from the chart and these were converted to a swelling rate with the dimensions $\{1/(1/A)\} \times \{d(1/A)/dt\}$ in $(1/\text{hsec})$[1] by the following calculation:

$$\frac{1}{(1/A)} \cdot \frac{d(1/A)}{dt} \text{ in } (1/\text{hsec}) = \frac{d(\%T)}{dt} \text{ in } (1/\text{min}) \times \frac{43.43}{\%To\,(2-\log \%To)\,60}$$

where A=Absorbance at 450nm, %T=% Transmittance at 450nm, %To=initial % Transmittance.

Cells were grown with elaidic acid (18:1t), oleic acid (18:1c), or linoleic acid (18:2cc) plus the appropriate amount of palmitic acid (16:0) in the presence or absence of cholesterol, and swelling rates in D-glucose and in

---

[1]The rate of change of reciprocal absorbance is divided by (1/A) to normalize small differences in initial absorbance. 1 hsec (hecto-second) = 100 sec.

erythritol were determined at various temperatures. Swelling rates were also determined in the same way using a variety of other sugars, D-glucose analogs, and polyhydroxy compounds as permeants. In some cases various high-energy compounds or inhibitors were present in the permeant solutions, in the cell suspensions, or in both. Where concentrations of permeant other than 200mM were used, osmotic balance was maintained by the addition of sucrose. In order to determine the effect of pH on swelling rates with glucose and erythritol, the cell suspensions and the permeant solutions were made up using the following buffers at a concentration of 25mM as solvents: formic acid/NaOH, pH=4.0; acetic acid/NaOH, pH=5.0; hydroxylamine hydrochloride/NaOH, pH=6.0 or 7.0; tris/HCl, pH=7.0, 7.28, 7.43, 7.60, 7.78, 8.0, or 8.35; glycine/HCl, pH=9.0; and D,L-alanine/HCl, pH=10.0.

Photomicrography

Unfixed suspensions of cells in growth medium or in 200mM sucrose were photographed with Kodak No. 4166 Royal X Pan film (ASA=1250), using an American Optical Series 20 microscope equipped with a high intensity quartz-iodine illuminator, a No. 1067 lens and shutter assembly, a No. 1055 cut film camera back and a No. 1066 Photostar exposure meter. Photographs were made using phase contrast with the 100X oil-immersion objective. The illuminator was

set on maximum intensity without filters and a shutter speed of 1/30 or 1/60 sec was used. A stage micrometer, ruled in divisions of 0.01mm was photographed to determine the final magnification on the photograph. To determine the diameters of cells, several photographs were chosen and every focussed cell on the print was measured, using a 7X magnifier with a built in 10mm scale, graduated in tenths of a mm.

Differential thermal analysis

Differential thermal analysis was carried out on a DuPont 900 Thermal Analyzer using glass macro tubes with glass beads as a reference material. Analyses were done at the highest instrumental sensitivity at heating rates of 3–10 C° per min. Cooling rates of up to 10 C° per min could be obtained by circulation of nitrogen gas, chilled by passage through a copper coil immersed in liquid nitrogen, through the differential thermal analysis cell. Membranes were prepared by osmotic lysis of cells in distilled water and collected by centrifugation in a Beckman L2-65B ultracentrifuge at 30,800Xg for 60 min. The pellet was resuspended in distilled water and centrifuged again at 110,000Xg for 60 min, then the packed membranes were transferred to a DTA sample tube using a Pasteur pipet. This sample tube was spun at top speed for 3 min in an International Clinical Centrifuge to insure that all air bubbles were removed and that the membranes were tightly

packed. Aqueous dispersions of column-purified total membrane lipid were prepared by adding a 4-fold excess (w/w) of distilled water to a thin film of lipid, previously dried overnight under vaccuum, followed by vortexing with several glass beads. This suspension was added to sample tubes and packed by centrifugation before analysis in the same manner as the intact membranes.

Radioisotope tracer flux experiments

Cell suspensions and permeant solutions were made up using tris-buffered Bacto-Tryptose solutions (pH=8.2) containing 4g/l of fatty acid-poor BSA, or 10mM tris-HCl or potassium phosphate, pH=7.4, containing 10mM MgCl2 plus sucrose or NaCl to a tonicity of 150 to 300 mosM[1]. Cells were harvested in late log phase (Absorbance at 400nm = 0.5-1.0) by centrifugation for 20 min at 7000Xg in a Sorvall RC-2B or RC-3 centrifuge, then washed 3-4 times in the buffer used in the experiment before carrying out permeability measurements. "Quench" solutions for stopping permeation contained 0.15mM phloretin dissolved in the buffered saline solution used for suspending the cells, or in 100mM MgSO4 plus 10mM tris, pH=7.5. To measure flux rates, cell suspension was added at zero time to radioactively labelled permeant solution, or <u>vice versa</u>, in

[1]Osmolarity = Molarity X number of independent particles produced per molecule in solution.

a water-jacketed test tube maintained at the desired temperature . Aliquots of the reaction mixture were taken at the desired times, using either a Gilson Pipetman or a Fisher Scientific No. 13-687 automatic pipet, and added to 3 ml of ice cold quench solution. The volume dispensed by the automatic pipet was determined by measuring the absorbance at 600nm of a solution made by dispensing a standardized solution of buffalo black 10B into 10 ml of water. The quenched aliquots of reaction mixture were immediately filtered on 47mm diameter, 0.45 or 0.65 micron millipore filters at 15 psi negative pressure and the filters were washed with four 3 ml aliquots of ice cold quench solution. They were then folded and placed in scintillation vials while still wet. After drying at room temperature overnight, then in a 110° oven for 30 min, 10 ml of toluene-Omnifluor were added to each vial for radioactivity counting. Further details of individual experiments are given in the figure legends.

Binding measurements

Binding of [^{3}H]-phloretin to A. laidlawii was measured by equilibrium dialysis, using Bel Art model 260 1 ml micro dialysis cells. To one side of each cell was added 0.6 ml of A. laidlawii suspension in 145mM sucrose, 10mM $MgSO_4$, 20 mM tris, pH=7.5. The suspension had an absorbance at 400nm of 23. The other sides of the cells contained 0.6 ml of

[^{3}H]-phloretin in buffer, with unlabelled compound added to bring the final phloretin concentration after equilibration across the membrane to 10, 30, 56.7, or 120 micromolar. Dialysis was carried out at room temperature on a horizontal shaker for 2 hr in duplicate in the presence and absence of 50mM D-glucose. The attainment of equilibrium within this time was verified by adding labelled phloretin to one side of a dialysis cell, then monitoring radioactivity present in each side *vs* time in the absence of *A. laidlawii*. At the end of the dialysis period, duplicate 0.2 ml aliquots were taken from each side of each cell and dried on 2.3 cm Whatman No. 3 filter discs, then counted in 10 ml of toluene-Omnifluor after drying at room temperature overnight, then at 110°C for 30 min. The specific activities of the [^{3}H]-phloretin solutions were determined by counting on Whatman filter discs. Cell suspension was added to the filters containing aliquots from the non-cell sides of the dialysis membranes or to those with [^{3}H]-phloretin only in order to make any radioactive quenching due to the *A. laidlawii* cells reproducible.

To measure [^{3}H]-phlorizin binding, cells were separated from the suspension by centrifugation. This gave data equivalent to those obtained by dialysis. Binding assays were carried out in 1 cm X 7.5 cm Kimax tubes. To each tube were added: 0.4 ml of cell suspension (absorbance at 400nm = 74.2) in growth medium without added BSA, penicillin, or

glucose; 0.2 ml of [^{3}H]-Phlorizin in growth medium; and 1.0 ml of unlabelled phlorizin such that its final concentration was 0.033, 0.15, 0.50, 1.50, or 5.0mM. After mixing the contents of the tubes, duplicate 0.1 ml aliquots were taken onto 2.3 cm Whatman No. 3 filter discs. The cells were then separated from the medium by centrifugation at 12,000Xg for 5 min and duplicate 0.1 ml aliquots of each supernatant counted on Whatman filters. One tube contained [^{14}C]-sucrose instead of [^{3}H]-phlorizin in order to assess the significance of the excluded volume which was occupied by the cells themselves. Each determination was done in duplicate, in the presence or absence of 50mM D-glucose.

Analytical procedures

Protein assays: Protein concentration of cell suspensions was determined using the sensitive Biuret method described by Koch and Putnam (124), using Sigma Fraction V crystalline BSA as a standard. Duplicate aliquots of cell suspension containing approximately 4 Absorbance units[1] of cells were added to 30 ml corex centrifuge tubes, and suspending buffer was added to 0.25 ml. To each sample was added 0.75 ml of Biuret buffer (4.6 M NaOH, 1.5% (as NH3) NH4OH) or copper reagent (2.5g $CuSO_4 \cdot 5H_2O$ per 1 of Biuret buffer). The samples were mixed by vortexing, then heated for 5 min in a

[1] 1 Absorbance unit is defined as 1 ml of suspension having an Absorbance at 400nm of 1.

boiling water bath. After adding 4 ml of buffer or copper reagent and vortexing again, samples were incubated at room temperature for 30 min, then absorbance at 330nm was determined. The protein concentration is proportional to absorbance in the copper reagent minus absorbance in the buffer.

Determination of phospholipid phosphorus: After quantitative lipid extraction by the method of Bligh and Dyer (108) and purification on silicic acid columns, the lipid extract from about 0.4 Absorbance units of cells was added to a 2.5 cm X 20 cm tube[1] and the solvent was removed under a stream of nitrogen[2]. Phosphorus was then estimated by the method of Chen et al (125). Four drops of concentrated sulfuric acid were added to the residue and the tube heated with a Bunsen burner until white fumes just appear. Two drops of 72% perchloric acid were then added and the samples heated until clear. After adding 3.95 ml of water plus 4 ml of freshly prepared reagent C (0.5% ammonium molybdate tetrahydrate plus 2% ascorbic acid in 1.2 N sulfuric acid), tubes were covered with parafilm and incubated at 37°C for 90 min. Absorbance at 820nm was read on the Spectronic 20 colorimeter, using the red filter and red-sensitive photomultiplier.

---

[1]This large size of tube was found to be most convenient to prevent loss of material by spattering during ashing.
[2]Incomplete removal of solvent results in explosion during the oxidation step.

Cholesterol assay: The total dry weight of lipid in a silicic acid-purified extract was determined by adding extract to a tared tube, then removing solvent under a stream of nitrogen and under vacuum overnight and reweighing. Cholesterol content was assayed by a modification of the Liebermann-Burchard method (126). The reagent was prepared by mixing together 150 ml of glacial acetic acid, 300 ml of acetic anhydride, 50 ml of 96% sulfuric acid and 10g of anhydrous sodium sulfate in an ice-water bath, allowing the flask to come to room temperature and shaking until the sodium sulfate dissolved. The solvent was evaporated under nitrogen from lipid containing approximately 0.25mg of cholesterol in a screw-capped glass tube with a teflon cap liner. After adding 0.1 ml of acetic acid and shaking, then 5 ml of reagent, the tube was capped, shaken vigorously and placed in a 25°C water bath. The absorbance at 632nm was read on the Spectronic 20 colorimeter after 25–30 min.

Extraction of labelled compounds for chromatography: After incubation of cells with the radioactive metabolite for the desired length of time, an aliquot of the reaction mixture containing about 80 absorbance units of cells was added to 18 ml of ice cold quench solution and immediatly filtered on 6–47mm, 0.65 micron millipore filters under 15 psi negative pressure. The filters were quickly washed four times with 3

ml aliquots of ice cold quench, then frozen in liquid nitrogen. The frozen filters were added directly to 20 ml of boiling distilled water and boiled for 5 min, then the extracts were transferred to 125 ml flasks, rinsing the filters twice with 5 ml of water. These extracts were lyophilized to dryness, then the residues were taken up in 2 ml of water and transferred to 1.8 X 15 cm test tubes, rinsing with 1 ml of water and again lyophilized to dryness. The final residue was taken up in 0.15 ml of water with warming, then 0.05 ml of acetic acid was added and precipitated material was centrifuged out with the clinical centrifuge at top speed for 5 min. As much of the supernatant as possible, avoiding excess salt (about 0.05 ml), was spotted on Whatman No. 1 filter paper for chromatography. The amount of insoluble radioactive material was determined by washing the filters under the tap, then folding and inserting them in a scintillation vial. After drying overnight in vacuo, radioactivity in the filters was counted in 15 ml of toluene-Omnifluor.

Fatty acid analysis: The fatty acid compositions of whole lipid extracts of cells were routinely determined by gas-liquid chromatography after acid-catalyzed transesterification, as described in Chapter II. Chromatography was carried out on a 6 ft by 1/4 in column of 10% diethyleneglycol succinate on Anakrom 60/70 AS mesh using helium as the carrier gas with a flow rate of 75cc/min. The

temperature program consisted of an initial 4 min isothermal period at 160°C, followed by an increase to 200°C at 4 C°/min and a sufficient isothermal period at 200°C to elute all material from the column.

III Results

Relationship of absorbance to cell volume

The validity of the assay of permeation by rate of change of reciprocal absorbance is dependent on the behavior of the cells as ideal osmometers whose volume is inversely proportional to the osmolarity of the medium, and on the linear relationship between cell volume and reciprocal absorbance. As shown in figure 1, these relationships are borne out by the response of absorbance to variation in the sucrose concentration of the suspending medium. The slight departure of the plot from linearity at low sucrose concentrations (40mM) may be due to cell lysis.

Effects of inhibitors on swelling rates

The effects on swelling rates in solutions of various permeants by the inhibitors tannic acid, or phlorizin, or its aglucone, phloretin (figure 2) present in the permeant solutions are shown in Table I. These results are not strictly comparable to each other, because differences in fatty acid composition and temperature will produce

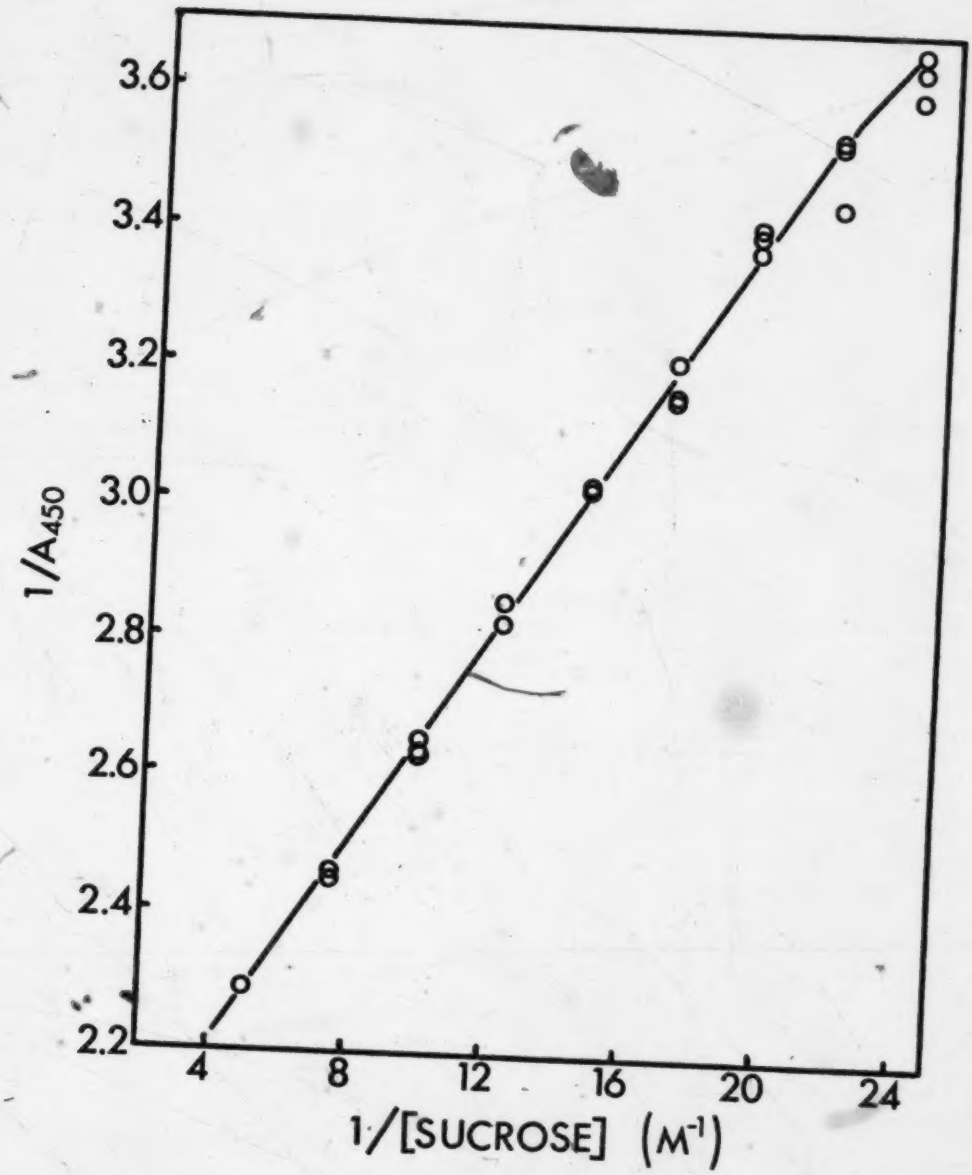

Figure 1. Effect of Osmolarity on Absorbance.
0.05 ml of a suspension in 200mM sucrose of Acholeplasma grown in the presence of 16:0+18:1t were added in triplicate to 5 ml of sucrose at various concentrations and the absorbance of the resulting suspensions at 450nm read with the Spectronic 20 colorimeter.

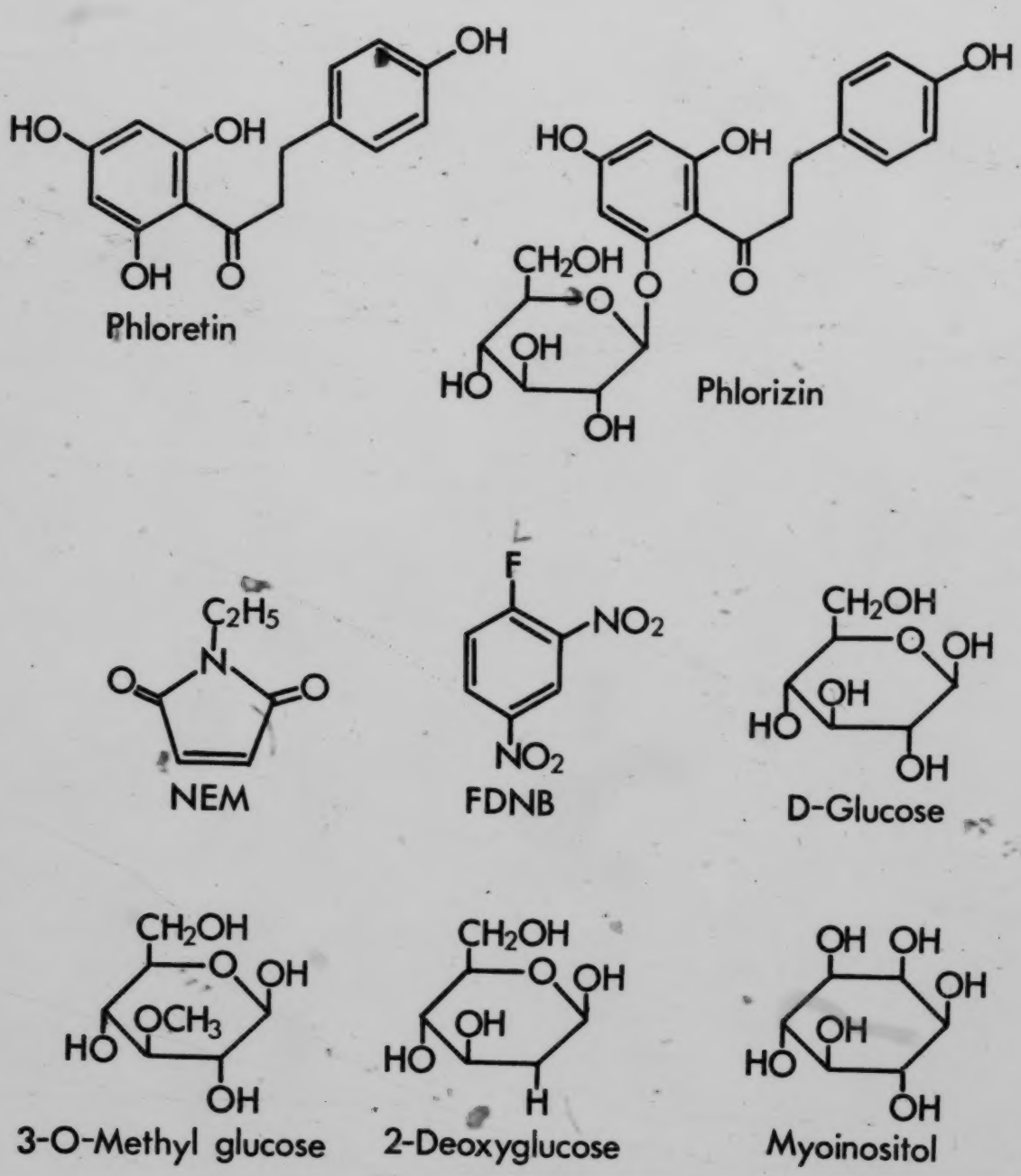

Figure 2. Chemical Structures of Transport Inhibitors and of Permeants.
1-Fluoro-2,4-dinitrobenzene can react with amino, sulfhydryl, imidazole, and phenolic hydroxy groups.

TABLE I

EFFECTS OF INHIBITORS ON SWELLING RATES

Permeant and Assay Conditions	0.01% Tannic acid	0.2mM Phloretin	0.2mM Phlorizin	2.0mM Phlorizin
D-Glucose 25°C 16:0/18:1t	100%	100%	43%	100%
Erythritol 25°C 16:0/18:1t	38%	13%	18%	13%
Xylose 37°C 16:0/18:1c + cholesterol	100%	73%	52%	——
Ribose 37°C 16:0/18:1c + cholesterol	53%	46%	34%	——
D-Glucose 41°C 16:0/18:2cc	——	97%	——	——
Sorbitol 41°C 16:0/18:2cc	——	44%	——	——
2-Deoxyglucose 25°C 16:0/18:2cc	——	85%	39%	85%
3-O-Methyl-D-Glucose 16:0/18:1c 31°C	——	71%	——	——
Myoinositol 31°C 16:0/18:1c	——	67%	——	——

The left-hand column gives the permeant used (present at 200mM), the temperature at which swelling was measured, and the fatty acids that were added to the growth medium. The body of the table is percent inhibition.

different degrees of membrane lipid fluidity, thus the relative contributions of passive flux to the swelling measured may vary. Nevertheless, it is clear that both phloretin and phlorizin cause a very significant inhibition of swelling in D-glucose, but have little effect on erythritol flux. It is also seen that phloretin is a more potent inhibitor than its glucoside, phlorizin, and that tannic acid seems to cause some general disruption of the membrane which affects all permeabilities. The inhibition of D-glucose- and L-glucose- induced swelling of Acholeplasma laidlawii are shown as a function of phloretin concentration in figure 3. The fluxes of both permeants are inhibited by micromolar concentrations of phloretin, with L-glucose showing a greater susceptibility. If it is assumed that D- and L-glucose permeate the cells via the same pathway, this greater susceptibility of L-glucose permeation to phloretin inhibition indicates some antagonistic effect of D-glucose on the inhibition. Such an antagonistic effect is also seen by the effect of D-glucose concentration on phloretin inhibition of glucose flux, shown in figure 4. These results cannot be explained by a simple competition by phloretin with glucose for binding to the transport site, since unlabelled D-glucose bound to this site would then be expected to inhibit uptake of [^{14}C]-D-glucose as effectively as the same amount of phloretin bound to the site.

The effects on swelling rates in glucose and erythritol

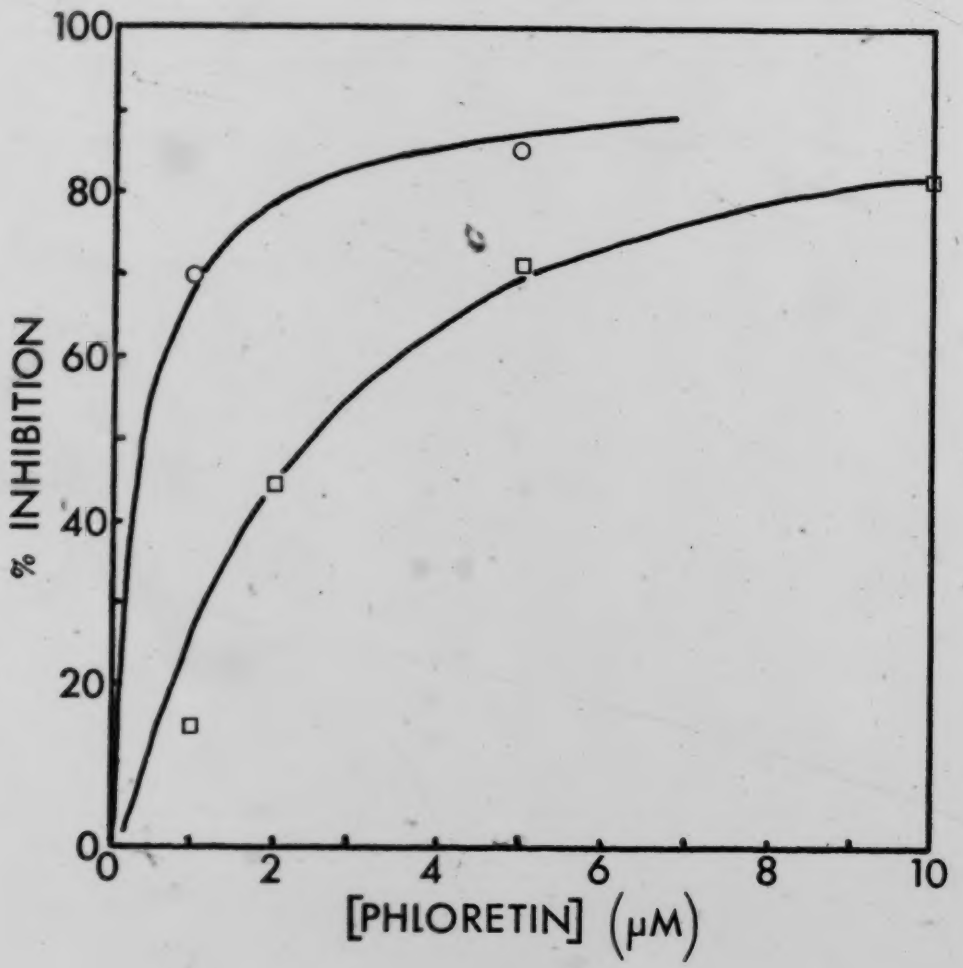

Figure 3. Inhibition of Swelling of A. laidlawii in D- or L-Glucose by Phloretin
Cells grown in the presence of palmitic plus oleic acids were suspended in 200mM sucrose and 0.05 ml of this suspension added to 7.5 ml of 200mM D- or L-glucose at 31°C containing phloretin to determine swelling rates. Each determination was done at least in triplicate.
o–o, L-glucose; □–□, D-glucose.

Figure 4. Effect of 0.001mM Phloretin on Uptake of [^{14}C]-D-Glucose.
A. laidlawii cells grown in the presence of palmitic plus oleic acids were incubated at 25°C with a fixed amount of [^{14}C]-D-glucose plus unlabelled D-glucose to 1mM or 10mM in the presence or absence of 0.001mM phloretin. Aliquots were then taken and washed on Millipore filters with ice cold quench solution at the times shown.

(a) CPM in cells vs time: □–□, 1mM D-glucose; ■–■, 1mM D-glucose plus 0.001mM phloretin; o–o, 10mM D-glucose; •–•, 10mM D-glucose plus 0.001mM phloretin.

(b) Difference between cpm in absence and presence of phloretin vs time
□–□, 1mM D-glucose; o–o, 10mM D-glucose.

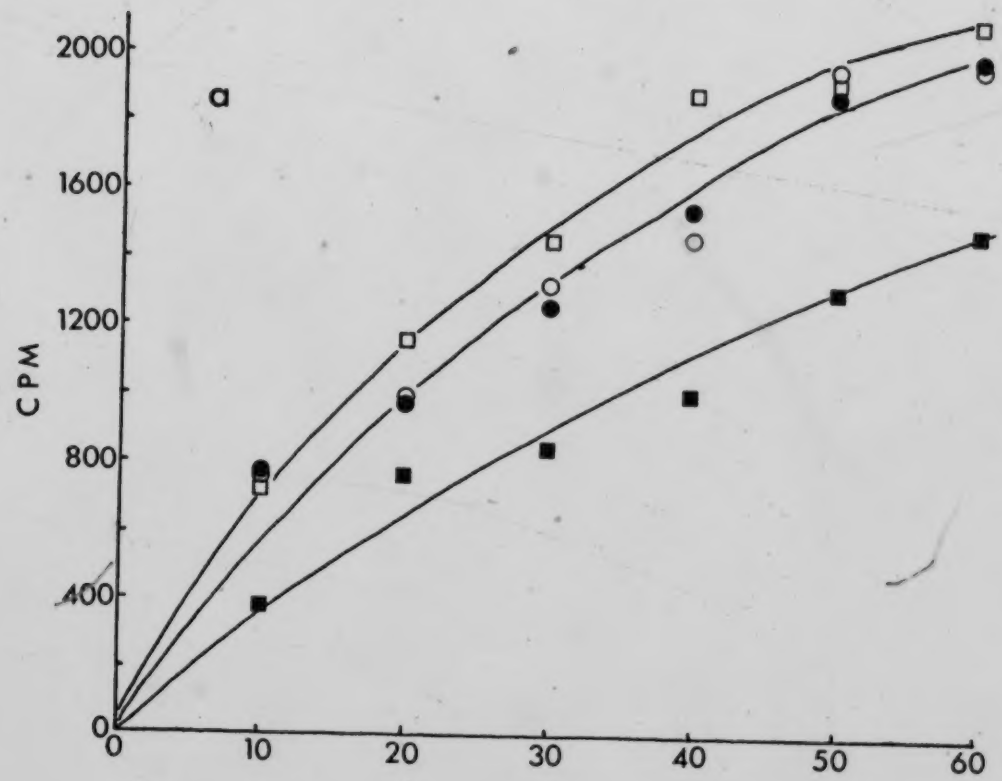
a
CPM
2000
1600
1200
800
400
0
0
10
20
30
40
50
60

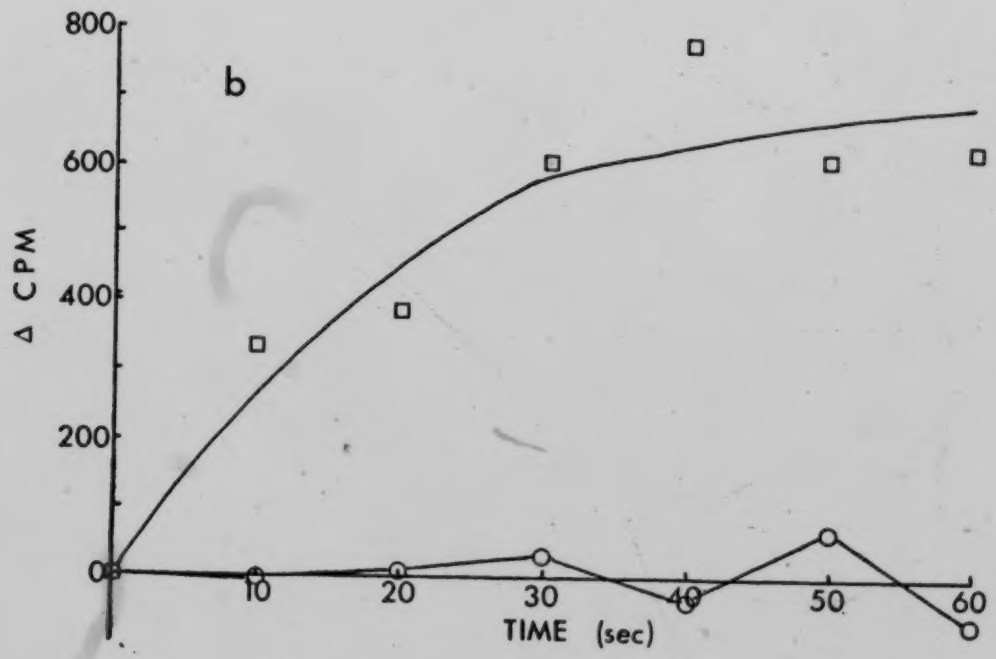
b
Δ CPM
800
600
400
200
0
10
20
30
40
50
60
TIME (sec)

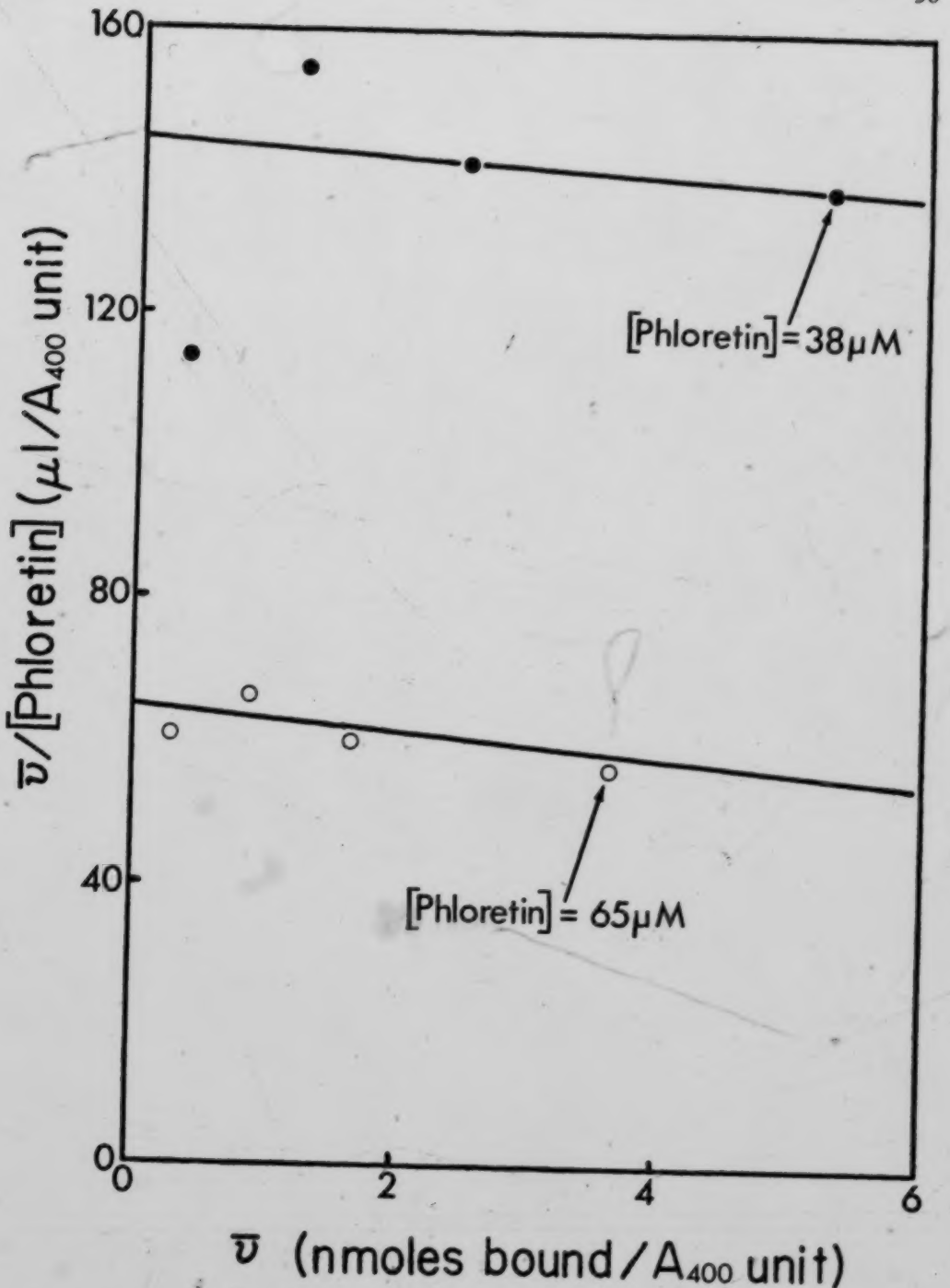

Figure 5. Scatchard Plot of Phloretin Binding to Acholeplasma laidlawii.
Cells grown in the presence of palmitic plus oleic acids were dialyzed against [^{3}H]-phloretin for 2 hr in the absence (•–•) and presence (o–o) of 50mM D-glucose until equilibrium was attained.

of treating cells with trypsin, pronase, 1-fluoro-2,3-dinitrobenzene (DNFB), and N-Ethyl-maleimide (NEM) are shown in table II.

The binding of [^{3}H]-Phloretin to Acholeplasma laidlawii is shown plotted according to the method of Scatchard (127) in figure 5. This plot is based on the law of mass action expressed as:

$$\bar{\nu}/c = k(n-\bar{\nu})$$

where $\bar{\nu}$=average number of small ligands bound per large molecule, c=concentration of free ligand, k=association constant and n=number of binding sites per large molecule. The intercept on the abcissa gives n and the slope is -k.

While the precision of the data plotted here does not allow an exact calculation of the number of binding sites, the plots extrapolate to a value of the order of 10^7 to 10^8 binding sites per cell, using a value of 10^9 cells per absorbance unit of suspension (128). The association constants appear to be 1 to 2 mM^{-1}. This extremely weak binding and apparent large number of sites can be interpreted as a partitioning of phloretin into the membrane rather than binding at discrete saturable sites. Although a direct comparison of association constants or numbers of binding sites is not possible, it is evident from the relative positions of the regression lines that binding of phloretin to the cells is reduced by the presence of glucose. About 2/3 of the phloretin added to the assay

TABLE II

EFFECTS OF PROTEIN MODIFICATION ON SWELLING RATES

	% of Control Swelling Rate	
Treatment Used	D-glucose	erythritol
0.01mg/ml trypsin[1]	34%	63%
1mg/ml pronase[1]	99%	226%
0.5mM DNFB[1] [3]	27%	56%
2.0mM NEM[2] [4]	72%	—

[1]Cells grown in the presence of palmitic plus oleic acids were suspended on 200mM sucrose, then treated for 30 min at 30°C with 0.01mg/ml of TPCK trypsin, 1mg/ml of pronase, or 0.5mM DNFB. The reactions were terminated by the addition of 200mg of BSA to the 5.5 ml reaction mixtures, then cells were washed twice in a large volume of 200mM sucrose before measuring swelling rates at 30°C.

[2]Cells grown in the presence of palmitic plus linoleic acids were suspended in 200mM sucrose, then treated for 20 min at 20°C with 2.0mM NEM. The reaction was terminated by the addition of 3.0mm 2-mercaptoethanol and cells were washed in a large volume of 200mM sucrose before measuring swelling rates at 37°C.

[3]DNFB = 1-Fluoro-2,4-dinitrobenzene.

[4]NEM = N-ethylmaleimide.

mixture is associated with the cells in the absence of glucose, vs less than 1/2 in the presence of glucose. These values are obtained from the concentrations of free phloretin present at the points where 0.12mM phloretin was added to the assay mixture (shown on figure). A similar type of experiment carried out with [^{3}H]-phlorizin showed no evidence of any binding of this substrate to cells.

Effect of pH on Swelling Rates

The effect of pH on swelling rates in erythritol or glucose is shown in figures 6 and 7. A rise in swelling rates with both permeants is seen as pH increases within a physiological range, however glucose seems to show a more pronounced discontinuity between pH=7.6 and pH=7.8 than is observed with erythritol.

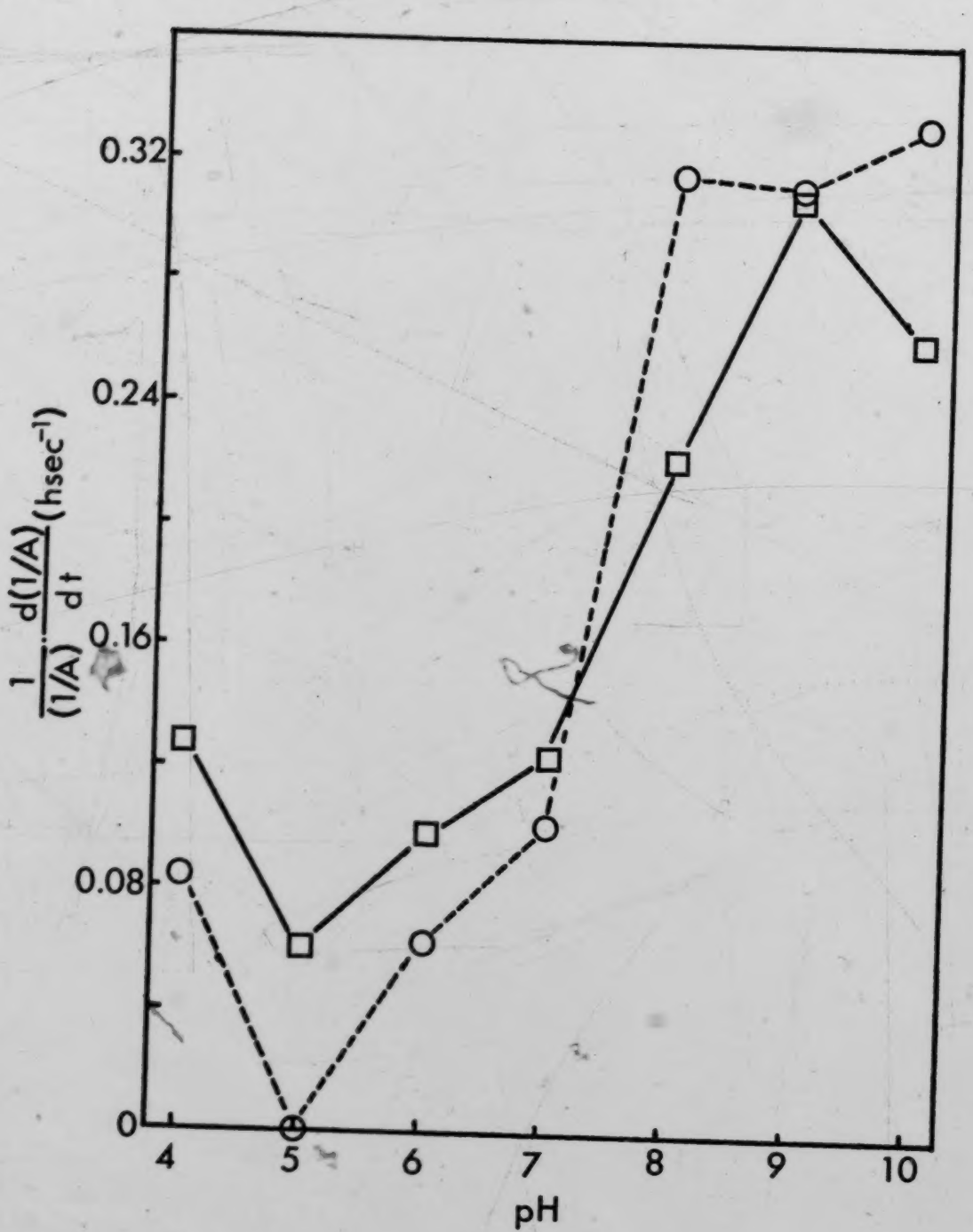

Figure 6. Swelling Rates vs pH
Cells grown in the presence of palmitic plus elaidic acids were used to determine swelling rates at 20°C in buffered solutions of 200 mM erythritol (□–□) or glucose (○–○).

Figure 7. Swelling Rates *vs* pH.
Cells were grown in the presence of palmitic plus oleic acids, and swelling rates were measured at 30°C. Each point is the mean of at least three determinations. The error bars represent range. 7(a)=erythritol; 7(b)=D-glucose.

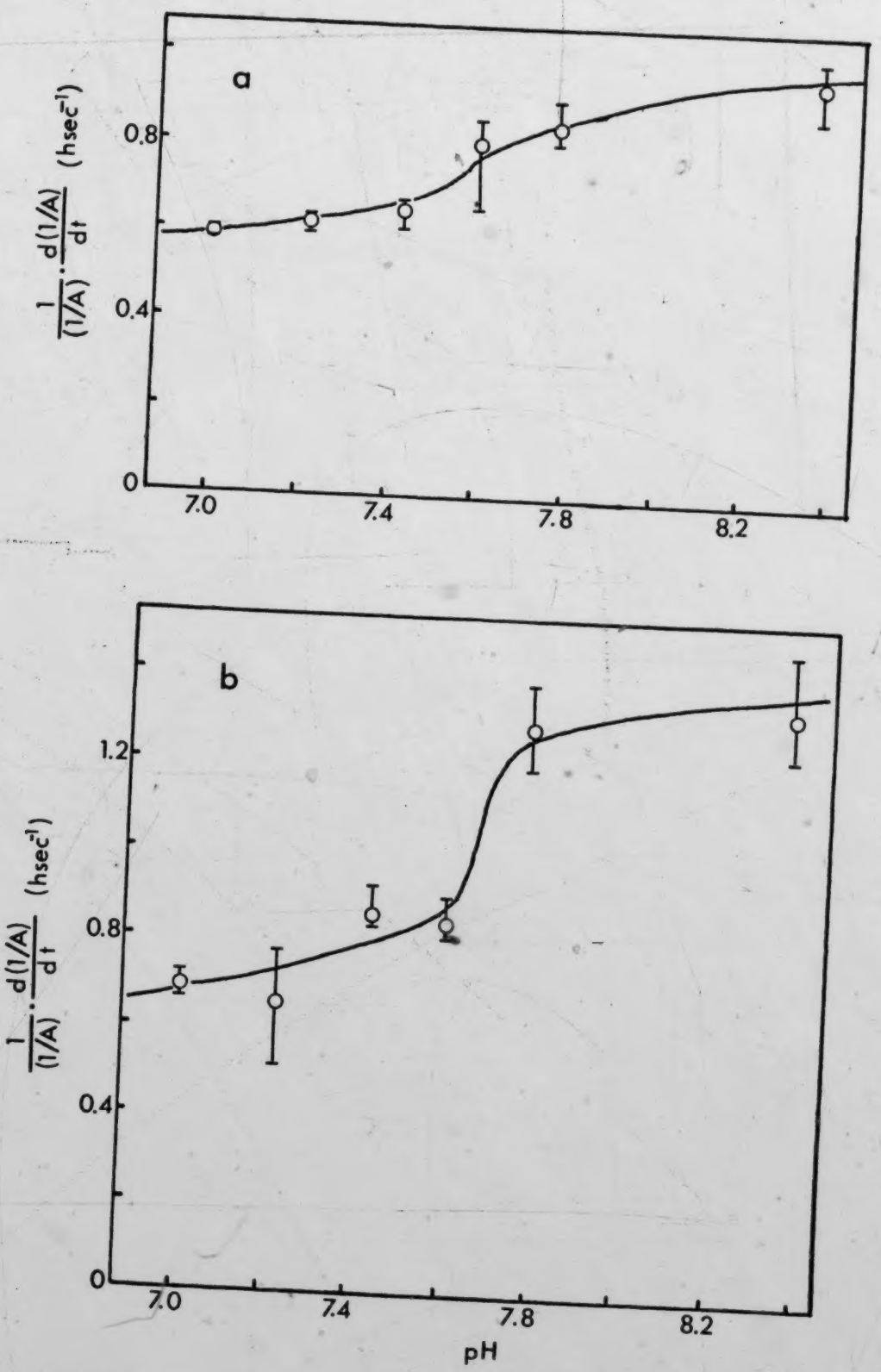
a
b
$\frac{1}{(1/A)} \cdot \frac{d(1/A)}{dt}$ (hsec^{-1})
0
0.4
0.8
1.2
7.0
7.4
7.8
8.2
pH

Effect of glucose concentration on swelling rates

The swelling rate of cells grown in the presence of palmitic plus linoleic acids was determined at 37°C as a function of D-glucose concentration to see if saturability could be detected. The results are shown in figure 8.

The fact that this plot does not pass through the origin is evidence for some saturable process involved in swelling, but the points do not seem to be approaching a plateau, even at 200mM glucose. This may indicate an extremely low affinity of glucose for the carrier, or more likely, it may be due to two superimposed parallel pathways for glucose uptake, one being saturable, the other not.

Effect of high temperature on swelling rates

Figure 9 shows the relationship of swelling rates in erythritol and in D-glucose to temperature, up to 60°C. A clear-cut difference in behavior is seen between erythritol and glucose. The decrease in swelling rate in D-glucose occuring above 45°C can be interpreted as being due to inactivation of some heat-labile component of the transport system and is evidence for the uptake of glucose by a non-passive mechanism. The subsequent increase at 60°C may be due to passive flux which becomes significant at this high temperature.

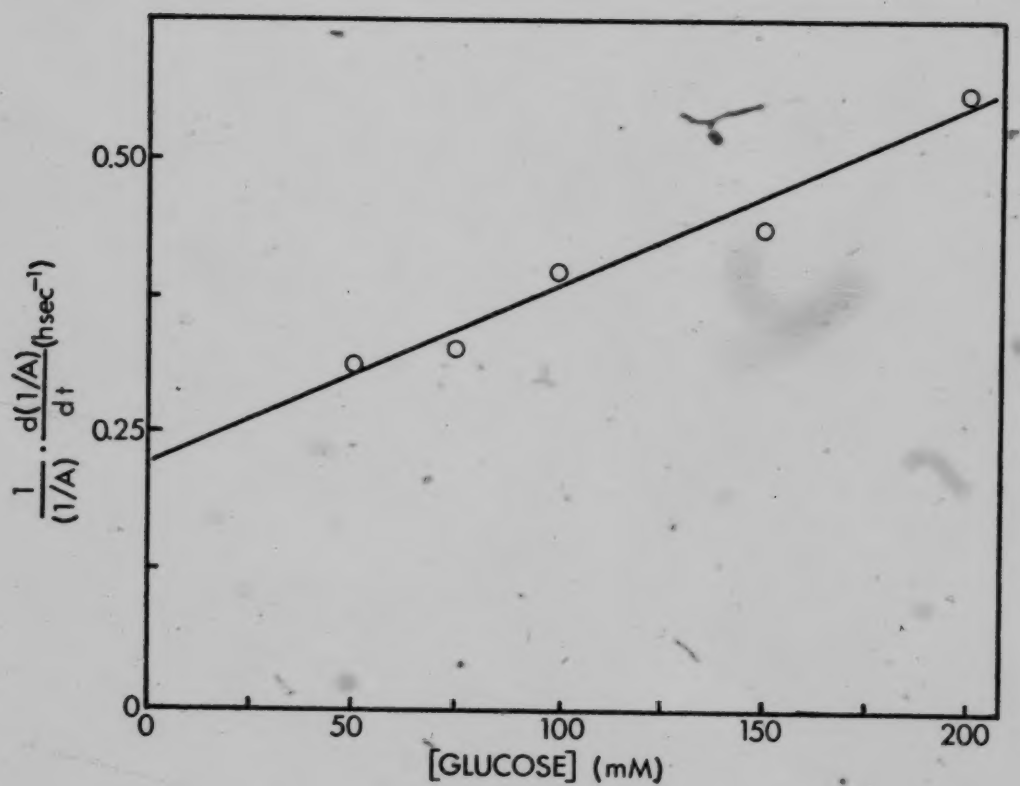

Figure 8. Swelling Rate vs Glucose Concentration. Cells suspended in 200mM sucrose were added to D-glucose at various concentrations, with sucrose added to maintain tonicity at 200mosM

Passive permeation of liposomes by glucose

To determine whether the permeation of cells by glucose is faster than would be predicted for passive diffusion through the lipid bilayer, a comparison was made of swelling of cells and of liposomes in erythritol and in glucose. Permeation of liposomes can be assumed to occur by passive

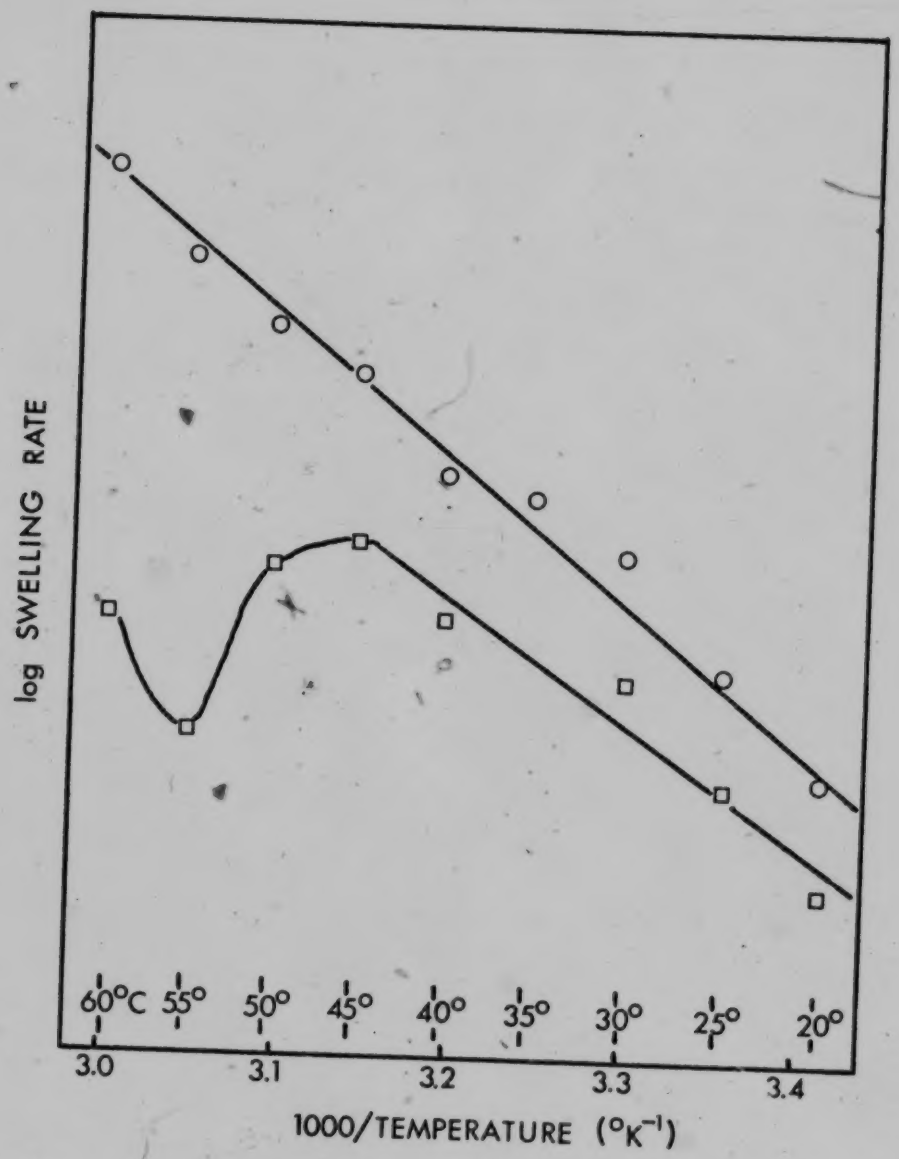

Figure 9. Inactivation of Glucose Transport by High Temperature.
The logarithm of swelling rate in D-Glucose (□–□), or in erythritol (o–o) is plotted vs reciprocal of temperature (Arrhenius plot).

diffusion, since there is no protein present which could function as a carrier. The results are shown in figure 10. At 25°C, glucose permeates cells at about 2/3 the rate that erythritol does. The apparent swelling rates of liposomes are lower than those of cells because of differences in their optical properties. Nevertheless, it is apparent that glucose permeation of liposomes at 25°C is not 2/3 the rate of erythritol permeation. At 45°C, where liposomes in erythritol show an apparent swelling equivalent to whole cells at 25°C, the swelling of liposomes in glucose is still undetectable. Therefore glucose permeates cells at a faster rate than would be predicted for passive diffusion through the lipid bilayer, via some mechanism which is not available in liposomes.

Effect of fatty acid composition on swelling rates

Cells were grown in the presence of palmitic acid (16:0), plus either elaidic (18:1t) oleic (18:1c), or linoleic acid (18:2cc) so that an approximately equimolar amount of each supplemented fatty acid was incorporated into the membrane. For each experiment fatty acid compositions of the cellular lipids were analyzed by gas-liquid chromatography. Table III shows a typical analysis. In the cases where cholesterol was also added to the growth medium, no change in the patterns of fatty acid incorporation was seen. Cholesterol was incorporated to a level of about 10%

Figure 10. Swelling Rates of <u>Acholeplasma laidlawii</u> and Derived Liposomes in Glucose and Erythritol. Cells were grown in the presence of palmitic plus oleic acids and a portion was suspended in 200mM sucrose and used to assay swelling rates. Lipids were extracted from the remainder, purified, and used to form liposomes, which were also used to measure swelling rates.

•–•, □–□ = erythritol; •–•, o–o = glucose

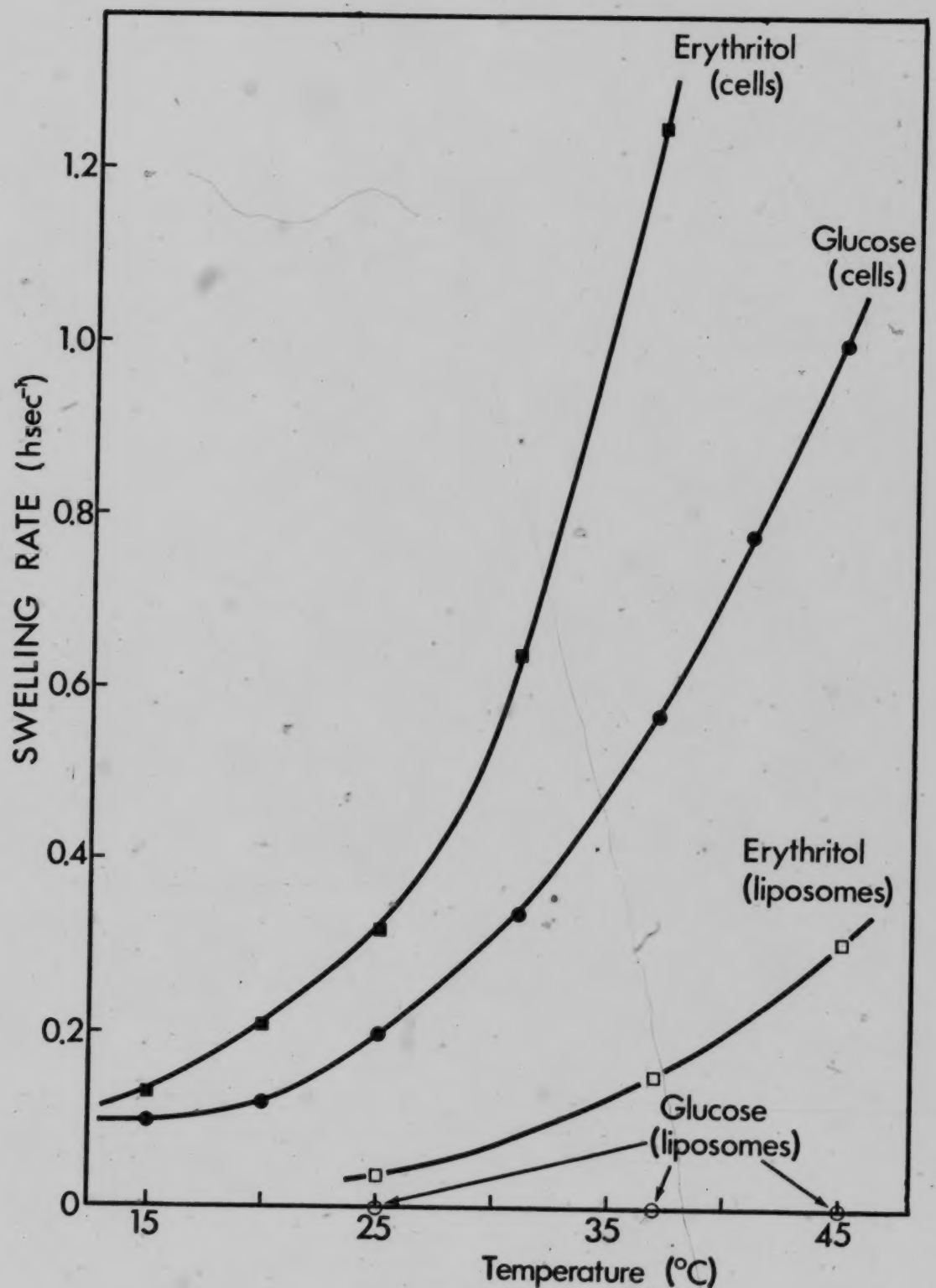
Erythritol
(cells)
Glucose
(cells)
Erythritol
(liposomes)
Glucose
(liposomes)
SWELLING RATE (h sec⁻¹)
1.2
1.0
0.8
0.6
0.4
0.2
0
15
25
35
45
Temperature (°C)

TABLE III

FATTY ACID COMPOSITION OF *ACHOLEPLASMA LAIDLAWII* LIPIDS

IDENTITY	FATTY ACIDS ADDED AS SUPPLEMENT		
	16:0/18:1t[1]	16:0/18:1c[2]	16:0/18:2cc[3]
12:0	6.0	4.3	2.2
13:0	0.9.	0.5	0.1
14:0	8.0	6.8	4.4
15:0	0.6	0.8	0.6
16:0	40.1	38.7	32.5
17:0	0.1	0.1	0.2
18:0	—	0.7	1.4
18:1t	44.2	?[4]	—
18:1c	?[4]	46.0	3.5
18:2	0.1	1.2	44.4
20:1	—	1.0	—
20:2	—	—	10.5

[1] 0.06mmoles 16:0 + 0.07mmoles 18:1t per 1 of medium

[2] 0.055mmoles 16:0 + 0.075mmoles 18:1c per 1 of medium

[3] 0.02mmoles 16:0 + 0.11mmoles 18:2cc per 1 of medium

[4] 18:1c and 18:1t are not resolved by conventional GLC analysis so it is not possible to determine whether all the material in the peaks is the isomer designated.

of the dry weight of the total membrane lipid.

Figure 11 shows the effect of fatty acid composition on swelling rates of A. laidlawii in erythritol and in glucose. Each point on the graphs represents the mean of several experiments. The erythritol serves as a control to demonstrate that the passive permeability, and thus the fluidity of the bilayer, has actually been altered in the expected direction. The permeabilities to erythritol increase in the order 16:0/18:1t < 16:0/18:1c < 16:0/18:2cc, with cholesterol decreasing permeability in each case, exactly as would be predicted from the effects of these fatty acids on transition temperatures (10). The swelling rates in D-glucose increase in exactly the same order.

Arrhenius plots of swelling rates are all linear over the range of temperatures studied, with the single exception of cells grown with palmitic plus elaidic acids in the absence of cholesterol. These showed a change in slope occurring at about 25°C (figure 12). This temperature is within the range of the thermal phase transition of whole membranes or lipid extracts of cells grown in the presence of these fatty acids (See next section). The heats of activation for permeation above the transition temperature obtained from the Arrhenius plots are given in Table IV. There is no significant or systematic fatty acid composition-dependent variation of heat of activation for permeation of either compound. The values for glucose are

Figure 11. Effect of Membrane Lipid Composition on Swelling. Rates

Acholeplasma laidlawii cells were grown in the presence of the supplements identified on the figure, then harvested and resuspended in 200mM sucrose. The swelling rates were determined when aliquots of these suspensions were added to a much larger volume of 200mM erythritol (a), or 200mM D-glucose (b).

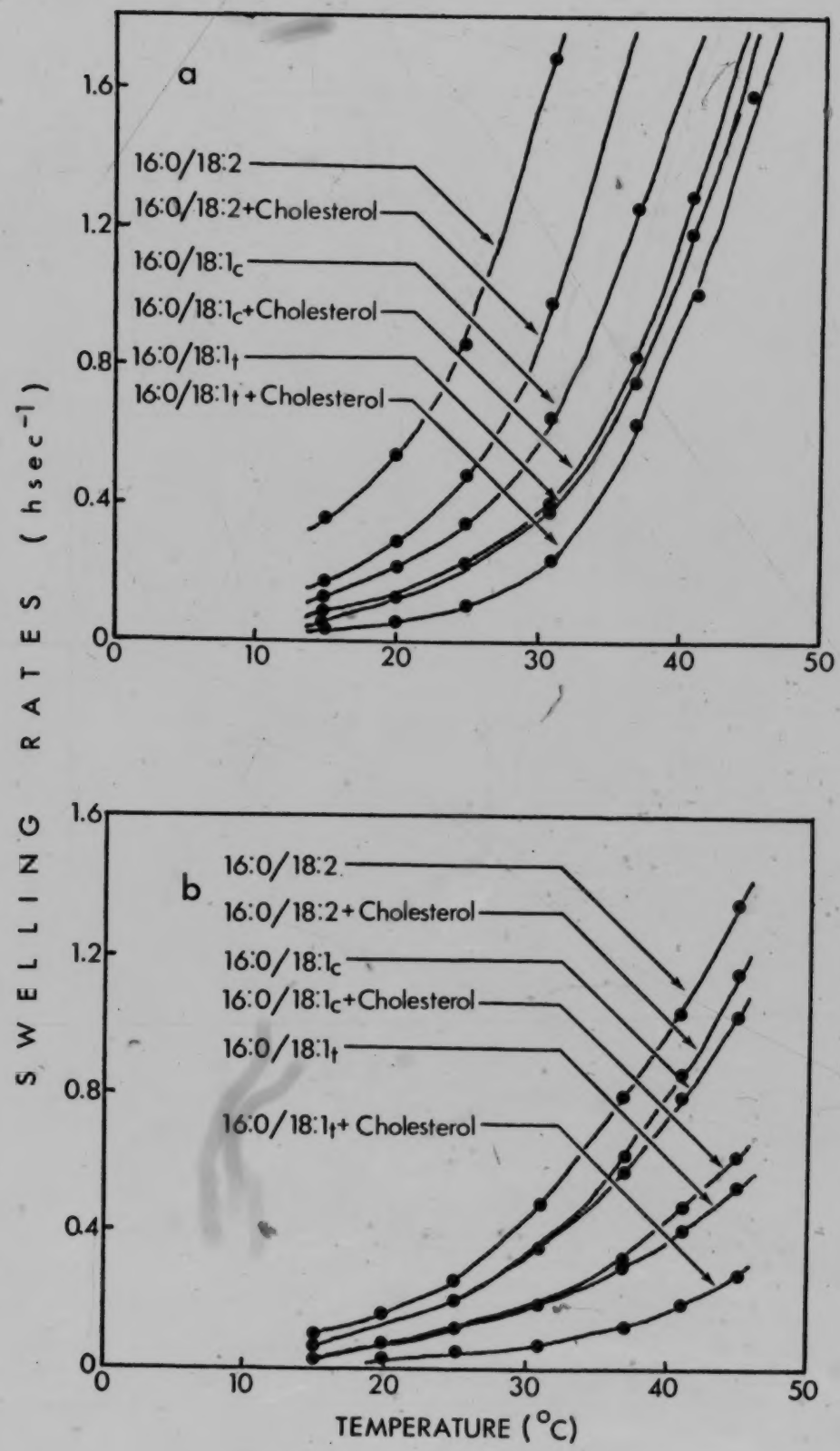
a
16:0/18:2
16:0/18:2+Cholesterol
16:0/18:1c
16:0/18:1c+Cholesterol
16:0/18:1t
16:0/18:1t + Cholesterol
b
16:0/18:2
16:0/18:2+Cholesterol
16:0/18:1c
16:0/18:1c+Cholesterol
16:0/18:1t
16:0/18:1t+ Cholesterol
SWELLING RATES (hsec⁻¹)
TEMPERATURE (°C)
0
0.4
0.8
1.2
1.6
10
20
30
40
50

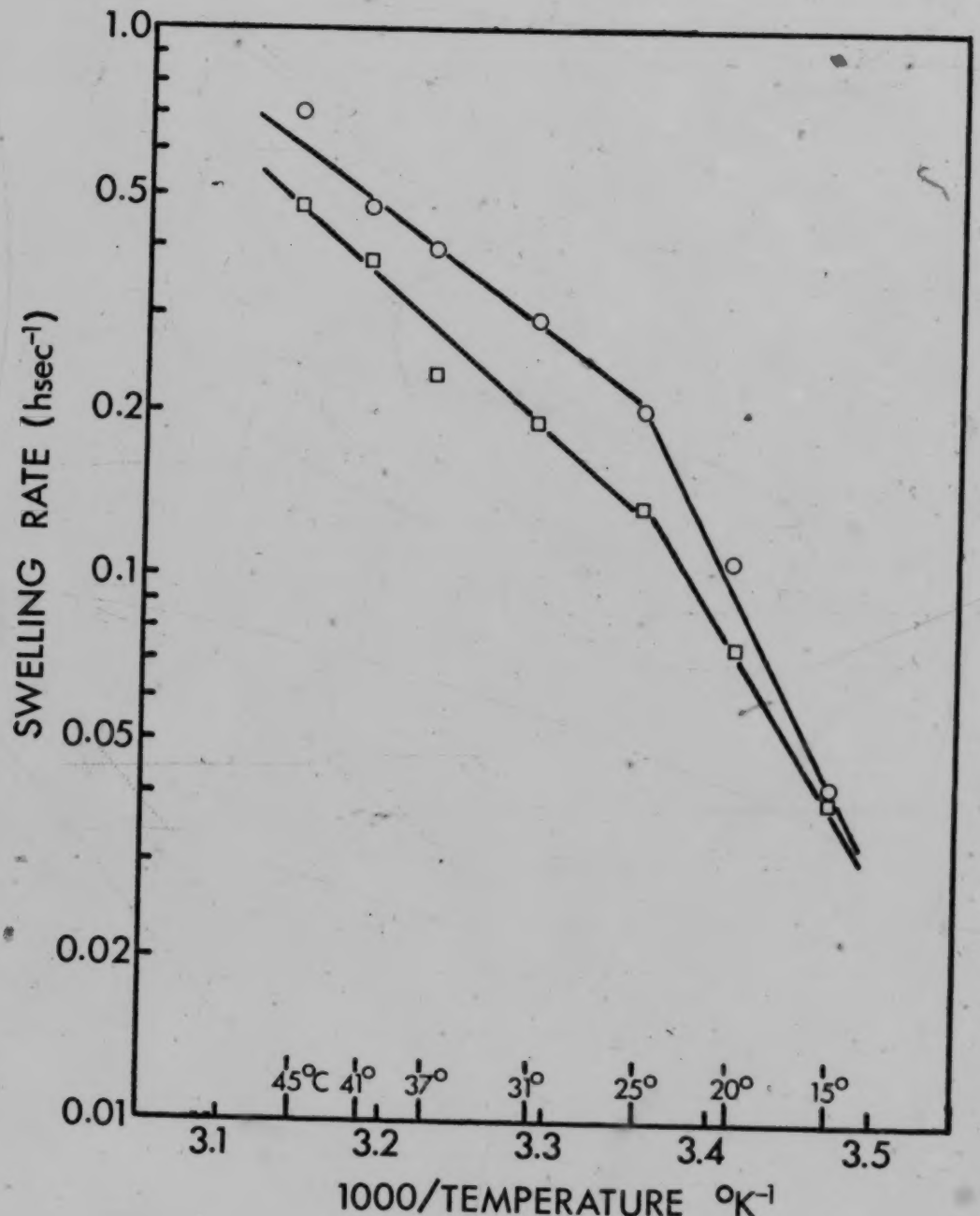

Figure 12. Arrhenius Plots of Swelling of 16:0/18:1t-Grown Cells

Acholeplasma laidlawii cells grown in the presence of palmitic plus elaidic acids, without cholesterol were harvested and resuspended in 200mM sucrose. Swelling rates were measured in 200mM solutions of permeant.
o—o, D-xylose; □—□, D-glucose.

TABLE IV

EFFECTS OF LIPID COMPOSITION ON HEATS OF ACTIVATION

ADDITIONS TO GROWTH MEDIUM	HEAT OF ACTIVATION (kcal/mole) ERYTHRITOL	GLUCOSE
16:0/18:1t	20.4	16.0
16:0/18:1t + cholesterol	21.4	16.2
16:0/18:1c	19.7	15.6
16:0/18:1c + cholesterol	20.1	16.1
16:0/18:2	18.5	16.6
16:0/18:2 + cholesterol	19.6	17.3
MEAN	19.0	16.3
STANDARD DEVIATION	0.9	0.3

significantly lower than would be predicted for passive permeation through the hydrocarbon region, based on other studies of glucose permeation of bilayers. Activation energies of 19–22 kcal/mole and 26–29 kcal/mole have been quoted for the passive efflux of D-glucose from sonicated, unilamellar phosphatidylethanolamine bilayer vesicles and multilamellar phosphatidylcholine bilayer vesicles, respectively (129,130).

Differential thermal analysis

The temperature-based thermograms from the differential thermal analysis of whole membranes and of extracted lipids

from cells grown in the presence of palmitic plus elaidic acids are reproduced in figure 13. The temperatures of onset and finish of the phase transitions are defined by the points where the traces first deviate from the baseline (arrows). The transitions of membranes and of extracted lipids, respectively, are from 13°C to 41°C with the peak at 29°C, and from 11°C to 46°C with the peak at 30°C. The discontinuity in Arrhenius plots of permeation seen with these cells lies within the transition and near the peak.

Effect of fatty acid composition on cell size

The morphology of A. laidlawii B cells is dependent on the fatty acids supplied in the growth medium. Cells whose membranes have a high Tm appear as single spheres, while those with more fluid membranes exhibit morphologies like a string of beads, or like filaments. Suspension of the cells in 200mM sucrose, which is hypotonic to the growth medium, transformed most of the cells in any culture to fairly uniform spheres, however it was necessary to demonstrate that the sizes of these spheres did not vary systematically with membrane fluidity. If it did, then apparent differences in swelling rates may arise artifactually from geometrical factors causing differences in light scattering or from the different surface area/volume ratios. The results of measurements made of photomicrographs of cell suspensions in sucrose are given in Table V. Although the standard

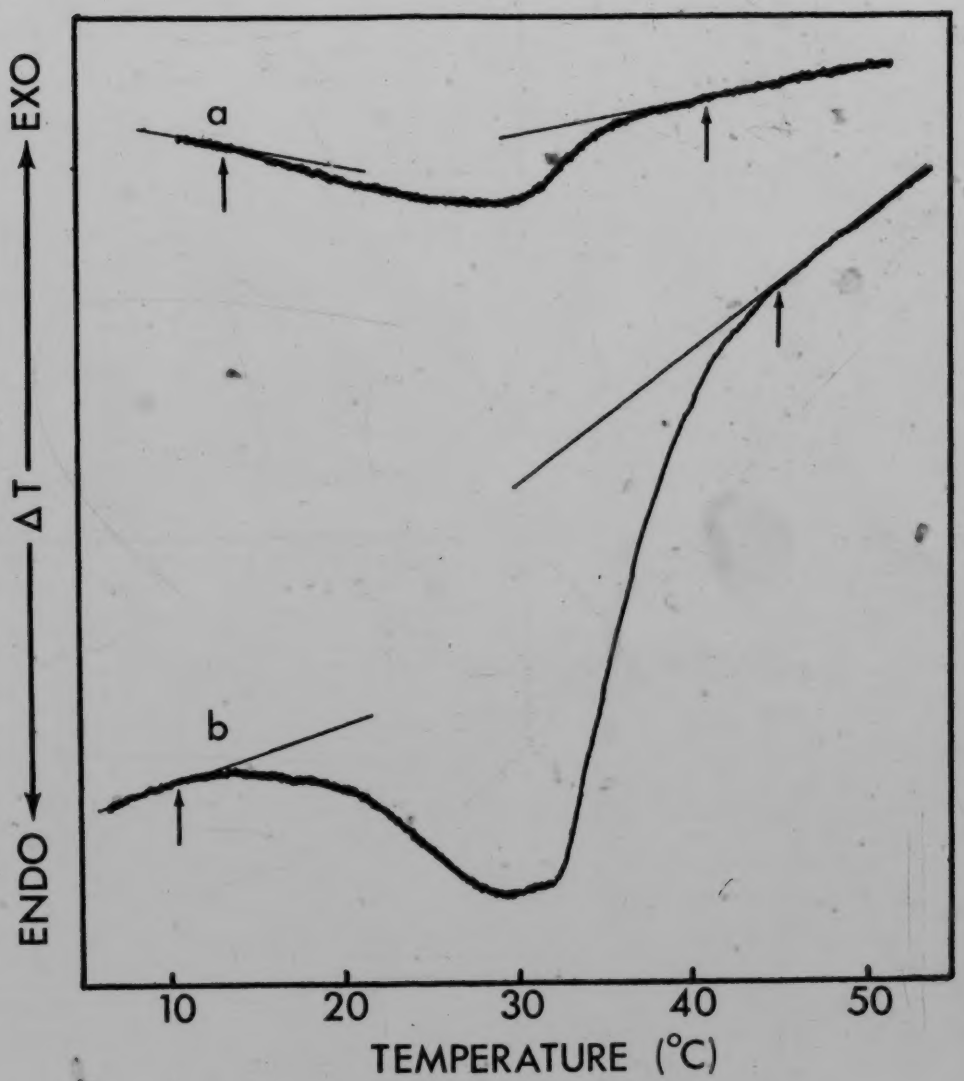

Figure 13. Differential Thermal Analysis of Membranes and Lipids from Cells Grown in the Presence of Palmitic plus Elaidic Acids.
Membranes and lipids were prepared and DTA run as described on page 40. Heating curves are shown here, at heating rates of 10°C/min.
a=membranes, b=lipids.

TABLE V

EFFECT OF MEMBRANE LIPID COMPOSITION ON CELL SIZE

Supplemented Fatty acids	Number of Measurements	Mean Diameter (microns)	Standard Deviation (microns)
16:0/18:1t+ cholesterol	203	0.579	0.170
16:0/18:1t	58	0.595	0.130
16:0/18:1c	308	0.474	0.118
16:0/18:2cc	190	0.508	0.109

deviations are large and the mean diameters are considerably different in some cases, no systematic alteration of cell size with membrane lipid fluidity is apparent. It was concluded that the effects of lipid composition on permeability are not artifacts due to varying cell size.

Metabolic fates of permeants

To determine whether permeation is the rate-limiting process for accumulation of label, or whether other factors play a role, it is necessary to know in what form the radioactively labelled permeants are present inside the cell. Therefore, cells were incubated with various labelled permeants under a variety of conditions, then radioactively labelled compounds were extracted and the products analyzed by paper chromatography as described in Chapter II and the

Methods section of this chapter. For chromatography of glucose and its analogs, solvent 28 (1M aqueous ammonium acetate, pH=5.0:95% ethanol 3:7 (v:v)), or solvent 36 (ethyl acetate:acetic acid:water 3:1:1 (v:v:v)) were used (131). For maltose, n-butanol: pyridine: water, 6:4:3 (v:v:v) was used (109). The results of chromatographic analyses using a number of labelled permeants under a variety of conditions are given in figures 14-20.

Figure 14 shows the effects of various enzyme inhibitors on the extent of metabolism of 1mM D-glucose after 90 sec at 30°C. Under these conditions, there is a significant conversion of glucose to other compounds, probably phosphates. It seems, however, that a large amount of unaltered glucose is present as well, so the rate limiting step for uptake of counts can not be readily assigned as would be the case if either metabolism were insignificantly slow, or so rapid that no free glucose was found.

Iodoacetic acid has been used to inhibit glucose metabolism and energy production in Mycoplasma gallisepticum and in Saccharomyces cerevisiae (123,132). Sodium azide, sodium cyanide, and sodium fluoride all inhibit thiomethyl-galactoside accumulation in E. coli, presumably by inhibiting energy-yielding metabolic steps (133). Sodium fluoride also shows some inhibition of sugar uptake, perhaps by depleting energy, in Mycoplasma gallisepticum, while

Figure 14. Effect of Inhibitors on D-Glucose Metabolism. Acholeplasma laidlawii cells were incubated for 90 sec at 30°C with 1mM [^{14}C]-D-Glucose in the presence of various inhibitors after a 10 min preincubation with the inhibitor being used. Cells were then filtered and washed with ice cold quench solution on Millipore filters, and the radioactive material extracted and chromatographed for 18 hr using solvent 28 (1M aqueous ammonium acetate, pH=5.0:95% ethanol, 3:7 (v:v)). The positions on the paper of standards are indicated on figure 14(a).

(a) o–o, control; Δ–Δ, 10mM NaCN; □–□, 10mM FDNB

(b) o–o, 10mM sodium azide (NaN3); □–□, 10mM NaF Δ–Δ, 10mM iodoacetic acid (IAA).

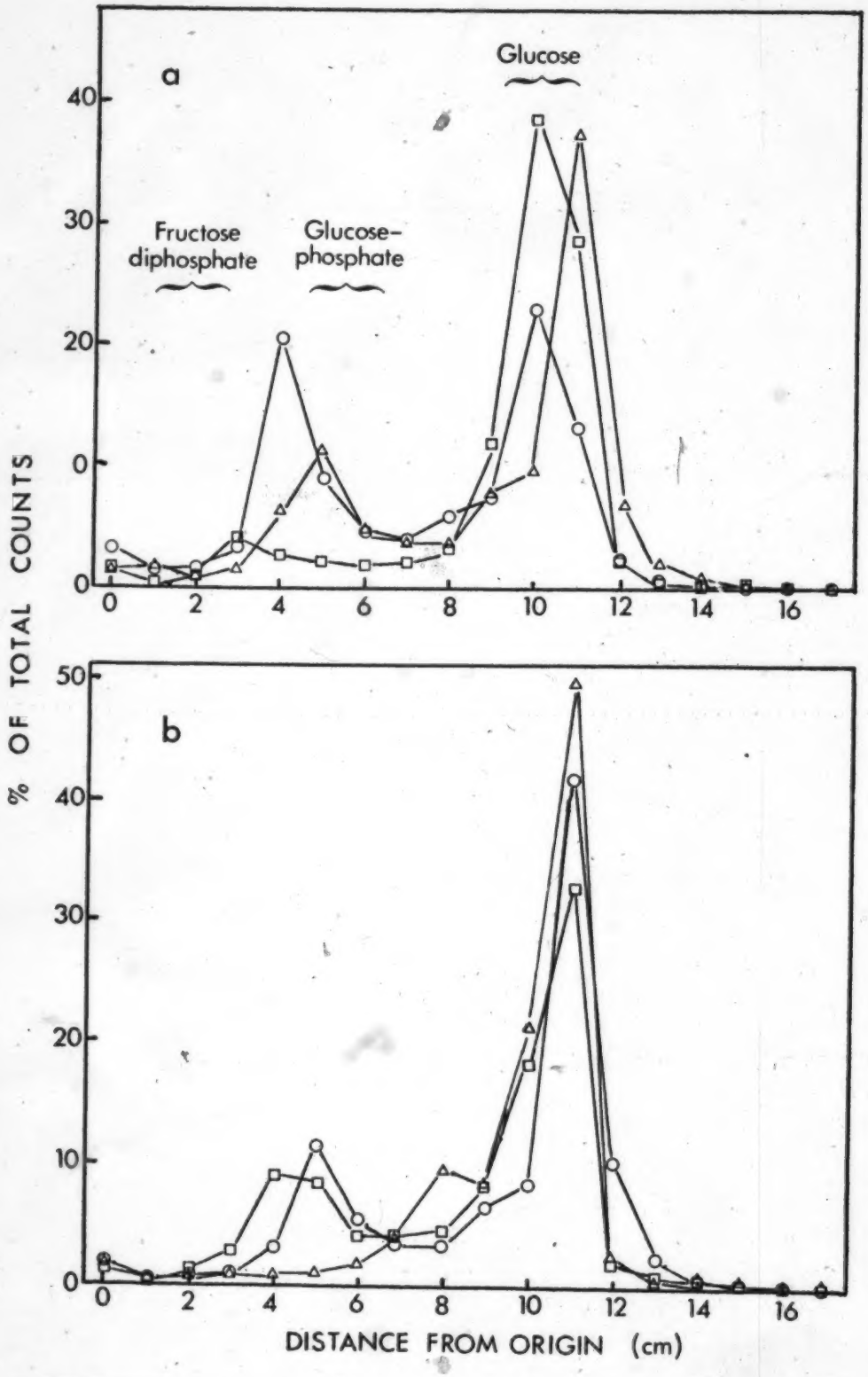
a
Glucose
Fructose diphosphate
Glucose-phosphate
40
30
20
0
0
2
4
6
8
10
12
14
16
b
50
40
30
20
10
0
% OF TOTAL COUNTS
DISTANCE FROM ORIGIN (cm)

sodium azide and potassium cyanide have no effect (123). DNFB (1-fluoro-2,4-dinitrobenzene) can react with amino, sulfhydryl, imidazole, and phenolic hydroxyl groups, and has been shown to inhibit glucose transport and anion uptake in red blood cells and L-glutamate uptake by rat liver mitochondria (134). Of these compounds, DNFB and IAA seemed to show a significant inhibition of glucose metabolism in A. laidlawii, while the other three inhibited to a much lesser degree.

Figure 15 shows the chromatographic pattern of radioactivity obtained from extracts of cells incubated in the presence of 0.02mM [^{14}C]-D-glucose at 37°C for various periods of time. This concentration is of the same order of magnitude as the glucose concentrations used by Tarshis et al. in studying transport in A. laidlawii (120). It is obvious that, at this concentration, a large portion of the glucose inside the cells is metabolized, at times as early as 1 minute, to some component whose Rf matches that of glucose-6-phosphate, and that the proportion in this form remains fairly stable up to 30 minutes, so the chromatographic pattern obtained seems to represent a steady state. There is also a significant proportion of counts at the position where standard glucose is found. These may or may not represent unaltered glucose.

Figure 16 shows the pattern obtained by chromatography of extracts of cells incubated for 1 min at 37°C in the

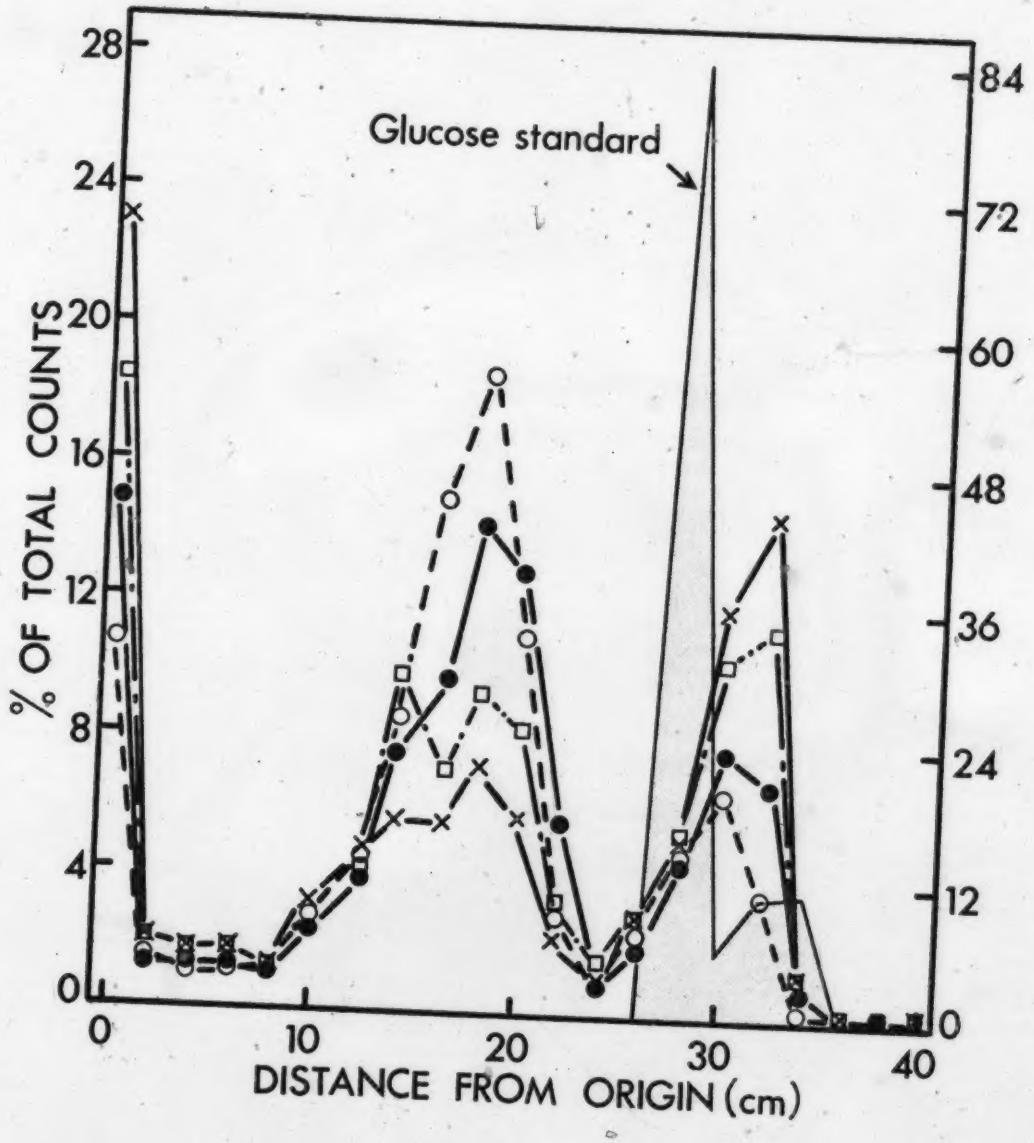

Figure 15. Metabolism of 0.02mM D-Glucose by Acholeplasma laidlawii.
Cells were incubated at 37°C with 0.02mM [^{14}C]-D-glucose for various periods of time. Aliquots were removed, washed on Millipore filters with ice cold quench solution, then extracted and chromatographed for 18 hr with solvent 28. The shaded peak is standard D-glucose.
o–o, 1 min; •–•, 10 min; □–□, 20 min; x–x, 30 min.

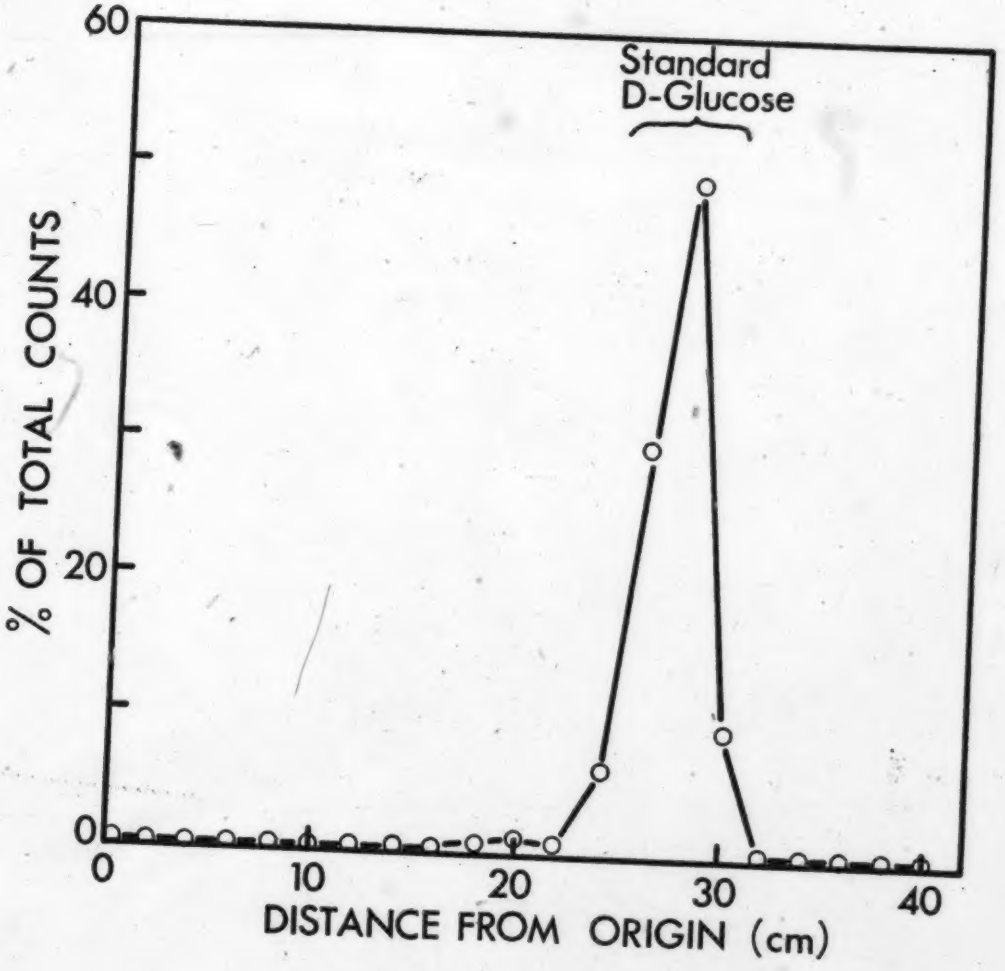

Figure 16. Metabolism of 200mM D-Glucose by Acholeplasma laidlawii.
Cells were incubated at 37°C for 1 min in the presence of 200mM [^{14}C]-D-glucose, then washed on Millipore filters with ice cold quench solution, extracted and chromatographed for 18 hr using solvent 28.
The position of the D-glucose standard is indicated by the bracket on the figure.

presence of 200mM [^{14}C]-D-glucose. At this concentration the proportion of glucose taken up by the cell which is metabolized is negligibly small. These conditions are similar to those used in the swelling rate assays of permeability, and these data indicate that metabolism of glucose does not interfere with the measurement of transport by swelling rates.

Figures 17 and 18 are the chromatographic patterns obtained after incubation of [^{14}C]-L-glucose or 2-deoxyglucose with A. laidlawii at 30°C. Figure 19 is the pattern with [^{14}C]-3-O-methyl glucose after incubation for 3 min at 30°C.

2-Deoxyglucose appears to be transported by human erythrocyte ghosts (135), and to be transported and phosphorylated, but not further metabolized by Chlorella vulgaris (136), adipose cell ghosts (137), mammalian tissue culture cells (138), and cultured chick embryo fibroblasts (139). On the other hand, it was oxidized to 2-deoxygluconic acid rather than phosphorylated by Pseudomonas aeruginosa (140), and was not phosphorylated by cell-free extracts of A. laidlawii which were able to phosphorylate glucose (119). L-Glucose is not transported in erythrocytes (141,142), mouse pancreatic beta cells(143), or membrane vesicles from rat adipose tissue (144), but may be a substrate for the D-glucose transport system in rat small intestine brush border membrane cells, having a lower affinity for carrier

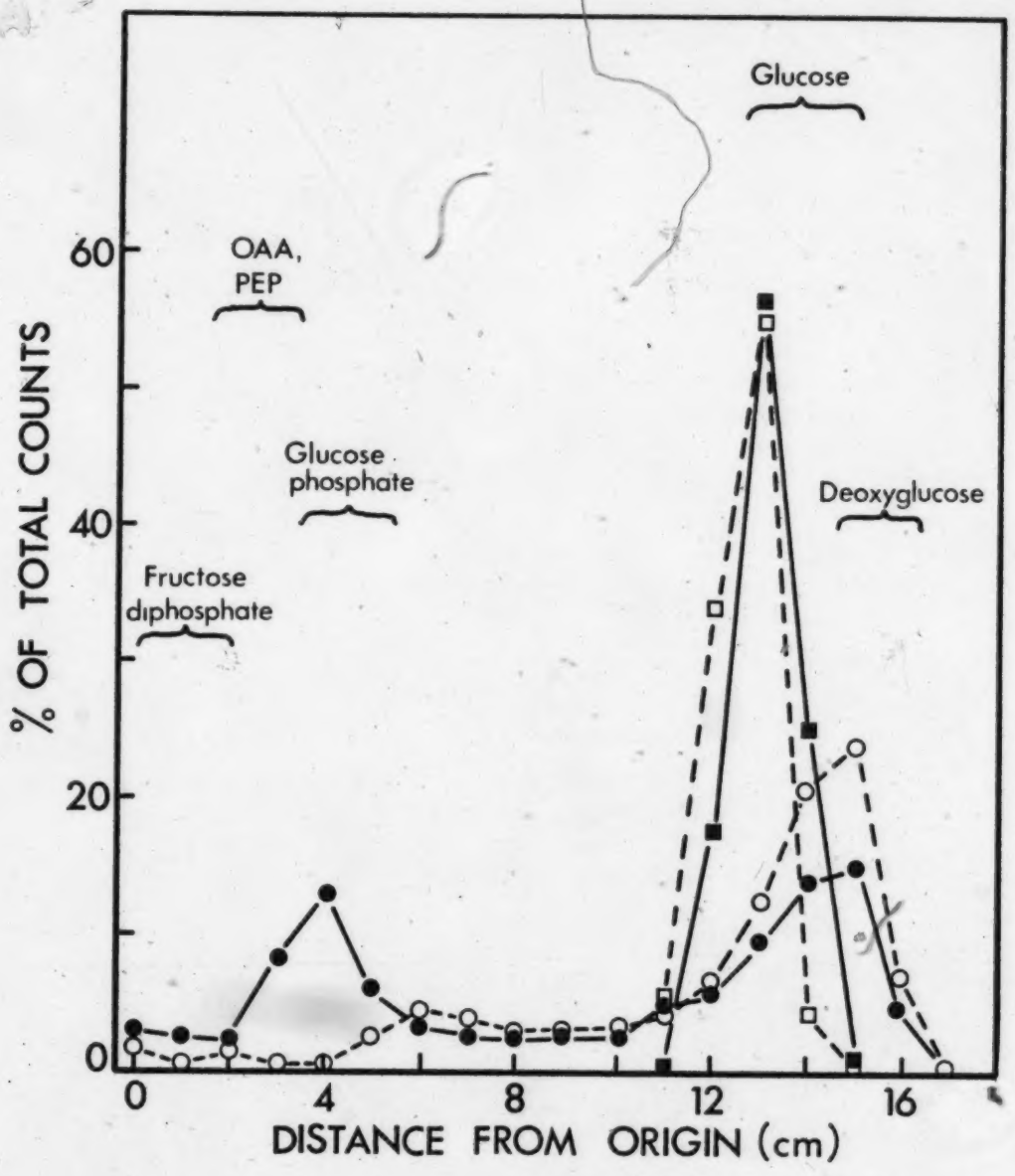

Figure 17. Metabolism of L-Glucose and 2-Deoxyglucose by Acholeplasma laidlawii.
Cells were incubated at 30°C in the presence of labelled sugar, then washed on Millipore filters with ice cold quench, extracted, and chromatographed for 18 hr using solvent 28. The positions of standard compounds are indicated by brackets.
o–o, •–• = 2-deoxyglucose; □–□, ▪–▪ = L-glucose
Open symbols = 40 sec incubation,
closed symbols = 10 min incubation.

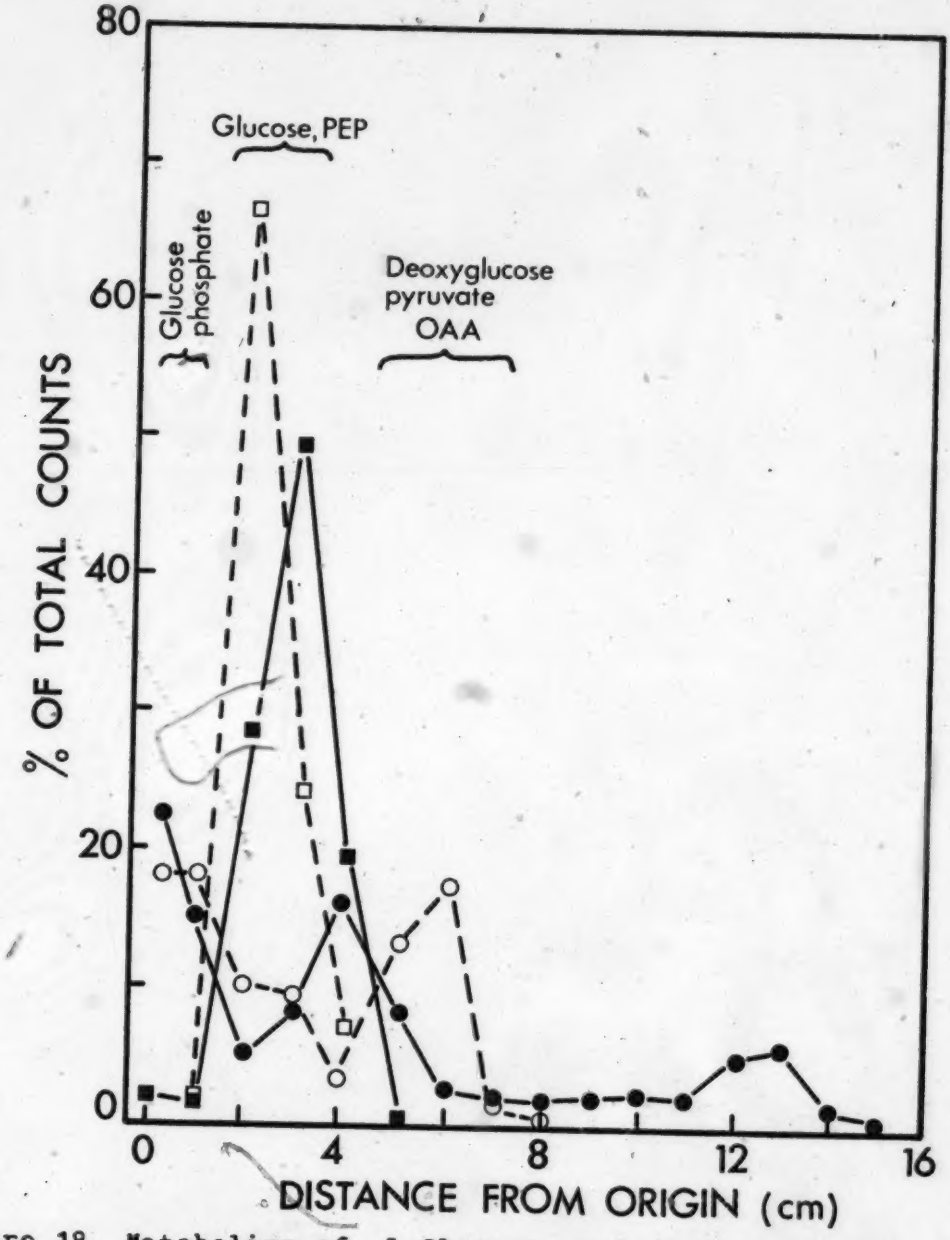

Figure 18. Metabolism of L-Glucose and 2-Deoxyglucose by Acholeplasma laidlawii.
Cells were incubated at 30°C in the presence of labelled sugar, then washed on Millipore filters with ice cold quench solution, extracted, and chromatographed for 18 hr using solvent 36. The positions of standard compounds are indicated by the brackets.
o–o, •–• = 2-deoxyglucose; □–□, ■–■ = L-glucose
Open symbols = 40 sec incubation,
closed symbols = 10 min incubation.

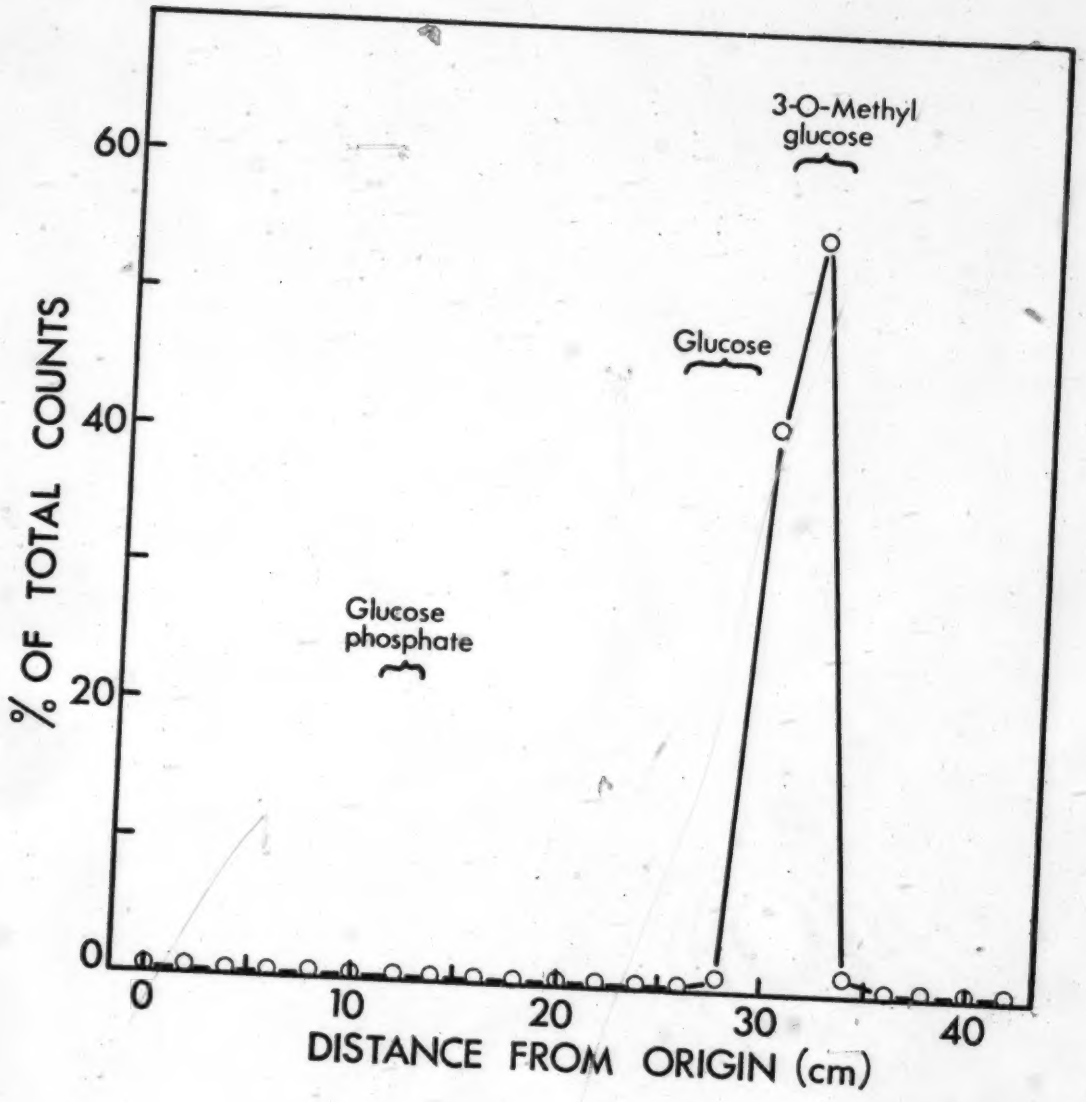

Figure 19. Metabolism of 3-O-Methyl-D-Glucose by Acholeplasma laidlawii. Cells were incubated for 3 min at 30°C in the presence of labelled 3-O-Methyl-glucose, then washed on Millipore filters with ice cold quench solution, extracted, and chromatographed for 18 hr, using solvent 28. The position of standard 3-O-methyl-glucose is indicated by the bracket.

than the D-isomer (145). 3-O-Methyl glucose is transported but not phosphorylated by beef erythrocytes (146), Chlorella vulgaris (136), chick embryo fibroblasts (139), and human lymphocytes (147). The data in figures 17 and 18 indicate that L-glucose is not metabolized by A. laidlawii, but that 2-deoxyglucose is phosphorylated, as well as undergoing some other reaction. Figure 18 shows radioactivity derived from 2-deoxyglucose occurring at a position with an Rf which is greater than that of either 2-deoxyglucose itself, or that expected for the phosphate. This reaction seems rather slow, however, as the only material other than 2-deoxyglucose occurring at 40 sec has an Rf similar to that expected for the phosphate; the more mobile material is seen only after 10 minutes. Figure 19 shows that 3-O-methyl glucose is not detectably altered by A. laidlawii after 3 min at 30°C.

Figure 20 shows the patterns obtained by chromatographing cell extracts after incubating at 37°C for 5 min with [^{14}C]-maltose in the presence and absence of 1mM methylarsine oxide (CH_3AsO). This inhibitor was also added to the growth medium, dissolved in ethanol, for 2 hr prior to harvesting the cells. Control cells had ethanol only added at the same time. Methylarsine oxide has been reported to cause 100% inhibition of maltase after incubation of the enzyme with 0.47mM of this inhibitor for at least 30 min (148). The data shown in figure 20, however, indicate a rapid metabolism of maltose by A. laidlawi, which is not

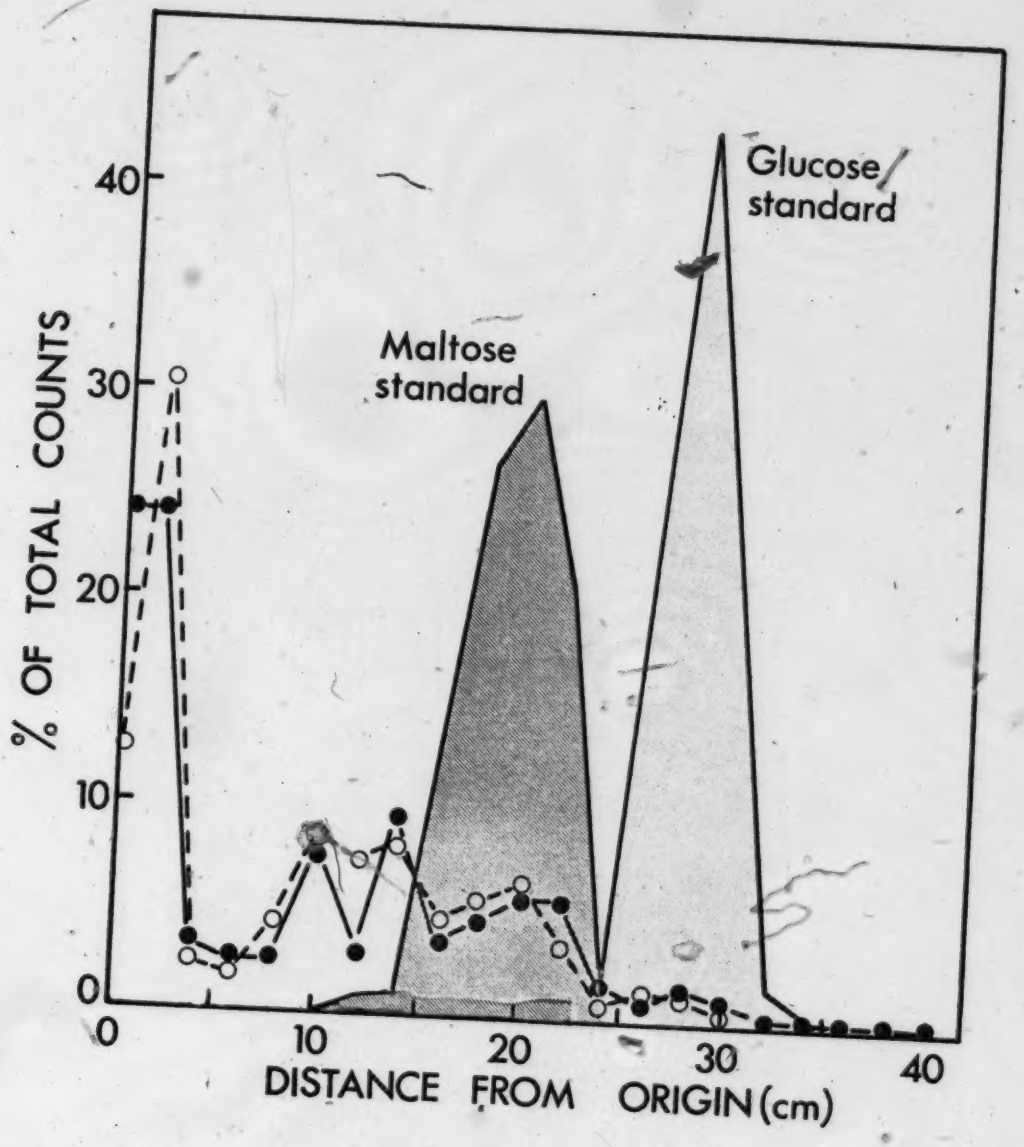

Figure 20. Metabolism of Maltose by Acholeplasma laidlawii. Control or CH3AsO-treated cells were incubated with [^{14}C]-Maltose for 5 min at 37°C, then washed on Millipore filters with ice cold quench solution, extracted, and chromatographed for 40 hr at room temperature, using butanol:pyridine:water 6:4:3 (v:v:v) as a developing solvent. The positions of glucose and maltose standards are indicated by the shaded peaks.
•—•, control; o—o, CH3AsO

affected by methylarsine oxide. This may be due to a difference in the enzyme which cleaves the maltose, or to failure of the inhibitor to penetrate the cell membranes.

Kinetics of radioactive sugar accumulation

The following section deals with the effects on the uptake of labelled sugars of the concentration of the same or a different competing sugar. Many of the experiments were performed by incubating the cells with a fixed amount of labelled compound, adding various concentrations of unlabelled sugar to change the specific activity. In others, the results are normalized to a constant radioactivity per volume of permeant solution, and so are also expressed as if the experiments were done in this way. The results in these instances are plotted as counts inside the cells *vs* time, and saturability or competition will be manifested as a decrease in slope as the concentration of the saturating or competing compound increases. The effect of glucose concentration on uptake rates in the first 60 sec is shown in figures 21 and 22. In figure 21 very little, if any, saturability is evident at the level of 0.1mM glucose, but marked inhibition of uptake is seen at 10mM glucose. These results should reflect uptake only, not metabolism, if the 10mM IAA which is present is effectively inhibiting glucose metabolism, as is suggested by the data in figure 14. Figure 22 shows the uptake of 0.1mM [^{14}C]-D-glucose with 10mM IAA

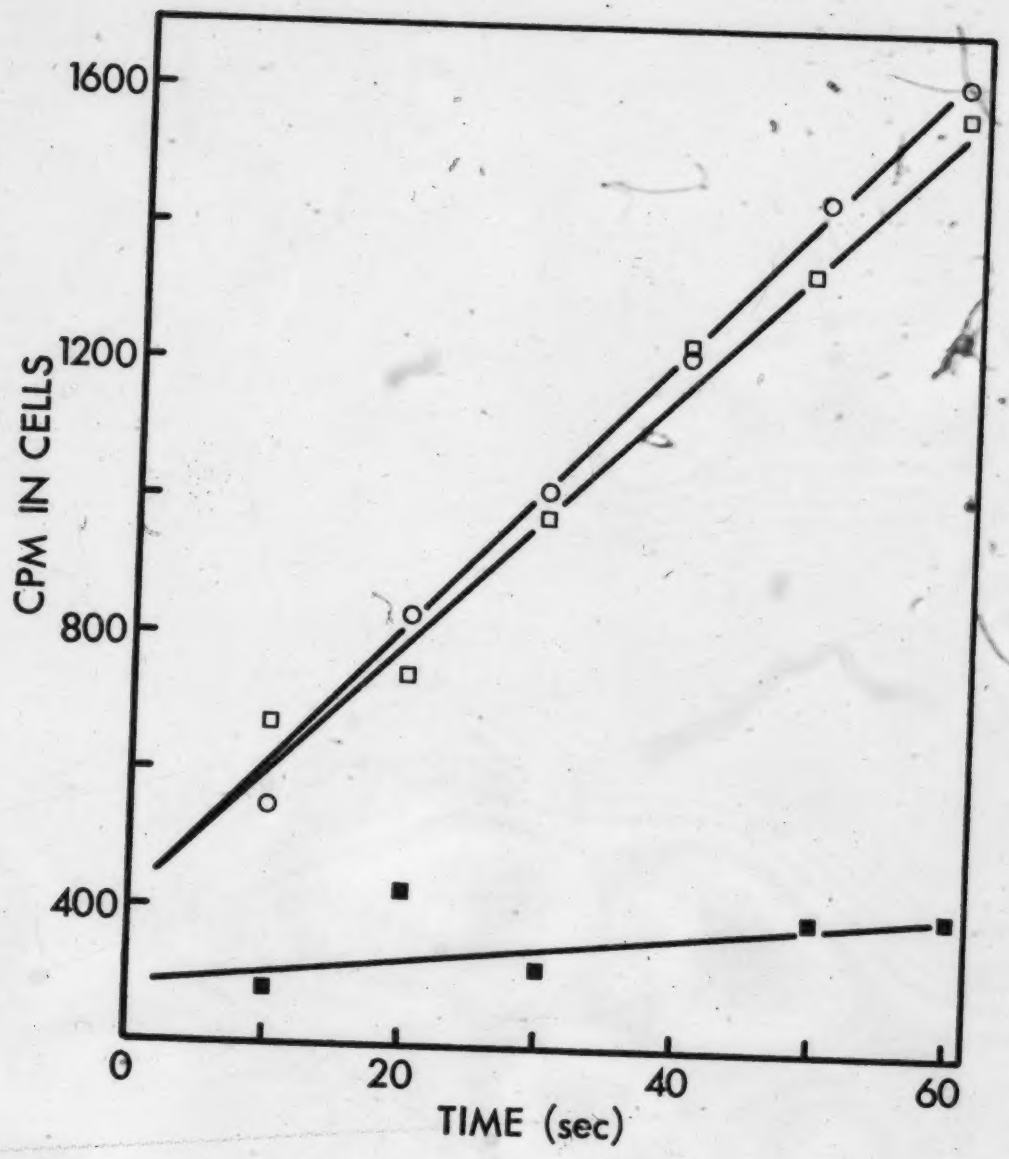

Figure 21. Saturability of [^{14}C]-D-Glucose Uptake by A. laidlawii in the Presence of 10mM IAA.
Cells grown in the presence of palmitic plus oleic acids plus cholesterol were incubated at 30°C in the presence of 10mM iodoacetic acid with [^{14}C]-D-glucose plus unlabelled glucose to the desired concentration. Aliquots were removed at 10 sec intervals into 3 ml of ice cold quench solution, then cells were washed on Millipore filters and counted
o–o, 0.0038mM; □–□, 0.104mM; ▪–▪, 10.0mM.

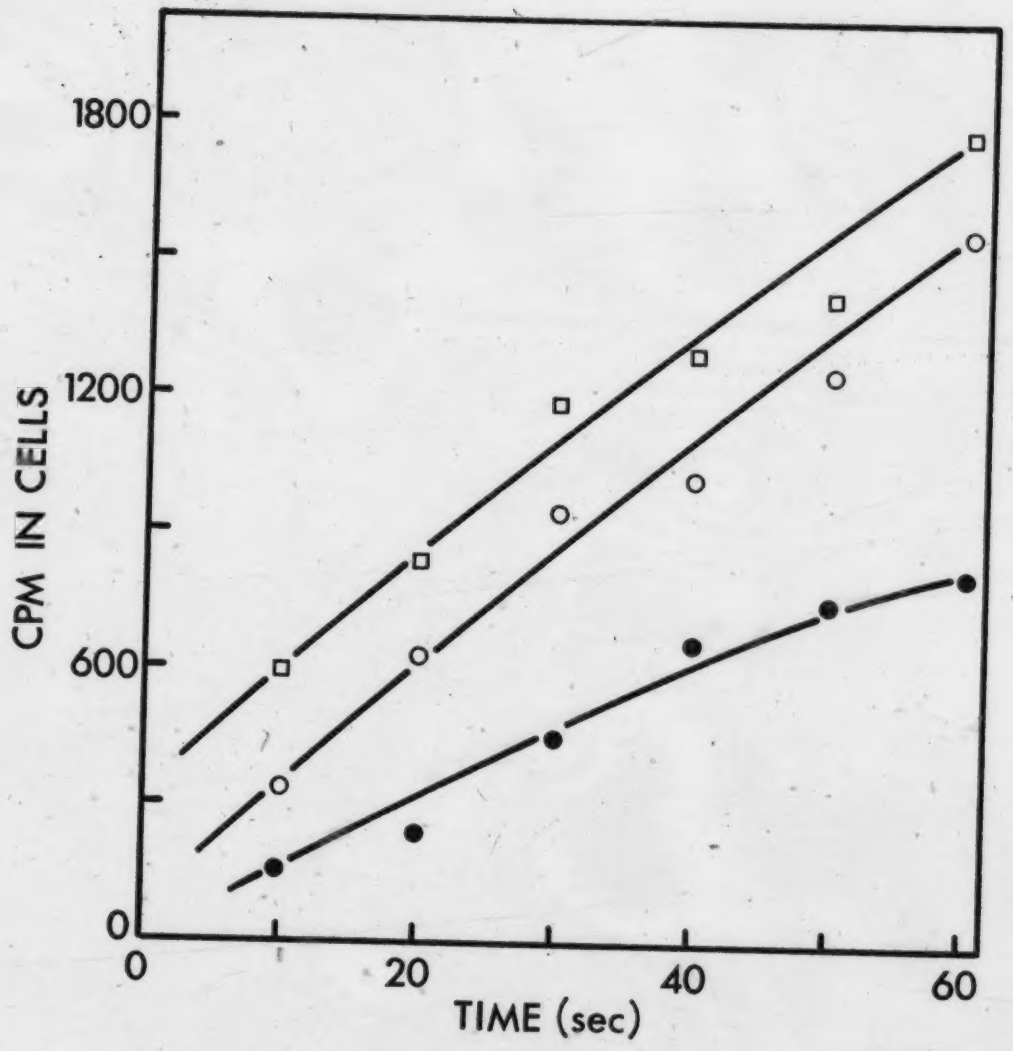

Figure 22. Competition by D-Glucose and 3-O-Methyl glucose for [^{14}C]-D-Glucose Uptake by A. laidlawii with 10mM IAA.
Cells grown in the presence of palmitic plus oleic acids plus cholesterol were incubated at 30°C in the presence of 10mM iodoacetic acid with 0.1mM [^{14}C]-D-glucose. To test competition, unlabelled D-glucose or 3-O-methyl glucose was added to a level of 25mM.

o–o, 0.1mM D-glucose; •–•, 25.1mM D-glucose
□–□, 0.1mM D-glucose + 25mM 3-O-methyl glucose

present in the presence or absence of added unlabelled 25mM D-glucose or 3-O-methyl glucose. Again, there is evidence of saturability of D-glucose uptake, but no competition by 3-O-methyl glucose is seen. To test whether 3-O-methyl glucose uses the D-glucose transport system, but shows no inhibitory effect on glucose uptake because of a much lower affinity, the effect of D-glucose on 3-O-methyl glucose uptake was determined. This is shown in Figure 23. The uptake of 0.0075mM [^{14}C]-3-O-methyl glucose in the absence of IAA is inhibited slightly by the presence of 25mM 3-O-methyl glucose, but not by 25mM D-glucose, thus the uptake of these two sugars seems to be via two distinct pathways. In studying sugar uptake by A. laidlawii, Tarshis and co-workers used concentrations of the order of 0.001 to 0.30mM and sampled at much later times, up to 40 min (120). No metabolic inhibitors were present. Figures 24-26 show the results of measurement of [^{14}C]-D-glucose uptake determined under conditions comparable to these. Figure 24(a) shows the effect of glucose concentration from 0.03 to 0.10mM on the uptake of D-glucose, and the effects of 1mM ATP or 1mM ADP + 1mM PEP (phosphoenol pyruvate). As shown in figure 24(b), no evidence for saturability of uptake is seen under these conditions. It is interesting that the presence of ATP or of ADP plus PEP, which should make energy for phosphorylation available, seems to decrease the initial rate, and causes a loss of radioactivity to occur after 5 min. This may indicate that what is really being seen is the ATP-dependent

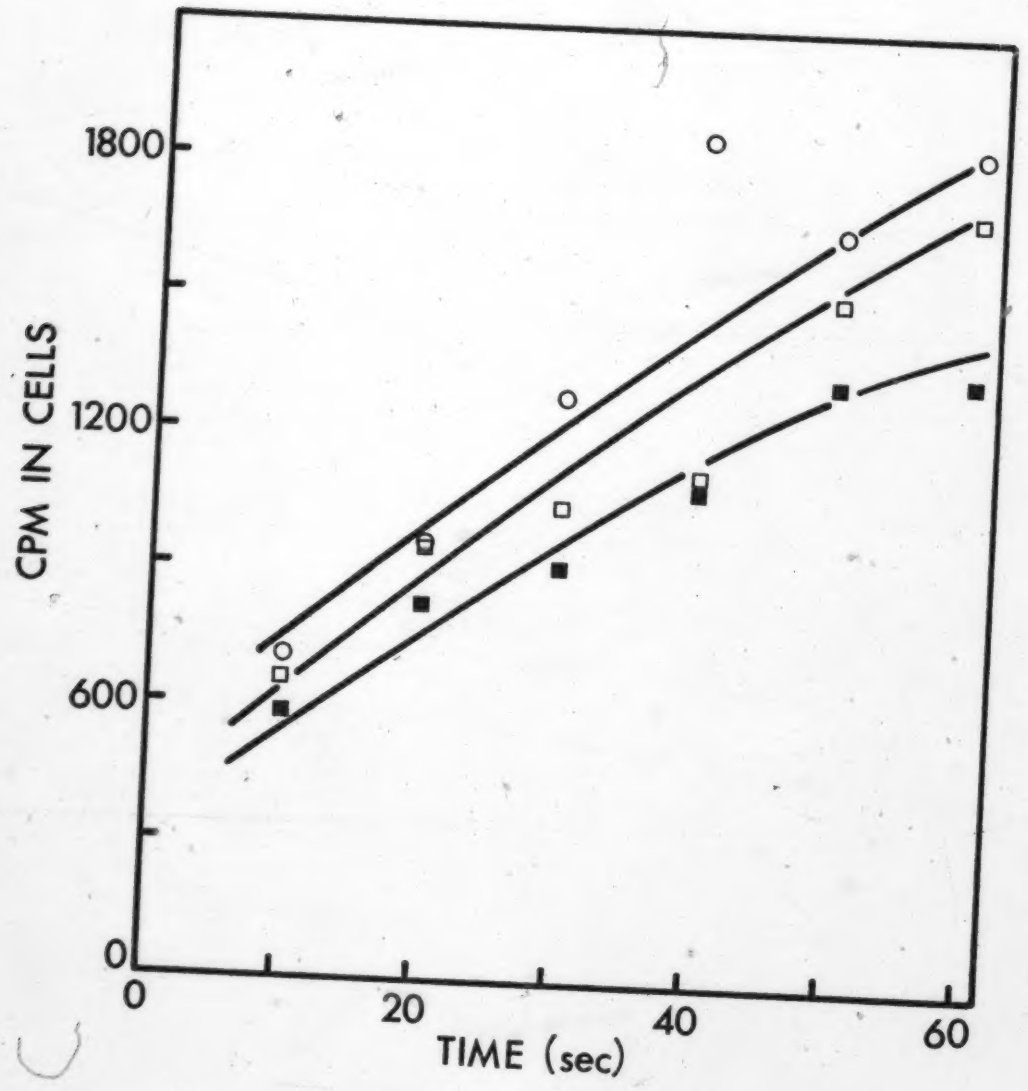

Figure 23. Competition by D-Glucose and 3-O-Methyl glucose for [^{14}C]-3-O-Methyl glucose Uptake by A. laidlawii.
Cells grown in the presence of palmitic plus oleic acids plus cholesterol were incubated at at 30°C with 0.0075mM [^{14}C]-3-O-methyl glucose. To test competition, unlabelled D-glucose or 3-O-methyl glucose was added to a level of 25mM. ▫—▫, 0.0075mM 3-O-methyl glucose; ▪—▪, 25mM 3-O-methyl glucose; o—o, 0.0075mM 3-O-methyl glucose plus 25mM D-glucose

Figure 24. Effect of Glucose Concentration on Uptake by *Acholeplasma laidlawii*
Cells grown in the presence of palmitic plus oleic acids plus cholesterol were suspended in 10mM phosphate, pH=7.4, 150mM NaCl, 10mM MgCl2 and then incubated at 37°C with various concentrations of [^{14}C]-D-glucose. Aliquots were taken into 3 ml of ice cold quench solution at 5 min intervals, washed on millipore filters, and counted.
(a) Uptake *vs* time: ▲–▲, 0.03mM; Δ–Δ, 0.04mM; •–•, 0.06mM; x–x, 0.09mM; o–o, 0.10mM □–□, 0.09mM+10mM ATP; ▪–▪, 0.09mM+10mM (ADP+PEP)
(b) Rate *vs* concentration: Rates were taken as the difference between the 5 min and zero values, divided by 5.

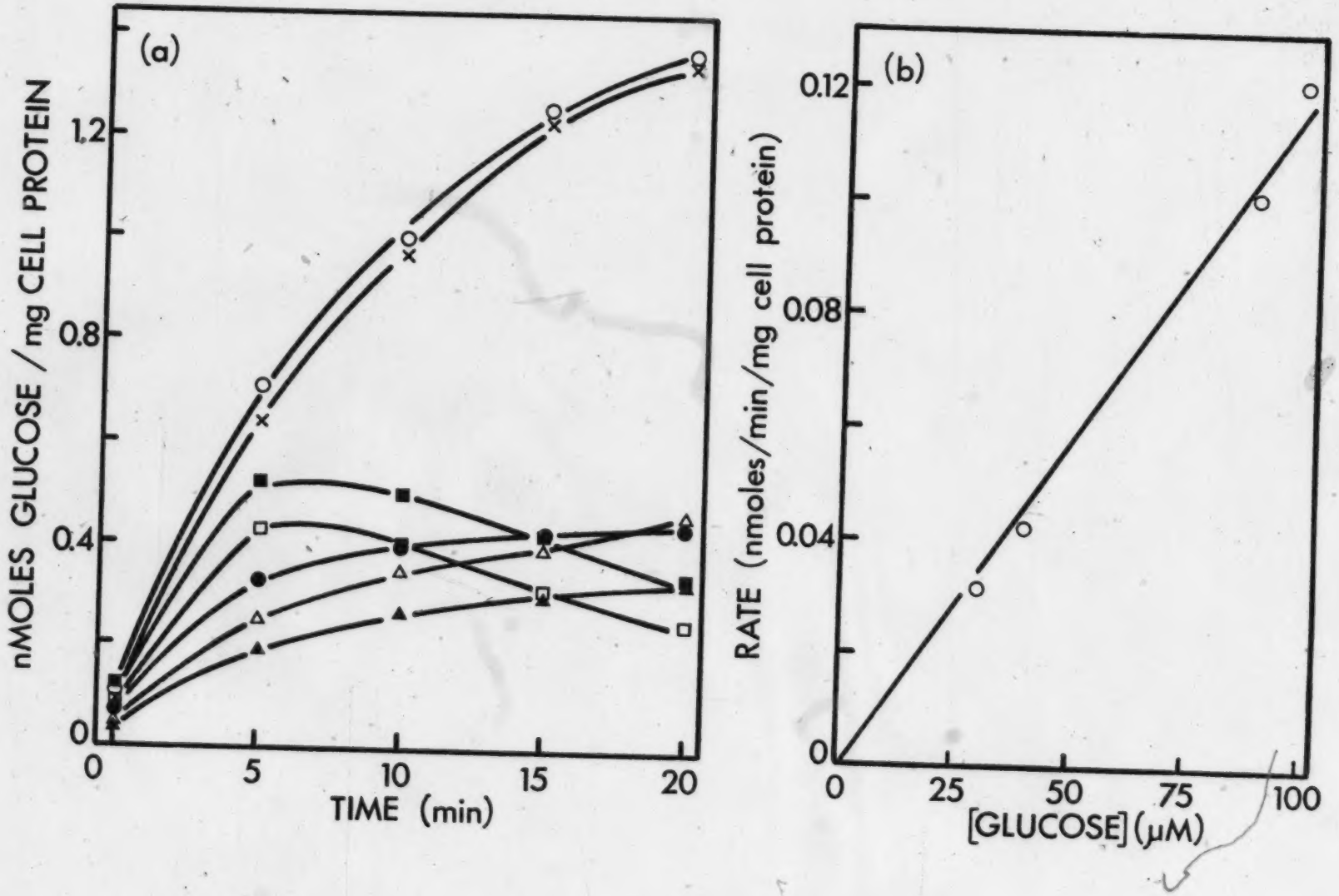
(a)
nMOLES GLUCOSE / mg CELL PROTEIN
1.2
0.8
0.4
0
0
5
10
15
20
TIME (min)
(b)
RATE (nmoles/min/mg cell protein)
0.12
0.08
0.04
0
0
25
50
75
100
[GLUCOSE] (μM)

labelling of metabolic pools, and that the availability of energy accelerates the loss of radioactivity in the form of metabolic products. The apparent reduction in uptake caused by ATP, or ADP plus PEP, could be an artifact due to the rapid rise to a peak, followed by loss of counts which occurs before the first 5 min sample is taken. Alternatively, the nucleotides may interact with the cell surface to make the membranes leaky.

Figure 25 shows the uptake of [^{14}C]-D-glucose, present at a constant radioactivity per volume of solution, in the presence of unlabelled glucose added to a final concentration of 0.02 or 0.20mM. The amount of radioactivity in the cells increased up to 10 min, then showed a decline with additional time, similar to the behavior seen in figure 24 in the presence of ATP or of ADP plus PEP. This suggests that the decline is due to metabolism of the glucose and loss of metabolic products. As shown in figure 15, most of the radioactivity present in these cells at all times has an Rf smaller than that of glucose. An increase in initial rate of uptake of radioactivity is seen here in the presence of added unlabelled glucose, rather than a decrease which would be expected from competition for carrier. This is probably due to stimulation of phosphorylation by the energy made available from the metabolism of the extra glucose. Figure 26 shows a stimulation of uptake of 0.2mM [^{14}C]-D-glucose by the presence of 0.5mM glucose. Again, the loss of

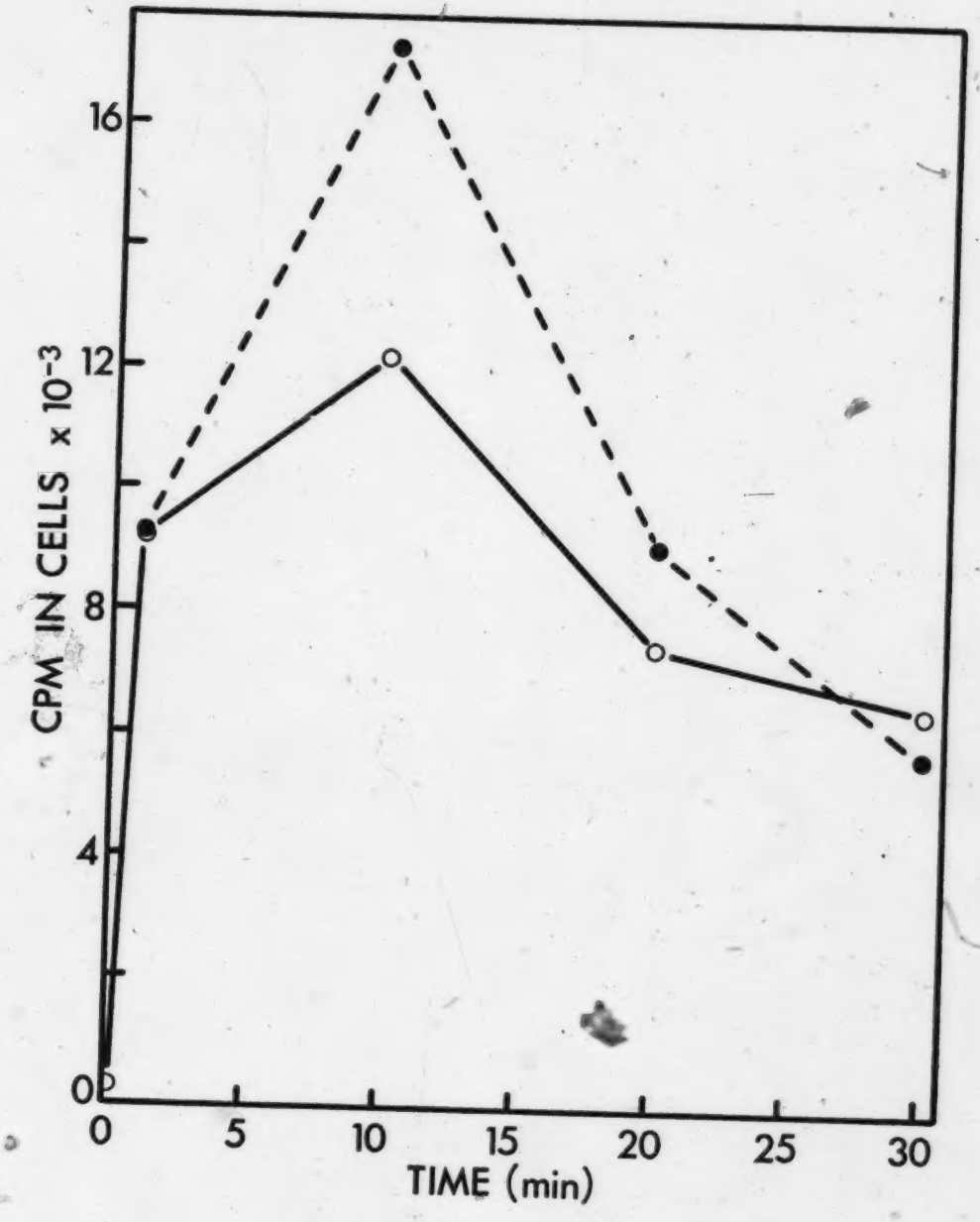

Figure 25. Effect of Glucose Concentration on Uptake by Acholeplasma laidlawii.
Cells grown in the presence of palmitic plus oleic acids plus cholesterol were incubated at 37°C with 0.02 or 0.20mM [^{14}C]-D-glucose having a constant radioactivity per unit volume.
o—o, 0.02mM; •—•, 0.20mM

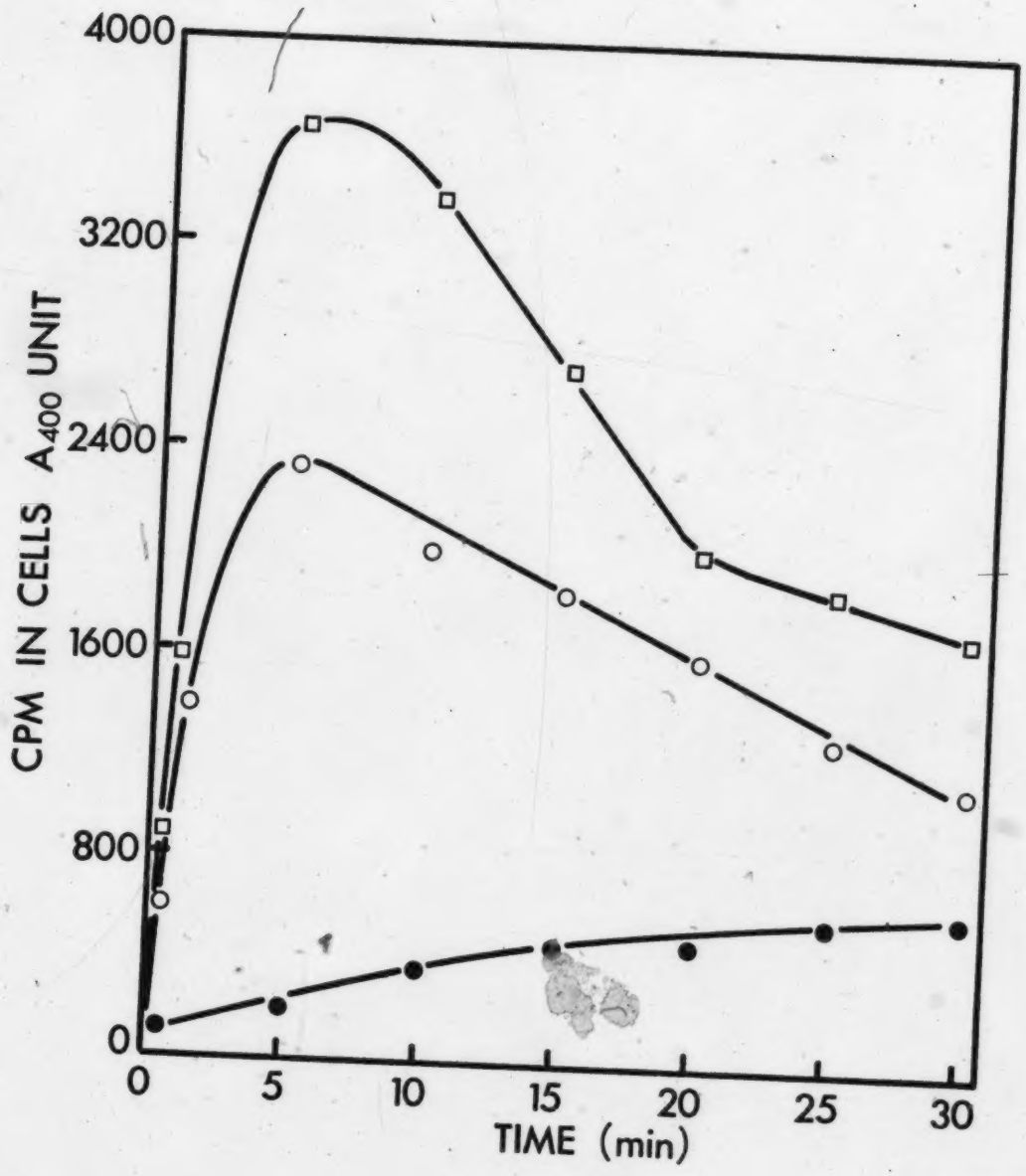

Figure 26. Effect of Glucose Concentration and of IAA on Glucose Uptake by Acholeplasma laidlawii. Cells grown in the presence of palmitic plus oleic acids plus cholesterol were incubated at 37°C with 0.2mM [^{14}C]-D-glucose with the addition of nothing (o–o), 0.5mM unlabelled D-glucose (□–□), or 10mM iodoacetic acid (•–•).

Figure 27. Chromatography of Cell Extract after 10 min Incubation with [^{14}C]-D-Glucose.
10 Min samples of cells from the experiment shown in figure 26 were extracted and the extracts chromatographed for 18 hr at room temperature using solvent 28. The position of the D-glucose standard is shown by the bracket.
o—o, 0.2mM glucose; □—□, 0.7mM glucose
•—•, 0.2mM glucose plus 10mM IAA.

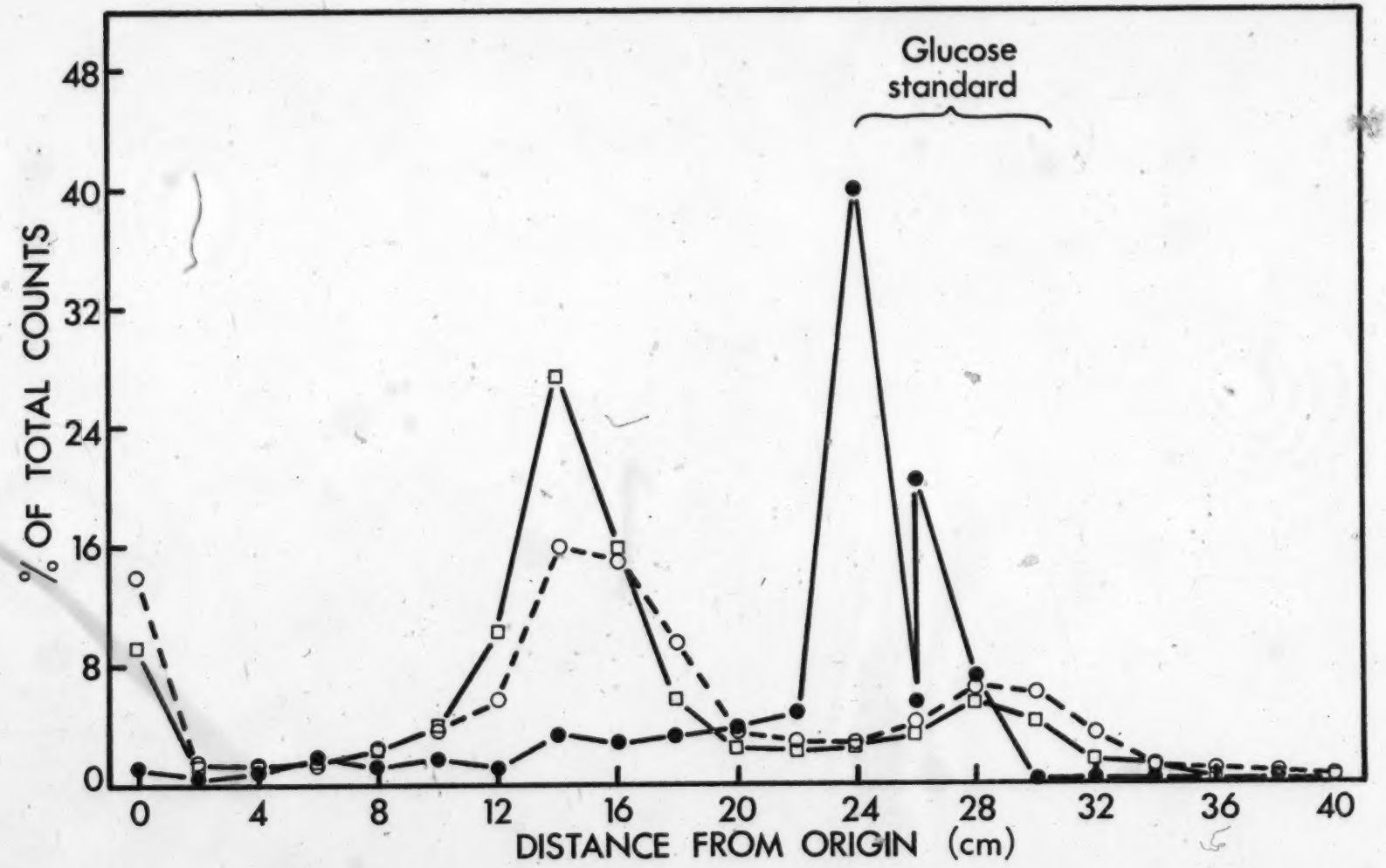
Glucose
standard
% OF TOTAL COUNTS
48
40
32
24
16
8
0
0
4
8
12
16
20
24
28
32
36
40
DISTANCE FROM ORIGIN (cm)

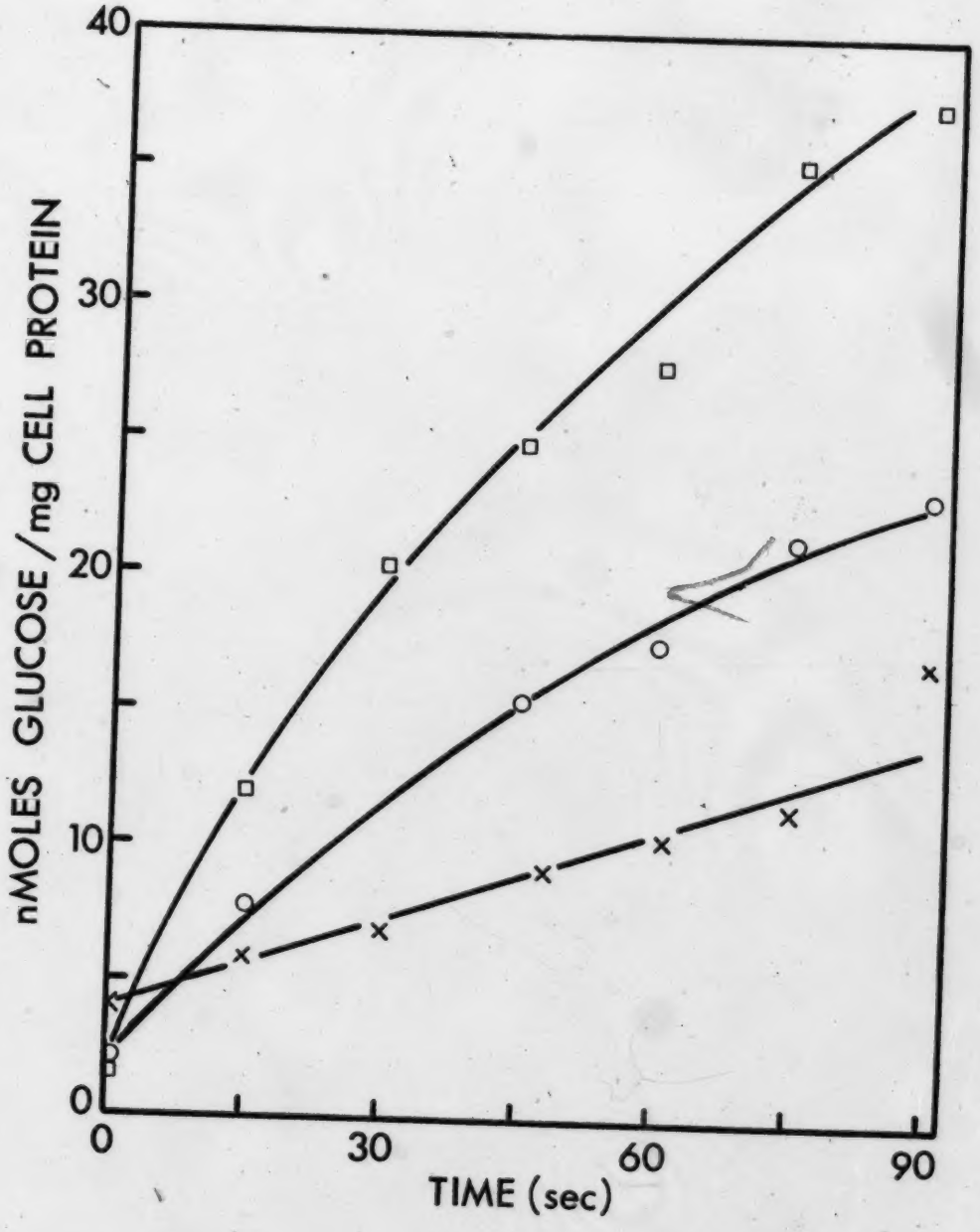

Figure 28. Effect of Fatty Acid Composition on Uptake of 0.1mM [^{14}C]-D-Glucose.
Cells grown in the presence of palmitic plus elaidic, oleic, or linoleic acids were incubated at 25°C with 0.1mM [^{14}C]-D-glucose, and portions taken into 3 ml of ice cold quench solution, filtered and washed at the times shown.
□-□, 16:0/18:2cc; o-o, 16:0/18:1c;
x-x, 16:0/18:1t.

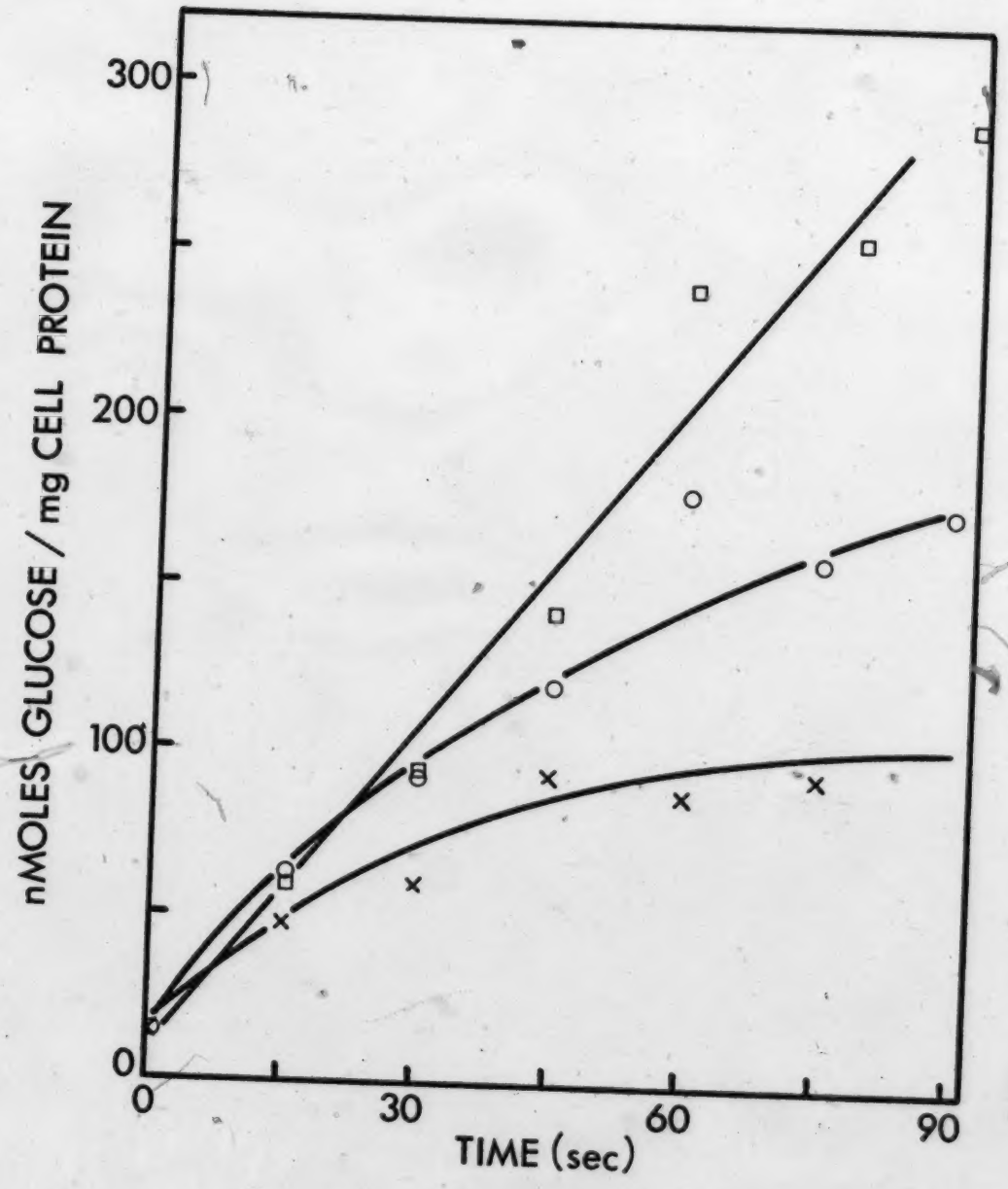

Figure 29. Effect of Fatty Acid Composition on Uptake of 1.0mM [^{14}C]-D-Glucose.
Cells grown in the presence of palmitic plus elaidic, oleic, or linoleic acids were incubated at 25°C with 1.0mM [^{14}C]-D-glucose, and portions taken into 3 ml of ice cold quench solution, filtered and washed at the times shown.
□–□, 16:0/18:2cc; o–o, 16:0/18:1c;
x–x, 16:0/18:1t.

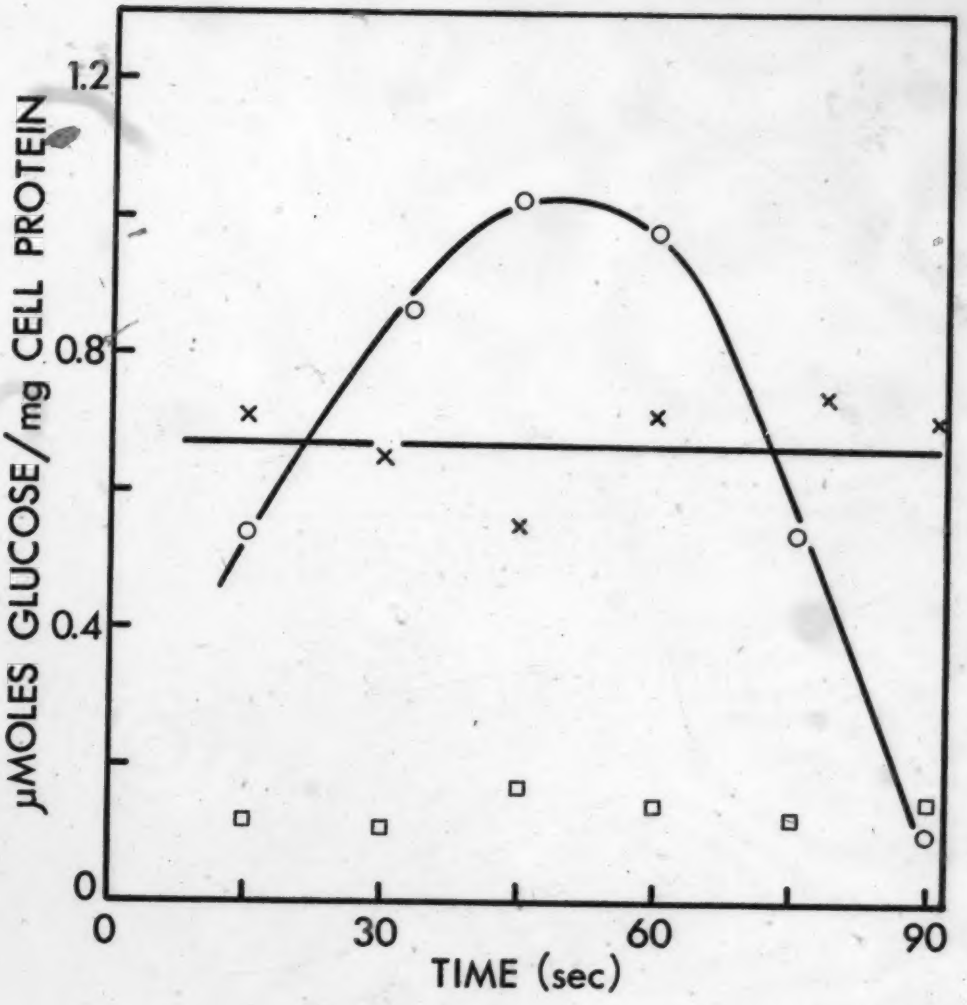

Figure 30. Effect of Fatty Acid Composition on Uptake of 10.0mM [^{14}C]-D-Glucose.
Cells grown in the presence of palmitic plus elaidic, oleic, or linoleic acids were incubated at 25°C with 10.0mM [^{14}C]-D-glucose, and portions taken into 3 ml of ice cold quench solution, filtered and washed at the times shown.
□-□, 16:0/18:2cc; o-o, 16:0/18:1c;
x-x, 16:0/18:1t.

radioactivity after the first 10 min is seen. The presence of 10mM iodoacetic acid prevents this net loss of label, as would be expected from its inhibition of metabolism. It also greatly decreases the rate of uptake. This could be due either to the absence of trapping of labelled glucose in large metabolic pools, or could also indicate some effect of IAA on the transport protein. Figure 27, which illustrates the chromatographic analysis of the intracellular radioactivity after 10 min, shows that a greater proportion of the radioactivity in these cells is in the form of compounds other than glucose in the presence of 0.5mM unlabelled glucose. This confirms the stimulation of metabolism by the added glucose. The inhibition of metabolism by IAA is also shown in figure 27. Although phosphorylation is obviously significantly curtailed, it is possible that some other reaction (eg oxidation) to a compound having a slightly lower Rf than glucose occurs.

The effect of fatty acid composition on the initial rates of uptake of [^{14}C]-D-glucose at 3 different glucose concentrations is shown in figures 28-30. At a concentration of 0.1mM (figure 28) or 1.0mM (figure 29), the rate of uptake of D-glucose increases with increasing lipid fluidity. At 10mM, however, the situation is more complicated (figure 30). The apparent amount of glucose inside cells with the most fluid membranes (16:0+18:2cc) is at all times equivalent to the amount which would be

calculated from the level of background radioactivity; in other words, no uptake of glucose is seen. The cells with the least fluid membranes (16:0+18:1t) show a plateau which is fairly constant, while those with intermediate fluidity (16:0+18:1c) exhibit a rapid rise to a peak at 45 sec, followed by a decline of counts inside the cells. It may be postulated that these effects are a result of enhancement of metabolism of the label by energy made available from the metabolism of the 10mM glucose which is present. Radioactivity inside the cells can be affected by the glucose permeability of the membranes in two ways: a higher permeability allows label to get into the cells faster, but also allows energy from glucose metabolism to be made available more quickly. This metabolic effect can tend to either increase or decrease radioactivity inside the cells, depending on whether labelled glucose in the medium is nearly depleted, so that loss from cells by metabolism is more significant, or not near depletion, so that the labelling of intracellular pools of metabolites is more significant. In addition, a more fluid membrane may increase the rate of loss of radioactive metabolites of glucose by cells. The most fluid cells seem to be unable to retain radioactive metabolic products during washing. Oleate-supplemented cells show an increase, followed by a decrease in radioactivity, as energy from the metabolism of glucose stimulates the movement of label through the intracellular pools. With elaidate-supplemented cells, some type of steady

state is seen.

Figure 31 shows the effects of various unlabelled sugars and similar compounds on the uptake of [^{14}C]-2-deoxyglucose. Only 2-deoxyglucose itself and D-glucose seem to significantly inhibit uptake, although there may be slight inhibition by L-glucose. Myoinositol and sucrose show no effect, while 3-O-methyl glucose and erythritol actually stimulate the uptake of label. This effect could occur by an activation of the transport carrier by these compounds through some type of co-operative effect, or by an inhibition of metabolic processes which lead to loss of label. The inhibition by D-glucose but not 3-O-methyl glucose is consistent with the lack of mutual competitive inhibition by these two compounds (figures 22 and 23). The reduced inhibition by L-glucose correlates with the evidence for weaker binding of this isomer from the phloretin inhibition of swelling (figure 3).

Because of the failure of the inhibitor methylarsine oxide to prevent the rapid metabolism of Maltose by A. laidlawii, the uptake of this permeant is subject to the same limitations as to interpretation that exist for D-glucose. Rather scattered data were obtained in initial attempts to measure uptake, perhaps due in part to ineffectiveness of the phloretin in the quench solution in inhibiting flux of this compound, so further attempts to characterize this transport system were not undertaken.

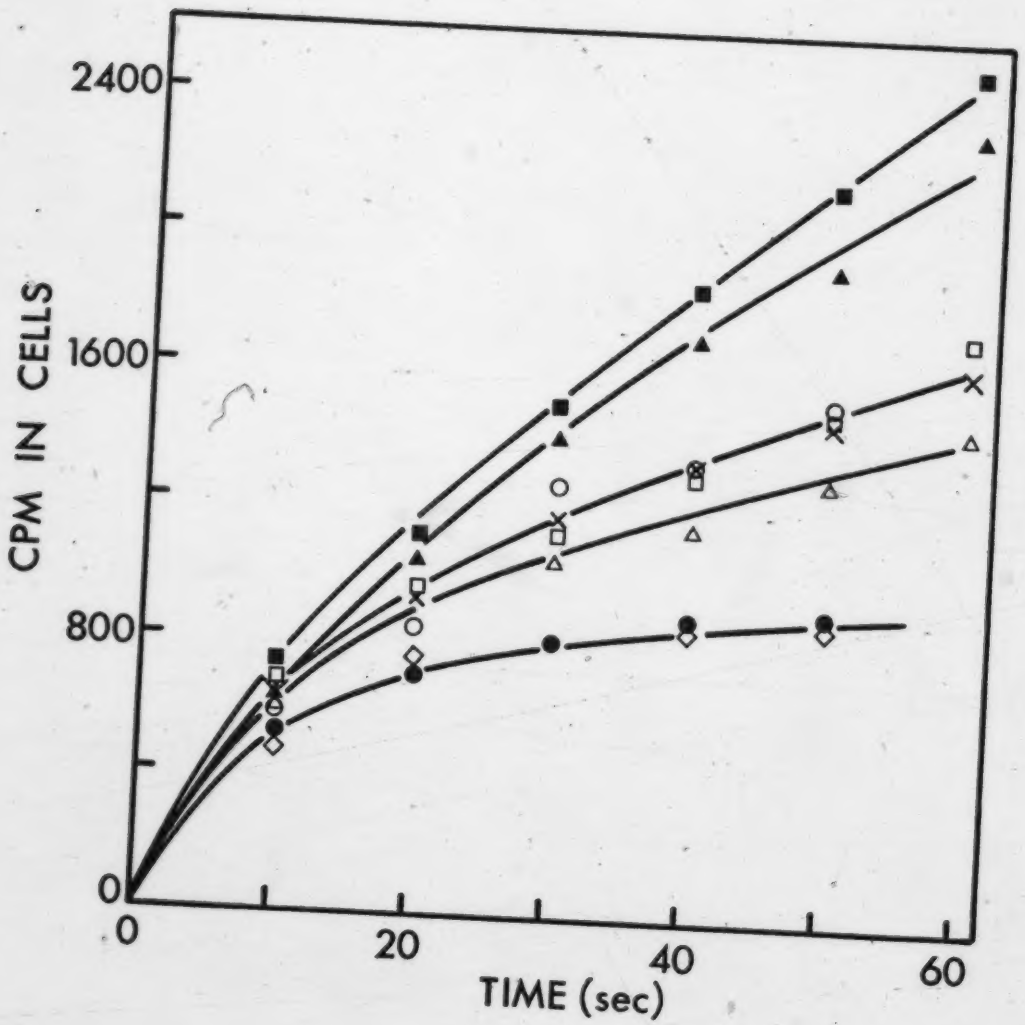

Figure 31. Inhibition of [^{14}C]-2-Deoxyglucose Uptake by Glucose and Glucose Analogs.
Acholeplasma laidlawii cells grown in the presence of palmitic plus elaidic acids were incubated at 30°C with 0.2mM [^{14}C]-2-deoxyglucose in the presence of various other compounds at 40mM. Aliquots were taken into ice cold quench solution at the times indicated, washed on Millipore filters and counted.
▪–▪, 3-O-methyl glucose; ▲–▲, erythritol;
o–o, control; x–x, myoinositol; □–□, sucrose;
△–△, L-glucose; •–•, 2-deoxyglucose;
◇–◇, D-glucose.

IV Discussion

It seems quite clear that glucose is taken up by A. laidlawii via some type of mediated process, that is, via some mechanism, probably involving membrane protein, other than simple passive diffusion through the lipid bilayer. This is indicated by several lines of evidence. The swelling rate in D-glucose is strongly inhibited by phloretin and phlorizin, compounds which are known to inhibit mediated sugar transport in many different systems (143,149-154). It is inhibited at temperatures above 45°C, whereas the swelling rate in erythritol continues to rise exponentially with increasing temperature, indicating the involvement of some heat-labile component in glucose, but not erythritol permeation. The swelling in glucose is much faster than would be predicted for passive diffusion, from a comparison of swelling rates of cells with those of liposomes, and shows a lower activation energy than does glucose permeation of lipid bilayers (130,131). Unfortunately, the assay of permeability by the use of radioactive tracers is complicated by the rapid metabolism of D-glucose. Several factors interact to determine the apparent rate of uptake of labelled sugar which is observed at various permeant concentrations. Competition for a saturable transport process will decrease the rate of entry of radioactivity into the cell as the concentration of unlabelled permeant increases. On the other hand, metabolism of the unlabelled

sugar can provide energy which tends to increase the counts in the cell measured at early times because of accelerated labelling of intracellular pools, but decrease the counts measured at later times when the loss of label by metabolism becomes significant. In addition, unlabelled sugar may be competing for metabolic enzymes. The fluidity of the cell membrane can have various opposing effects upon the uptake observed. A more fluid membrane may allow permeant to be taken up faster, but it can also allow labelled metabolic products to escape more readily. The dichotomous effect of the increased metabolism due to faster uptake of substrates through more permeable membranes must also be kept in mind. The net effect of these interacting parameters may depend on the concentration of permeant present, the times at which sampling is done, the temperature, the relative magnitudes of the permeability and the rate of metabolism of the permeant, the permeability of the membrane to metabolic products and the ratio of the amount of cells to the total amount of permeant present in the assay mixture.

The two most obvious approaches to this problem are to use non-metabolizable analogs of the permeant or to inhibit cellular metabolism. Of the analogs of D-glucose tried, 3-O-methyl glucose and L-glucose were not metabolized, but they also showed little affinity for the transport system. While 2-deoxyglucose showed competition with D-glucose for uptake, it was also metabolized, at least to the level of phosphate

and, in fact, this reaction may be the step at which competition is acting. Iodoacetic acid seemed to inhibit glucose phosphorylation, but could not be unequivocally shown to prevent all reactions of glucose. It was also uncertain what effect this inhibitor had on the presumed transport protein itself. An additional problem with these measurements was that curved rather than linear plots of intracellular counts *vs* time are nearly always obtained, even at very early times, so determination of initial rates is difficult. Nevertheless, at early times, and at low (0.1mM) glucose concentrations, the membrane lipid fluidity could be shown to have an effect on glucose uptake, with the more fluid membranes allowing faster permeation. The conditions of the swelling rate assays were such that metabolism of radioactive material by the cells was not a problem. At the high permeant concentrations used (200mM), the proportion of material taken up which was chemically altered by the cell in the time of measurement was insignificantly small, indicating that intracellular metabolism is more readily saturable than the transport process. Since a continuous tracing is obtained, sampling at early times is not required, so this problem of measuring uptake of labelled permeants is eliminated. The swelling rates show a definite increase with increasing lipid fluidity, produced by manipulation of both fatty acid composition and cholesterol content. This increased rate of uptake arises from entropic terms, as the heat of activation does not

change significantly, and thus appears to be a direct consequence of the ease of some type of movement of carrier which occurs in the lipid environment. The Arrhenius plot of uptake in 16:0/18:1t-supplemented cells showed a discontinuity in slope occurring within the lipid phase transition at about 25°C.

Because of the difficulties presented by the metabolism of glucose, the characterization of this transport system is incomplete. Without good kinetic data at low glucose concentrations, reliable estimates of Km and Vm were not possible. It was also not possible to determine whether uptake against a concentration gradient occurred in order to establish whether this was an active transport system or a facilitated diffusion system. The other phenomenon which it would have been desirable to examine is that of counterflow. This is a transient flux of labelled compound against its concentration gradient driven by a large flux in the opposite direction of unlabelled compound down its concentration gradient, which is often seen in facilitated diffusion systems (155). This phenomenon is explained by competition for permeant binding sites by the unlabelled compound, which prevents the flux in one direction of label, thus causing accumulation as long as the concentration gradient of the unlabelled compound is present. In this system, the metabolism of D-glucose precluded such a measurement, and counterflow was not seen with L-glucose or

3-O-methyl glucose, possibly due to their low affinities for the transport sites.

Although no saturable component of phloretin binding to the cells is seen, a large amount of phloretin does bind, and this binding is reduced by the presence of 50mM glucose. This altered binding may be a result of some general alteration of the cell surface by the presence of glucose rather than its competition with phloretin for binding to specific sites. On the other hand, the increased inhibition of uptake of 1mM *vs* 10mM D-glucose by 0.001mM phloretin does suggest competition between phloretin and glucose for binding to transport sites. There may be a small number of such binding sites for phloretin which are involved in the inhibition of glucose flux. Binding of phloretin to them could have been obscured in the determination of binding by a general partitioning of much larger amounts of phloretin into the membrane.

To summarize, D-glucose uptake in *A. laidlawii* is mediated and is dependent on lipid fluidity, but a complete characterization of the glucose uptake system was not achieved.

CHAPTER IV

URIDINE AND GLUCOSE TRANSPORT IN HUMAN ERYTHROCYTES

I Introduction

Although *Acholeplasma laidlawii* provides a system with readily-alterable membrane lipid fluidity, the characterization of the transport system investigated was somewhat equivocal. It was therefore decided to study a system with a well-defined facilitated diffusion system, even if the manipulation of membrane fluidity then became more difficult.

The human erythrocyte has facilitated diffusion systems for D-glucose (101-104) and for uridine (105-107) which have been studied in some detail. There are several procedures which can be used to determine kinetic parameters of these systems, and the complexity of the transport phenomena are reflected in the fact that the values determined for Km and Vm vary greatly depending upon which method is used. In the zero-*trans* procedure, flux from one side of the membrane, in contact with various concentrations of permeant, to the other side, where the permeant concentration is zero, is measured. In the equilibrium exchange experiment both sides of the membrane are in contact with the same concentration of permeant, but labelled permeant is present at one side only, and its flux is measured at various permeant concentrations. The infinite-*cis* experiment follows flux of

labelled permeant from one side, having a saturating concentration, to the other, which has unlabelled permeant present at varying concentrations. Lieb and Stein have collected data for glucose transport from various workers which show that the values for Km determined by the zero-*trans* and equilibrium exchange procedures are at least an order of magnitude higher than by the infinite-*cis* procedure, and that the value of Vm determined by equilibrium exchange is about double that obtained by the other methods (156). Various modifications of a simple, symmetrical, shuttle-type carrier have been proposed to account for the kinetic anomalies which have been noted. These include different mobilities of permeant-bound and free carrier (102), the presence of unstirred layers of water outside the erythrocyte (94,157), and an asymmetric carrier system exhibiting different binding constants at the two surfaces (158). Lieb and Stein have presented a proposal featuring a tetrameric transport protein with two binding sites, one with high affinity and one with low affinity, exposed at each surface (156). Transport is accompanied by an internal transfer of permeant from one subunit to another which is at the opposite face of the membrane. Using a diverse body of kinetic data, they present an argument for this model and against the other proposals which is quite convincing, provided that the data used can all be accepted. One problem is that the experiments were done by a number of different investigators under a variety of different

conditions, so may be subject to differences caused by temperature and other experimental conditions, as well as the normal deviations which may exist between erythrocytes from different individuals.

In spite of some complicating aspects of the kinetics, the glucose transport system in human erythrocytes seemed like a very useful one to use in investigating the effects of lipid fluidity. At glucose concentrations of 5mM or higher, the rate of permeation is far in excess of the rate of glucose utilization, so that interference with permeability measurements by metabolism is not a serious problem (159). At 25°C, the cells can even be incubated with glucose for extended periods of time to preload them with permeant without significant metabolism of the glucose occurring (102). Large quantities of human erythrocytes are readily available and, because the cells are large, washing by centrifugation and the determination of cell volume in suspensions (hematocrits) can be done easily and quickly. The potent inhibition of flux by phloretin (160) or mercuric ions (161) allows transport to be rapidly terminated by a solution containing these compounds in order to measure flux rates (162).

For many of the same reasons, the uridine transport system of human erythrocytes also appeared to be a promising one to investigate. Uridine is not chemically altered by the human erythrocyte, and is taken up by facilitated diffusion

(105). A large number of compounds show accelerative exchange diffusion, that is, they increase the rate of unidirectional flux of uridine from a saturating concentration when they are present at the *trans* membrane surface. This effect is explained by a faster return of the carrier binding site to the *cis* membrane surface when bound to the accelerating substrates than when empty, implying that the accelerating substance must be a substrate for the transport system (155). The acceleration of flux by substances present at the *trans* side of the membrane has been used to investigate the specificity of the uridine transport system. This system in human erythrocytes exhibits specificity for un-ionized nucleosides of a fairly large number of both purines and pyrimidines, but a more stringent specificity toward the sugar portion (106). There is little tolerance for substitution at the 2' or 3' positions of ribose, although the 2'-hydroxyl group can be replaced by a hydrogen. Uridine shows values of Km and Vm of 0.71mM and 0.5 micromoles/min/ml of packed cells for the zero-*trans* experiment at 15°C (105), 0.1mM and 4.3 to 7.1 micromoles/min/ml packed cells measured by accelerative exchange diffusion at 25°C (106,107), and a Km of 1.0mM at 25°C for equilibrium exchange flux (163). The S-substituted thiopurine ribonucleoside 6-[(2-hydroxy-5-nitrobenzyl)-thio]guanosine (HTG), and a number of other analogous compcunds, bind tightly ($K_d=10^{-9}M$) to the membrane and inhibit uridine transport (106,163,164).

In the work described here, equilibrium exchange efflux was measured because the kinetic analysis of this type of experiment is simpler and because of certain technical advantages. Since the concentration is the same at both sides of the membrane, washing of the cells with large volumes of solution containing permeant at the desired concentration eliminates any uncertainty about the concentration present at either face. Volume changes induced by osmotic inbalance during transport are also eliminated.

One of the methods used to alter membrane lipid fluidity was treatment with anesthetics. An anesthetic may be broadly defined as a drug which, when applied directly to a nerve or muscle cell, reversibly blocks the action potential without appreciably affecting the resting membrane potential (165). The term anesthetic, thus defined, encompasses a very large number of compounds which have a variety of pharmacological effects. Most of these are hydrophobic or amphipathic molecules. Several lines of evidence demonstrate that many of the lipid-soluble anesthetics have a fluidizing effect on membrane lipids. Anesthetics cause an increase in area of lipid films at the air/water interface and of biomembranes. This expansion is 10-fold more than can be explained by the volume occupied by the anesthetic molecules (165). An increase in mobility of anesthetics in membranes with increasing anesthetic concentration, up to a certain point, was shown by the NMR

spectrum of benzyl alcohol (166). A fluidization of the membrane by a large number of aliphatic alcohols, by halothane, and by methoxyflurane, which can be reversed by increased atmospheric pressure, was seen in studies using fluorescent or spin-labelled probes (167,168). The generalization has been made that anesthetics may either increase or decrease passive fluxes, but invariably inhibit facilitated diffusion, presumably due to some effect on the conformation of transport proteins (165). This postulate, however, has not been thoroughly tested and verified, nor does there seem to be any *a priori* reason for all facilitated fluxes to be inhibited, so it seemed worth while to look at the effects of some anesthetics on glucose and uridine fluxes in erythrocytes.

The second procedure used for the manipulation of erythrocyte membrane fluidity was the partial exchange of a cholesterol analog, cholest-4-en-3-one, for membrane cholesterol. Cholesterol comprises about 40 mole% of the membrane lipid of human erythrocytes (169). Cholesterol seems to be required for the maintenance of membrane integrity as its depletion from human erythrocytes *in vitro* leads to hemolysis (170), and depletion from rat erythrocytes *in vivo* leads to increased fragility and the formation of morphologically abnormal cells (171). Cholesterol is thought to act in biological membranes as a regulator of lipid fluidity, fluidizing fatty acid chains at

temperatures below Tc, but rigidifying them at temperatures above Tc (172,173). Fluorescent probe analysis has indicated that the effect of cholesterol in erythrocyte membranes at 37°C is to restrict molecular motion in the hydrophobic region (174). Investigations of the effects of cholesterol on erythrocyte permeabilities have yielded varying results. In vivo or in vitro cholesterol loading of guinea pig erythrocytes decreased their permeability to erythritol or Na^+ at 37°C, and to thiourea or monacetin at 22°C (175). Up to 39% depletion of cholesterol of pig, ox, or human erythrocytes does not seem to affect permeabilities, but depletion beyond this level increased the permeabilities of human erythrocytes to erythritol at 30°C, of pig erythrocytes to glycerol at 15°C, and of ox erythrocytes to acetate or propionate at 0°C (176,177).

It has been reported that significant amounts of certain other steroids can be exchanged for erythrocyte membrane cholesterol by incubating the erythrocytes with sonicated dispersions of the steroids plus lecithin (170). These replacements can cause significant increases or decreases, depending upon the sterol used, of swelling rates of the erythrocytes in glycerol at 37°C. Using a fluorescent cholesterol analog, evidence has been obtained that exchange of sterol molecules between the two sides of the bilayer occurs much faster than that of phospholipids (178). With the sterol used, the half time of this process at 30°C was

72 min, which means that cholesterol in both sides of the membrane should be exchanged under the conditions used here (2–8 hr at 37°C).

II Methods

Buffer systems

Because the cation pump responsible for maintaining high intracellular K^+ and low Na^+ levels, as well as the property of membrane deformability, requires the presence of ATP, and because the survival of red cells in stored Red Cross blood seems to be closely related to intracellular ATP levels, it was felt desirable to maintain high concentrations of ATP in erythrocytes used for permeability experiments (179). The presence of 0.5mM adenine has been shown to improve the survival of red cells in stored blood, by reacting with phosphoribosyl pyrophosphate (PRPP) to form AMP. This step is essential to the maintenance of ATP levels after AMP accumulation in stored blood triggers the reduction of adenine nucleotide pools by deamination to IMP, dephosphorylation to inosine, and phosphorolysis to hypoxanthine, because the cells can not synthesize new adenine nuclectide by the de novo pathway (179). Fresh red cells do not contain significant levels of PRPP unless they are incubated at 37°C with the pentose phosphate precursor,

inosine, or unless the concentration of inorganic phosphate is raised well above normal plasma levels (180). Significantly higher amounts of PRPP, which is derived from glucose, are found in stored red cells than in fresh cells (181). Incubation of red cells with inosine causes the accumulation of sugar phosphates, including a rise of fructose diphosphate and triose phosphate concentrations to 10 times their normal levels, as well as increasing the amount of PRPP. The presence of 10mM pyruvate prevents this accumulation of fructose diphosphate and triose phosphate, presumably by generating NAD from NADH, which is then available for the oxidation of triose phosphates.

Bearing these observations in mind, an isotonic buffer system was designed to keep ATP levels as high, and levels of other metabolites as near to normal, as possible. It contained 0.5mM adenine, 140mM NaCl, 2mM MgCl2, 5mM KH2PO4, 10mM Na^+-pyruvate, 20mM tris-HCl, pH=7.4, and 10mM of either D-glucose or inosine. Inosine was present in the buffer used for measuring glucose transport and uridine passive flux, but since inosine is a substrate for the uridine transport system, it was replaced by glucose in uridine facilitated diffusion experiments. After washing the erythrocytes, they were routinely incubated at 37°C for 1 hr in this buffer, then rewashed not more than one day before being used.

Preparation of egg yolk lecithin

Phosphatidylcholine (lecithin) was purified from a lipid extract of egg yolks by column chromatography on silicic acid (182,183). The yolks from three eggs were blended thoroughly in a Waring blender with 110 ml of acetone to remove cholesterol and cholesterol esters, glycerides, pigments, and water. After filtration through Whatman No. 1 paper, the filtrate was discarded and the residue blended with 110 ml of chloroform:methanol 2:1 (v:v) and filtered again. The filtrate was taken to dryness and the deposited material redissolved under nitrogen in 125 ml of 5% methanol in chloroform (v:v) with slight warming, then cooled to room temperature, filtered and the filtrate retained. For the first chromatography step, a slurry of 400 g of Unisil plus 50 g of celite in methanol was applied to a 6 cm-diameter glass column (height=35 cm) and washed with 1 l of chloroform. Lipids were applied in 5% methanol in chloroform, then eluted stepwise with increasing concentrations of methanol in chloroform, monitoring the effluent at all stages by micro-TLC. In this technique, plates are prepared by dipping two microscope slides held tightly together into a thick slurry of silica gel G in chloroform, so one side of each slide is coated. After the plates are separated and dried, samples are applied and can be developed within 5-10 min in a small covered bottle, using chloroform:methanol:water 60:25:4 (v:v:v) as a

solvent. Material on the plates is detected by spraying with 40 g/l of phosphomolybdic acid in 95% ethanol, then heating on a hotplate (184).

The column was eluted with 1 liter of 7.5% methanol in chloroform, 1 liter of 10% methanol, 1 liter of 12.5% methanol, 1 liter of 15% methanol, 1 liter of 17.5% methanol, 1 liter of 20% methanol, 1 liter of 22.5% methanol, and 1 liter of 35% methanol, and all of these fractions were discarded. The next elution was with 69 liters of 35% methanol. The first 35 liters showed very little contamination and this fraction was retained and the solvent evaporated, then lipid was taken up in 10% methanol in chloroform. A second column purification was carried out on a 3 cm-diameter X 15 cm column of Unisil. The sample was applied and the cclumn was eluted with 1.5 liters of 10% methanol in chloroform, discarding this fraction. Elution with 22 liters of 30% methanol was then carried out, and the first 13.5 liters retained and the solvent evaporated. The yield was 2.96 g of lipid which chromatographed as a single spot having the Rf of authentic egg yolk lecithin. This was stored at -20°C dissclved in chloroform under nitrogen, and in the dark.

Sterol exchange

Sterols and egg yolk lecithin were combined at a ratio of 0.6 g cholesterol/g lecithin, or 0.8 g (cholesterol + cholest-4-en-3-cne)/g lecithin in 40 ml stainless steel Sorvall centrifuge tubes, and 0.5 ml buffer per mg of lecithin was added to the mixture. The ratio of cholesterol to cholest-4-en-3-one varied and is given in the figure legends. A total volume of 10-20 ml (20-40 mg lecithin) was used per tube. These mixtures were sonicated on ice under nitrogen for 20 min each in four 5 min bursts using a Biosonik III probe-type sonicator at 180 watts. After sonication, the dispersions were centrifuged for 1 hr at 48,000Xg to remove titanium powder and undispersed lipid. The supernatants were then diluted 1-fold with buffer, and erythrocytes were added to a level of about 0.12 ml of packed cells per mg of lecithin. These mixtures were incubated for 2-8 hr at 37°C in the warm room, mixing by continuous inversion at 50 rpm, then cells were washed twice in buffer by centrifugation before equilibration with permeant (170).

Determination of intracellular volumes

The sum of intracellular plus extracellular volume of a suspension of erythrocytes was determined by dilution of [^{14}C]-3-O-methyl glucose, a non-metabolizable glucose analog which we found to rapidly permeate human erythrocytes, and

the extracellular space by dilution of [^{14}C]-sucrose, which does not permeate the cells (185). The hematocrit of an approximately 50% cell suspension was determined in quadruplicate, then 0.2 ml of suspension was diluted in triplicate with 0.2 ml of buffer containing either [^{14}C]-sucrose or [^{14}C]-3-O-methyl glucose. After allowing the 3-O-methyl glucose to equilibrate across the membrane for 30 min at room temperature, the cells were centrifuged out of the suspension at top speed on the clinical centrifuge for 5 min, then 0.2 ml aliquots of the supernatants, and of the original label solutions, were counted for radioactivity in Aquasol. The intracellular and interstitial volumes per ml of packed cells were calculated as follows:

$$\frac{\text{Sugar space}}{\text{ml suspension}} = \frac{\text{(CPM/ml label-CPM/ml Supernatant)}}{\text{CPM/ml Supernatant}}$$

$$\frac{\text{Intracellular volume}}{\text{ml packed cells}} = \frac{\text{3-O-CH3-glucose space-sucrose space}}{\text{hematocrit}}$$

$$\frac{\text{Interstitial volume}}{\text{ml packed cells}} = \frac{\text{sucrose space+hematocrit-1}}{\text{hematocrit}}$$

Transport measurements

Rapid sampling method: A 10 ml Hamilton gas tight syringe (Hamilton 1010LT) was used as a reaction vessel, and aliquots of 0.2 ml were expelled at various times with a

Hamilton repeating dispenser (Hamilton P16600), which delivers 1/50 of the total volume of the syringe each time the button is pressed.

The apparatus was fitted with a water jacket to control temperature, constructed from acrylic plastic, and with an adjustable stop on the repeating dispenser so that a reproducible volume of solvent could be rapidly sucked up. The reproducibility of the volume dispensed was determined by repeatedly dispensing aliquots of a solution of amido black 10B stain into 10 ml of water, then measuring the absorbance at 600nm of the resulting solutions.

The efflux of permeants was initiated by rapidly sucking buffer into the syringe containing a small volume of a thick suspension of preloaded erythrocytes. To assess the efficiency of initial mixing with this procedure, the homogeneity of the suspension created by sucking up buffer into a thick erythrocyte suspension was determined by delivering aliquots at various times, then lysing the cells and measuring the concentration of the hemoglobin released.

To lyse the erythrocytes, 0.2 ml aliquots were dispensed into 10 ml of oxygen-saturated buffer (5mM NaCl, 5mM tris-HCl, pH=6.5), and the solutions were mixed at room temperature, then centrifuged for 20 min at 48,000Xg. The hemoglobin was assayed by the absorbance at 540nm of the supernatants (186).

D-Glucose efflux: Erythrocytes were washed three times by suspending in buffer containing D-glucose at 5, 7, 10, 20, or 40mM and incubating for 30 min at room temperature to allow equilibration of the glucose across the cell membrane, then centrifuging and aspirating the supernatant. The final suspensions, at hematocrits of approximately 40%, were then preloaded with labelled permeant by adding 0.8 ml of each suspension to an analytically insignificant amount of dry [^{14}C]-D-glucose and incubating for 45 min at room temperature. To measure efflux, preloaded cell suspensions were centrifuged briefly in the clinical centrifuge, then supernatants were aspirated and 0.2-0.4 ml of packed cells were added to the Hamilton syringe and the plunger inserted far enough to expel all the air. Efflux was initiated by rapidly sucking up buffer containing the same concentration of unlabelled D-glucose as is in the cell suspensions, thus diluting extracellular radioactivity. After discarding one aliquot, a zero time sample was added to quench solution immediately (within 4 seconds), and the timer started at the same time. Five more 0.2 ml aliquots were taken at 3 or 5 sec intervals. The quench solution consisted of the complete suspending buffer, plus 1.25mM KI, 0.001mM HgCl2 and 0.1mM phloretin (162). Three ml of this solution were layered over 6 ml of dibutyl phthalate in 15 ml conical centrifuge tubes, and these tubes were kept at 0°C on ice. Within two minutes of sampling, the tubes were centrifuged at top speed on the

clinical centrifuge for 3 min. This caused the resolution of the components of the mixture into an upper layer of cell-free aqueous medium, and a pelleted cell mass, separated by the dibutyl phthalate (103). To determine the amount of radioactive glucose released by the cells at various times, 1 ml of the aqueous supernatant was added to 10 ml of Aquasol and counted. The infinite time samples were obtained in duplicate for each reaction by adding aliquots of the reaction mixture to 3 ml of buffer layered over dibutyl phthalate, then centrifuging these tubes after a 1 hr incubation at room temperature. The hematocrit of each reaction mixture was determined, after concentrating the suspension 3-fold by centrifuging a measured volume, removing a volume of supernatant which was 2/3 as great, then resuspending the cells in the fluid remaining.

Uridine efflux: The procedures for preloading cells and measuring efflux were the same as for glucose flux experiments. The concentrations of uridine were 0.2, 0.3, 0.5, 1.0, and 4.0mM and sampling was done at 5 or 10 sec intervals. The quench solution used consisted of 0.05mM 6-[(2-hydroxy-5-nitrobenzyl)thio]guanosine in buffer (106).

Uridine passive flux

We showed that uridine flux occurs by passive diffusion in the presence of 0.05mM 6-[(2-hydroxy-5-nitrobenzyl)thic]guanosine (HTG), by demonstrating lack of saturability under these conditions. Erythrocytes in buffer, or buffer containing added 4.5mM uridine, were preloaded by incubation for 30 min at room temperature with 0.02mM [^{14}C]-uridine, then 0.25 volumes of 0.25mM HTG in buffer were added to each suspension to a final concentration of 0.05mM. The cell suspensions were concentrated by centrifugation, and efflux at 37°C initiated by adding 2 ml of quench solution (0.05mM HTG in isotonic buffer), with or without 4.5mM uridine present, to 0.3 ml of preloaded cells. Aliquots of 0.2 ml of the reaction mixture were taken at various times up to 45 min and immediately added to 3 ml of ice cold quench solution layered over 6 ml of dibutyl phthalate and centrifuged. Portions of the aqueous supernatants were counted for radioactivity in Aquasol.

Since no evidence of saturability was seen, the buffer solution routinely used for measurement of passive uridine flux contained 10mM inosine, rather than glucose. In one experiment, the rate of passive uridine uptake was also measured in order to verify that the apparent change in passive flux rate seen when membrane cholesterol is exchanged with other sterols was not an artifact resulting from a differential susceptibility of the two erythrocyte

preparations to lysis. Subsequently, only uptake of uridine was routinely measured. To measure passive uridine uptake, 0.7 ml of cells suspended in isotonic buffer containing 0.05mM HTG was incubated at 37°C with an equal volume of [^{14}C]-uridine in the same buffer. Aliquots of 0.2 ml were taken at 0, 10, 20, 30, and 40 min into 3 ml of ice cold quench solution in 15 ml conical centrifuge tubes and immediately centrifuged for 1 min at top speed on the clinical centrifuge in the cold room. The supernatants were aspirated, and cells were washed 3 times by resuspending and recentrifuging. The hematocrit was determined on an aliquot of the reaction mixture, after concentrating the cells by centrifugation and removal of part of the supernatant. To extract radioactivity from the cells, they were lysed by the addition of 0.75 ml of distilled water, followed by vortexing. Then 0.75 ml of 10% TCA (trichloroacetic acid) was added to each sample to precipitate the proteins and the tubes were spun for 10 min at top speed in the clinical centrifuge. Aliquots of 1 ml of the supernatants were counted for radioactivity in 10 ml of Aquasol.

Glucose efflux from liposomes

The rate of diffusion of D-glucose out of liposomes prepared from erythrocyte membrane lipids was measured using a modification of the procedure outlined by Demel *et al.* (187). After extraction and column purification of lipids,

liposomes were prepared by vortexing the lipid under nitrogen with a 1 cm-diameter glass bead with 0.05 ml of 300mM D-glucose per mg of lipid. The resulting suspensions were stored at 4°C overnight, then dialyzed at 4°C against 70 ml of isctonic salt solution (75mM KCl, 72mM NaCl, 2mM Mg^{2+}-acetate) fcr 5 consecutive 45 min periods, stirring by bubbling nitrogen through the salt solution. When the effects of anesthetics were determined, the anesthetic tested was present in both the glucose solution and the salt solution used for dialysis. The reaction mixture used for glucose determination contained 8.8 units/ml of hexokinase (Sigma type F-300 sulfate-free), 0.9 units/ml of glucose-6-phosphate dehydrogenase (Sigma type XV), 1mM ATP, 0.5mM NADP, 75mM KCl, 72mM NaCl, 2mM Mg^{2+}-acetate and 28mM tris-HCl, pH=8.0. The solution used for a reference contained all of these components except for NADP. The double-beam spectrophotometer (Beckman model DB-GT) was zeroed at a wavelength of 340nm with 2.0 ml of reaction mixture in the sample cell and reference solution in the reference cell. For the initial reading, 0.01 ml of liposome suspension was added to each cell and mixed, then the absorbance read after 5 min. The same reference was used, with fresh reaction mixture, for each subsequent reading. The liposome suspensions were incubated at 50°C, and a sample removed for assay at 0, 20, 40, 60, and 80 min. After reading the absorbance of the 80 min sample, 0.2 ml of 10% triton X-100 was added to both cuvettes to release all the

glucose remaining in the liposomes for the infinite time reading. This last absorbance was multiplied by 1.1 to correct for dilution. This assay system couples NADP reduction tc oxidation of glucose-6-phosphate, so that the change in absorbance at 340nm due to the presence of NADPH is proportional to the amount of glucose accessible to the hexokinase. Since the lipid vesicles are impermeable to both enzymes, only extravesicular glucose is detected. Any glucose initially present because of incomplete dialysis is accounted for by subtracting the zero time absorbance from the other readings. The results are plotted as the % of the infinite time value vs time, which corrects for differences in the amount cf lipid, thus of trapped glucose, present.

Analytical procedures

Preparation of ghosts: Erythrocyte ghosts were prepared following the method of Dodge et al. (188). Cells were washed four times in 300mosM phosphate buffer, pH=7.4, aspirating the top layer of the pellet each time to remove all of the buffy coat. The washed erythrocytes were lysed by the addition of 19 volumes of distilled water, then centrifuged at 27,000Xg for 45 min after standing for 20 min at room temperature. The supernatant was carefully decanted and the membranes washed three times in 15mosM phosphate buffer, pH=7.4.

Lipid extraction and fatty acid analysis: Because it has been suggested that heme pigments catalyze autoxidation of erythrocyte membrane lipids, lipids were extracted from ghosts rather than whole cells (189). All the solvents were deoxygenated immediatly before use by vigorously bubbling nitrogen through them for 5 min, and all operations were carried out under nitrogen or carbon dioxide. Lipids were extracted and purified by the methods described in Chapter II, with the additional precaution that samples were not taken completely to dryness during solvent evaporation and the vacuum was always released to nitrogen rather than air to avoid oxidation of the lipids.

Sterol analysis: Purification of membrane sterols was carried out using methods described by Bruchovsky (190). For column chromatography, Mallinckrodt No. 2847 silicic acid was used. Seven grams of this adsorbant were washed on a sintered glass funnel with 4 changes of 3N HCl, then with distilled water until the pH of the effluent was between 4 and 5. After washing three times with acetone and drying under an infrared lamp, the silicic acid was activated at 100° for 1 hr and packed in a 1 cm-diameter glass column in a slurry in chlcroform:methanol 4:1 (v:v). The column was washed with 75 ml of this solvent, then 75 ml of chloroform. Erythrocyte membrane lipid extract was applied in chloroform and eluted with 225 ml of chloroform, then the effluent was concentrated by evapcration of solvent for thin layer chrom-

atography. For TLC, Woelm Neutral Alumina was activated at 150°C for 4 hr, then spread in a 0.25mm thick layer on a 20X20 cm glass plate as a slurry of 17 g adsorbant in 20 ml of water. The plate was dried at 37°C overnight before use. The column-purified lipid was applied in a line 10 cm long and standards of 0.02 mg each of cholesterol or cholest-4-en-3-one were also applied to the plate. The chromatogram was developed twice to within 3.5 cm of the top using cyclohexane:ethyl acetate 7:3 (v:v), containing 0.05% acetic acid. After staining the standards with phosphomolybdic acid, regions of the plate containing sterols were scraped off and the material eluted from the adsorbant with chloroform. The sterol content was analyzed by GLC at a temperature of 196°C on 3% QF-1 packed on Gas-Chrom Q (100-200 mesh) packed in a 210 cm X 3 mm glass column.

Measurement of hematocrits: Hematocrits of erythrocyte suspensions were determined in capillary tubes using an Adams-Readacrit micro-hematocrit centrifuge and spinning for 5 min. The values for independent determinations carried out on the same suspension varied by less than 1%.

III Results

Effect of HTG on saturability

Figure 32 shows the time course of efflux of [^{14}C]-uridine from erythrocytes in the presence of 0.05mM 6-[(2-hydroxy-5-nitrobenzyl)thio]guanosine (HTG) at 37°C. It is seen that the efflux of labelled uridine is not affected by the presence of 4.5mM unlabelled uridine. This lack of saturability was taken as evidence for the permeation of uridine by passive diffusion in the presence of 0.05mM HTG.

Mixing efficiency in syringe reaction vessel

Table VI shows the absorbances at 600nm of solutions prepared by dispensing aliquots of a concentrated dye solution into 10 ml of water with the syringe and repeating dispenser apparatus. The reproducibility of the volumes of solution delivered by this apparatus is very good, with a standard deviation of less than 0.5% of the volume.

Table VII shows the absorbance due to hemoglobin released from erythrocytes after mixing them with buffer, then delivering aliquots of the suspension into a lysing buffer at various times. The reproducibility seen (standard deviation < 1%) indicates that the suspension was quite homogeneous after mixing—that is, mixing was complete and settling of the cells did not occur to an appreciable extent

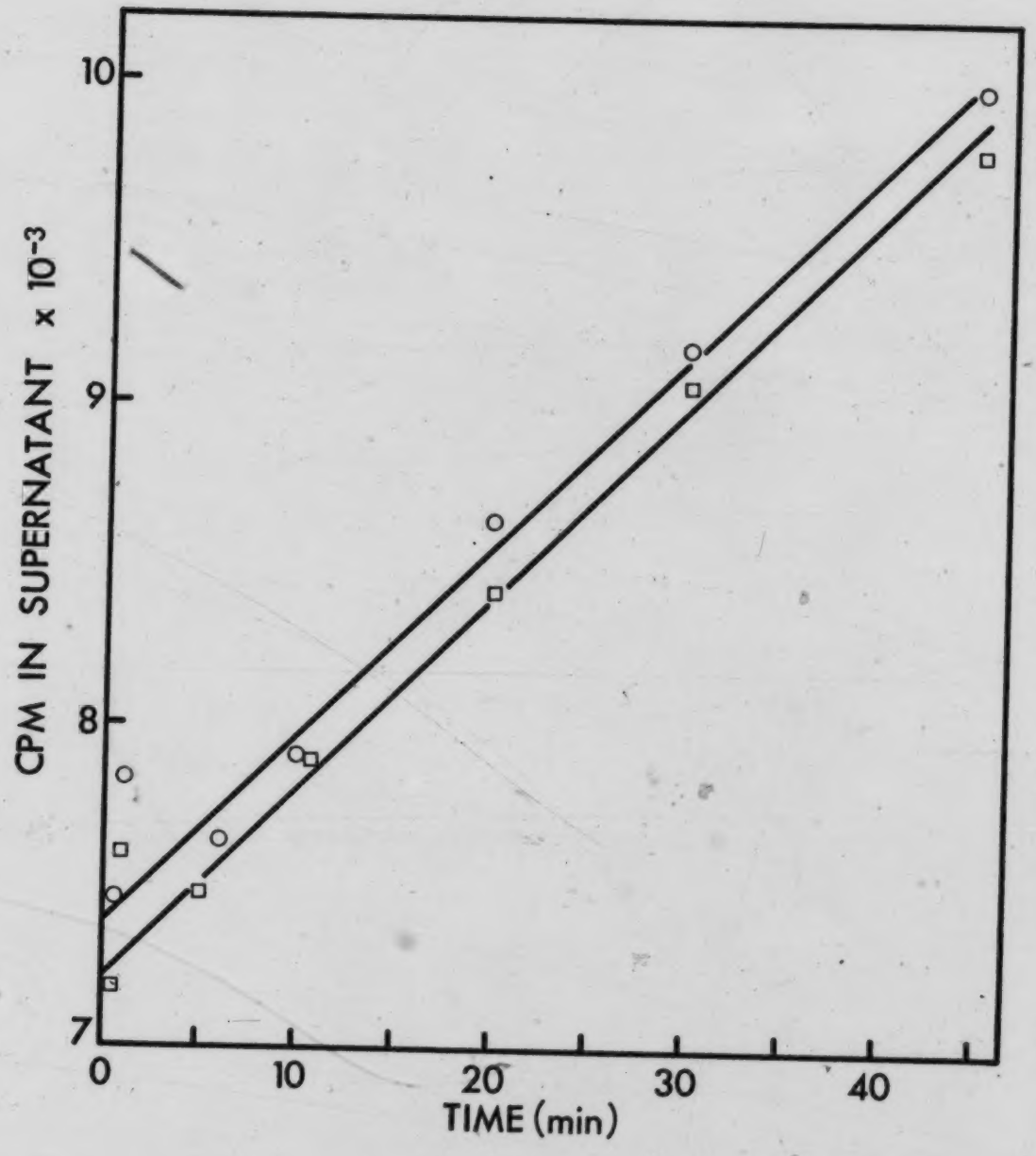

Figure 32. Passive Efflux of Uridine from Erythrocytes. Erythrocytes preloaded with 0.02mM [^{14}C]-uridine were incubated at 37°C in buffer in the presence of 0.05mM HTG, with or without 4.5mM unlabelled uridine present. The radioactivity external to the cells was determined after adding to ice cold quench solution at the times shown.
o–o, control (0.02mM); □–□, 4.52mM uridine

TABLE VI

REPRODUCIBILITY OF VOLUME DISPENSED BY SYRINGE

Number	Absorbance	Volume of Aliquot[1]
1	0.700	0.205 ml
2	0.688	0.201 ml
3	0.698	0.204 ml
4	0.701	0.205 ml
5	0.700	0.205 ml
6	0.698	0.204 ml
	Mean = 0.204 ml ± 0.001 ml (S.D.)	

[1]Volumes are calculated from the known absorbance of the original dye solution.

TABLE VII

HOMOGENEITY OF CONTENTS OF SYRINGE AFTER MIXING

Time after mixing	Absorbance at 540nm[2]
10 sec	0.305
20 sec	0.305
30 sec	0.308
45 sec	0.304
60 sec	0.302
2 min	0.301
3 min	0.310
Mean = 0.305 ± 0.003 (S.D.)	

[2]Absorbance is due to hemoglobin released, after lysing the cells in the aliquots delivered and centrifuging out membranes.

within 3 min. In the lysing buffer used, a plot of absorbance at 540nm *vs* amount of cells added was linear up to an absorbance of at least 1.4, so solubility of the hemoglobin was not a limiting factor.

Effects of anesthetics on permeabilities

The effects of 100mM ether and of 50mM procaine hydrochloride on the efflux of D-glucose from liposomes formed from human erythrocyte membrane lipids are shown in figure 33. Both of these anesthetics increase the permeability of liposomes to glucose, presumably by increasing the fluidity of the hydrocarbon interior of the bilayer. The fact that the first experiment (a) gives straight plots, while the second (b) gives curved plots may be due to some differences in the geometry of the liposomes, as they were prepared from different lipid extracts on different days. Within each experiment, however, the liposomes used with anesthetic and the control liposomes were prepared at the same time under exactly the same conditions. Because only lipids are present, the differences in permeability seen can be considered to be due to fluidization of the lipid region. The effects of these anesthetics on the uptake of [^{14}C]-uridine in human erythrocytes by passive diffusion is shown in figure 34. It is obvious that both ether and procaine increase the permeability of the membrane to uridine under these

Figure 33. Effect of 100mM Ether and of 50mM Procaine-HCl on Glucose Efflux.
Liposomes formed in the presence of 300mM glucose were incubated at 50°C, and the amount of glucose that had escaped measured at 20 min intervals by determining the absorbance at 340nm of NADPH produced by the reduction of NADP coupled to oxidation of glucose-6-phosphate.
(a) o–o, control; □–□, 100mM ether
(b) o–o, control; x–x, 50mM procaine-HCl

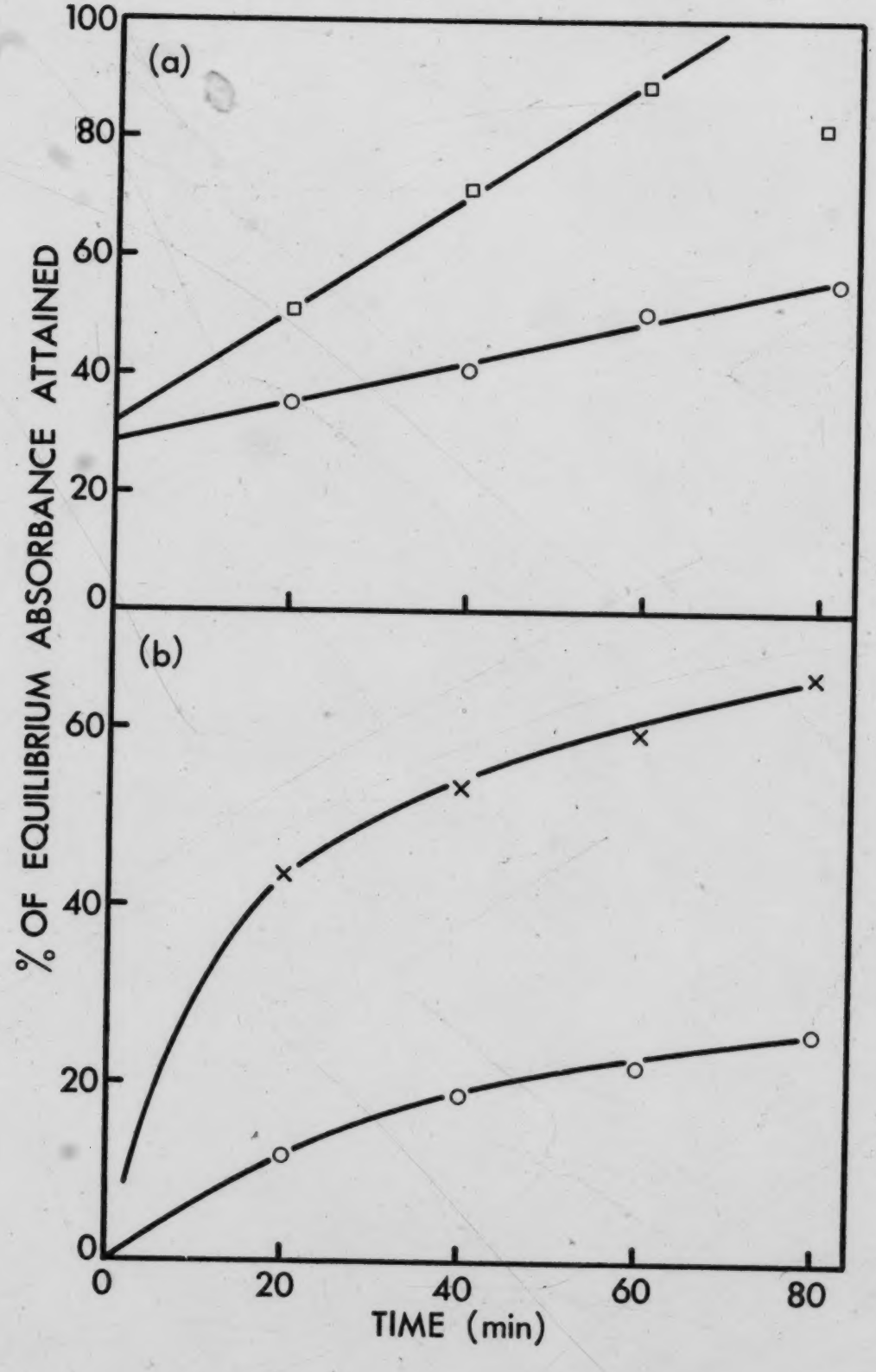
(a)
(b)
% OF EQUILIBRIUM ABSORBANCE ATTAINED
TIME (min)
0
20
40
60
80
100

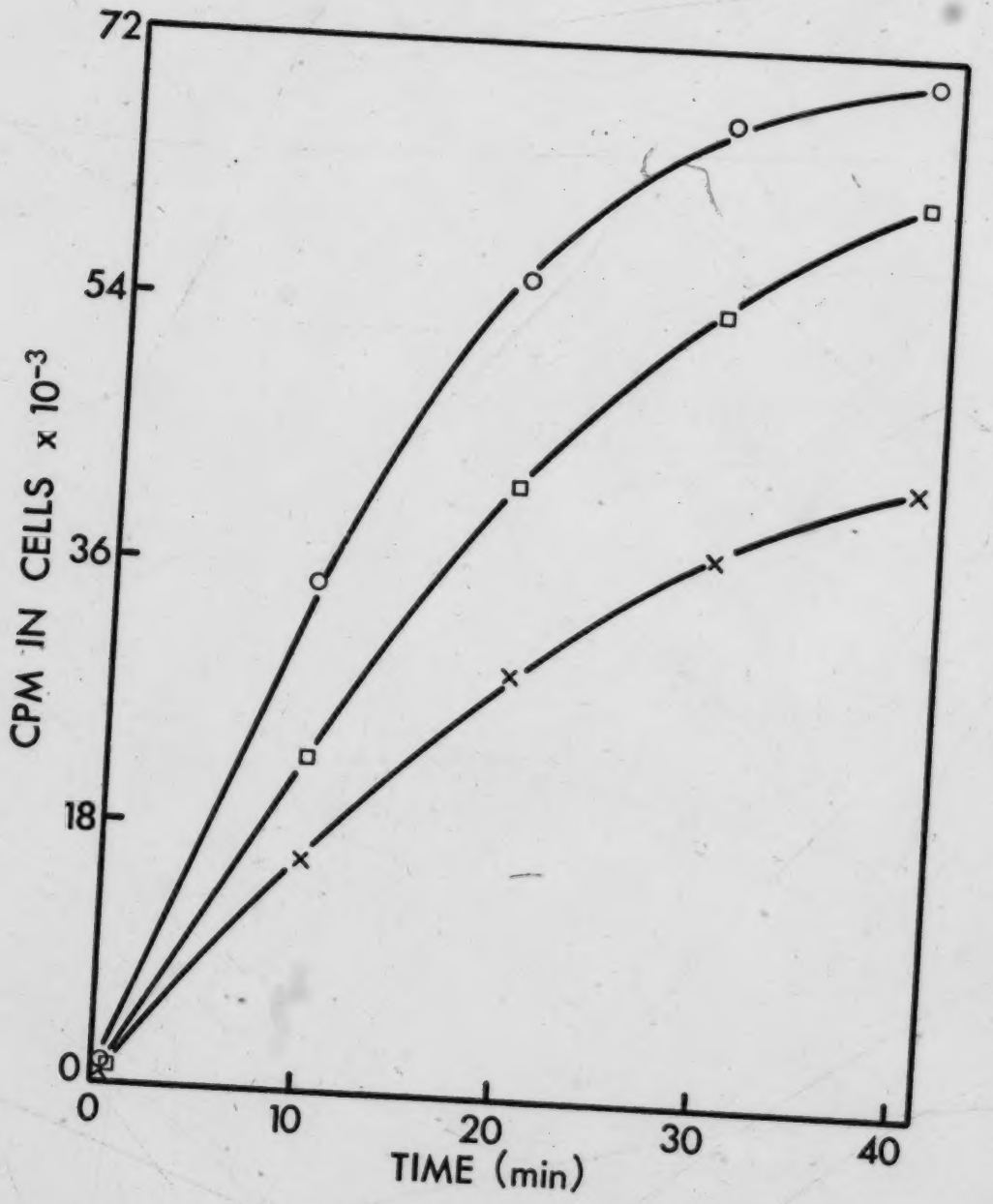

Figure 34. Effects of Ether and Procaine-HCl on Passive [^{14}C]-Uridine Uptake by Erythrocytes.
Erythrocytes were incubated at 37°C with [^{14}C]-uridine in the presence of 0.05mM HTG in the presence or absence of anesthetic.
x–x, control; □–□, 50mM procaine-HCl; o–o, 100mM ether.

conditions.

Figure 35 is a Lineweaver-Burk plot of D-glucose equilibrium exchange efflux from erythrocytes in the presence and absence of these anesthetics. The values for Km and Vm obtained from the reciprocals of the intercepts are 55.6mM and 100 micromoles/min/ml packed cells for the control, and 55.6mM and 73.5 micromoles/min/ml packed cells in the presence of 100mM ether. Thus, it appears that ether does not alter the affinity of the carrier for glucose, but reduces the maximum velocity. This is the opposite effect to what might be expected solely on the basis of the effect of ether on the lipid phase, since it seems to increase its bulk fluidity. In the presence of 50mM procaine-HCl, both the Km and the Vm are infinite; in other words efflux is occurring by a non-saturable process (passive diffusion). It seems that procaine inhibits facilitated diffusion, but at the same time increases the passive flux of glucose to a level comparable to the facilitated diffusional flux obtained in the absence of this anesthetic.

Figure 36 shows the equilibrium exchange efflux for uridine in the presence and absence of ether and procaine, with an inset Lineweaver-Burk plot of flux in the control and in the presence of 100mM ether. Although the data show relatively large deviations from linearity on the Lineweaver-Burk plots, it can be seen that the effects of these anesthetics on uridine flux are similar to their

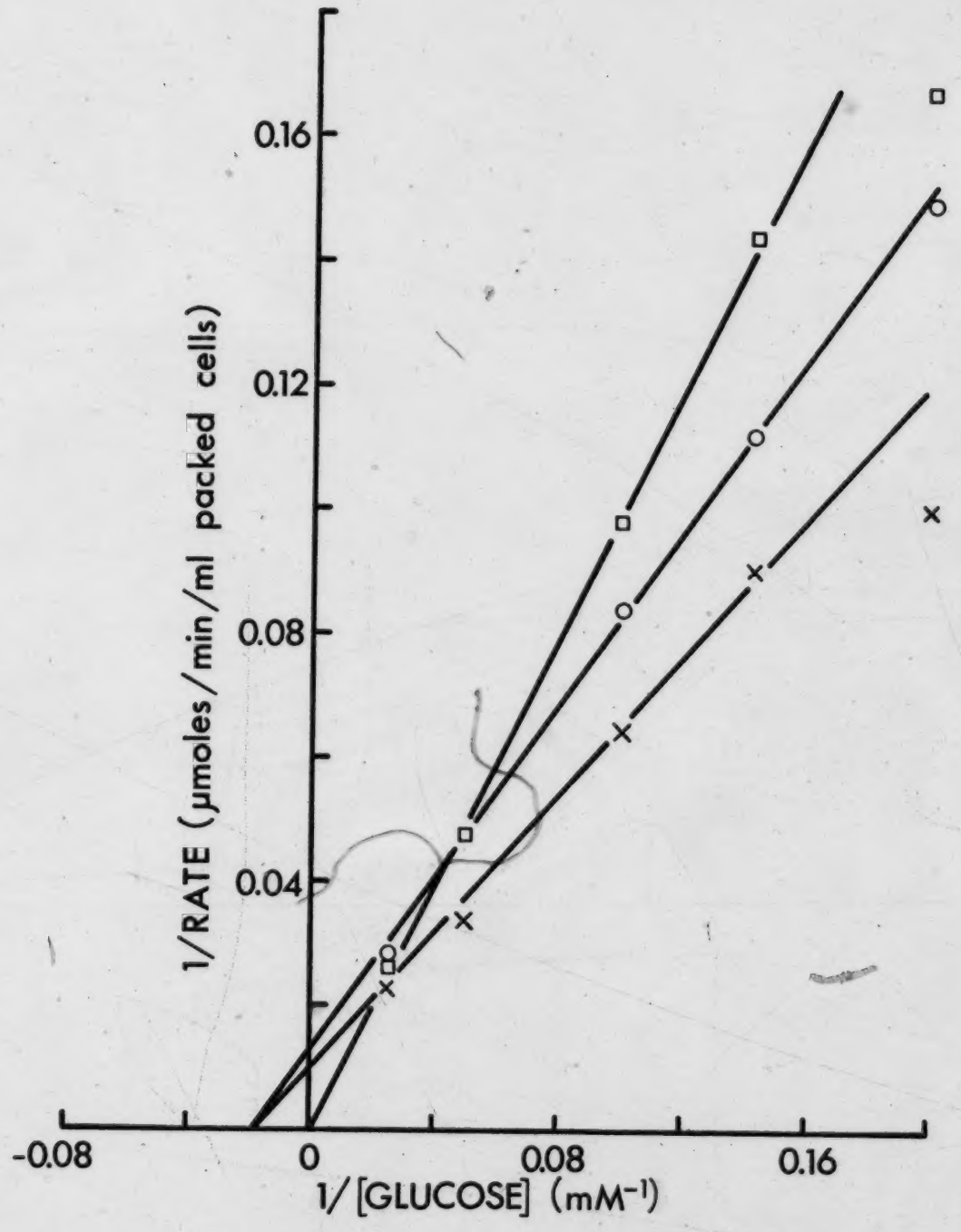

Figure 35. Effects of Ether and Procaine-HCl on D-Glucose Equilibrium Exchange Efflux.
Efflux rates were determined at 15°C as described on pages 126-127.
x-x, control; □-□, 50mM procaine-HCl; o-o, 100mM ether.

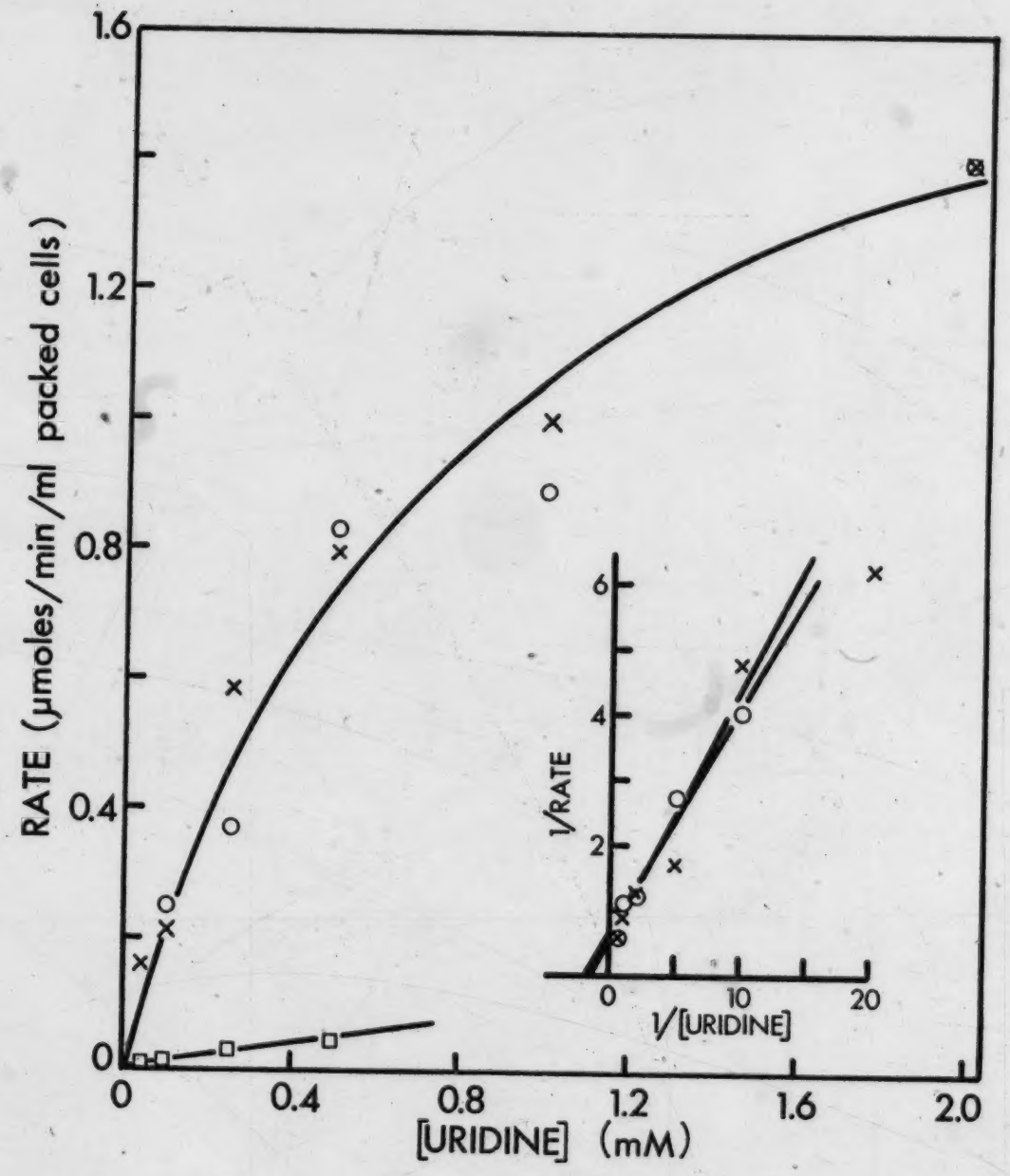

Figure 36. Effect of Ether and Procaine-HCl on [^{14}C]-Uridine Efflux from Erythrocytes.
Efflux rates were determined at 15°C as described in Methods. Inset=Lineweaver-Burk Plots.
x–x, control; □–□, 50mM procaine-HCl; o–o, 100mM ether.

effects on glucose flux. No unequivocal change in rate is seen with 100mM ether, but 50mM procaine strongly inhibits flux. This inhibition is more noticible than in the case of glucose, since the component of uptake which is mediated is apparently much greater for the uptake of uridine than of glucose. This means that compensation for the inhibition of facilitated diffusion by faster passive flux in the presence of procaine is much less significant. The values of Km and Vm obtained from the Lineweaver-Burk plot of these data are 0.59mM and 1.6 micromoles/min/ml packed cells in the control, and 0.81mM and 2.0 micromoles/min/ml packed cells in the presence of 100mM ether. Because of the quality of the data, it is difficult to say whether or not these values really differ significantly from each other.

Effects of sterol exchange on permeabilities

In contrast to the results presented by Bruckdorfer et al. (109), exchange of cholest-4-en-3-one for membrane cholesterol often made the cells so fragile that they all lysed upon subsequent manipulation. This effect was rather irreproducible from one batch of erythrocytes to the next; conditions which induce cell lysis in one case barely changed the passive permeability in another. For this reason, the passive permeation of the cells by uridine was determined in each experiment to serve as a control to demonstrate that a significant alteration in membrane lipid

fluidity had actually been achieved.

Figure 37 shows the effects of exchange of cholest-4-en-3-one for membrane cholesterol on the passive uptake and efflux of [^{14}C]-uridine. It is obvious that incubation of the cells with cholest-4-en-3-one increases the rates of both uptake and efflux of uridine, as compared to incubation with cholesterol, thus the apparent alterations in rate are not artifacts due to altered membrane fragility. Subsequently, only uridine uptake was determined for the controls.

Figure 38 shows the effect on passive uridine flux of incubating erythrocytes with 12 mg of cholesterol plus 12 mg of cholest-4-en-3-one per 30 mg of lecithin for 2 hr at 37°C. Control cells are incubated with cholesterol plus lecithin. Figure 39 is a Lineweaver-Burk plot of D-glucose equilibrium exchange efflux in these same cells. By measuring the slopes of the tangents to the curves in figure 38 at zero time, it is determined that the initial rate of uptake of uridine in the cells incubated with cholesterol is only about 65% of the rate in those incubated with cholest-4-en-3-one. However, the values of Km for glucose flux are approximately the same in both groups (33.3mM) and the value for Vm is actually about 15% smaller for cells incubated with cholest-4-en-3-one (75 micromoles/min/mg packed cells vs 90 micromoles/min/ml packed cells for the control).

Figure 37. Effects of Sterol Exchange on Passive Fluxes. Erythrocytes were incubated at 37°C for 6.5 hr with sonicated dispersions of 12mg cholesterol plus 20mg of lecithin, or 12mg cholesterol, 10mg cholest-4-en-3-one plus 20mg lecithin. Determinations of uridine flux at 37°C were carried out in the presence of 0.05mM HTG as described on page 131.
(a)=uptake, (b)=efflux
x–x, cholesterol; o–o, cholest-4-en-3-one.

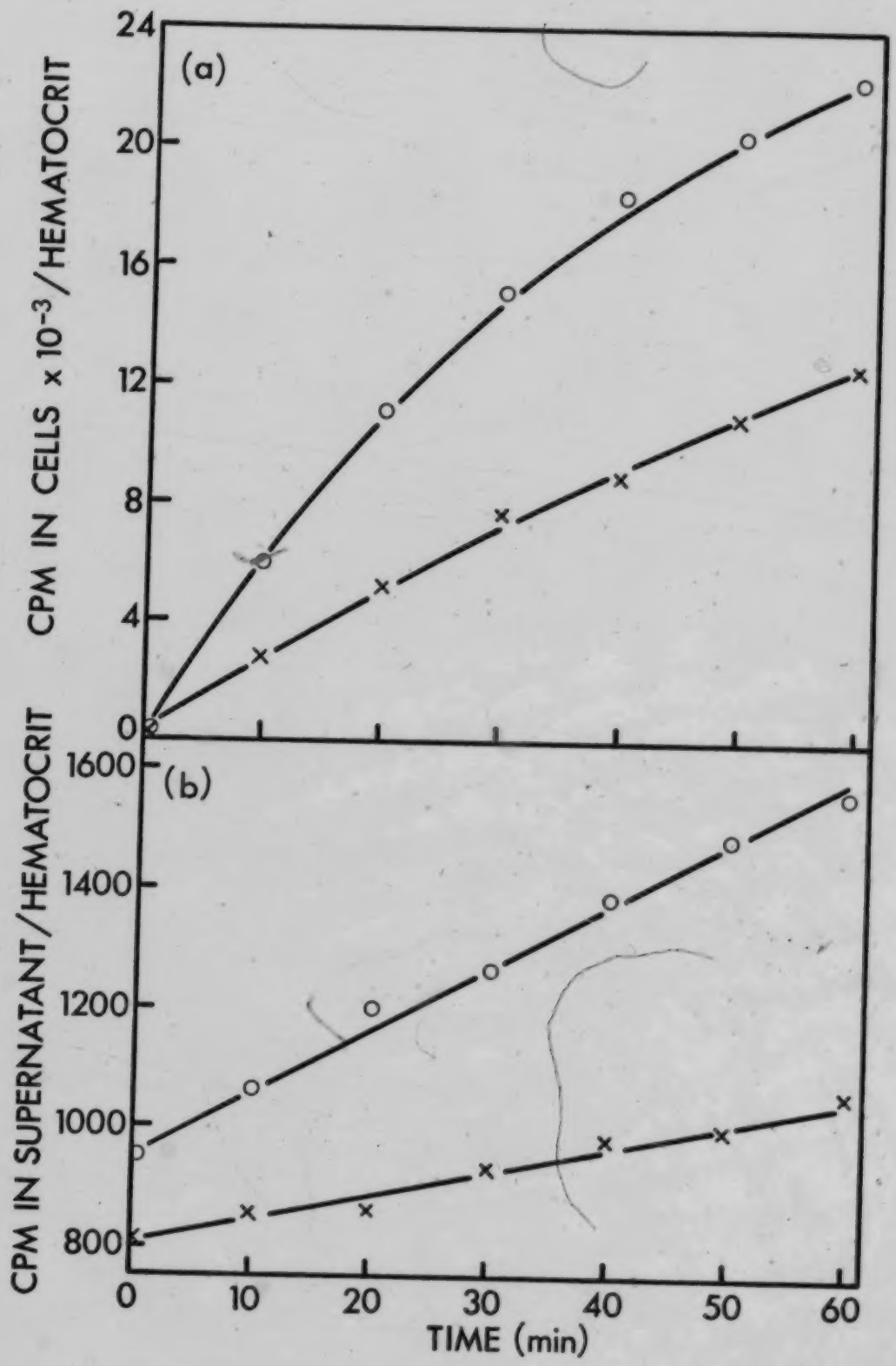
(a)
(b)
CPM IN CELLS x 10⁻³/HEMATOCRIT
CPM IN SUPERNATANT/HEMATOCRIT
TIME (min)
0
4
8
12
16
20
24
800
1000
1200
1400
1600
0
10
20
30
40
50
60

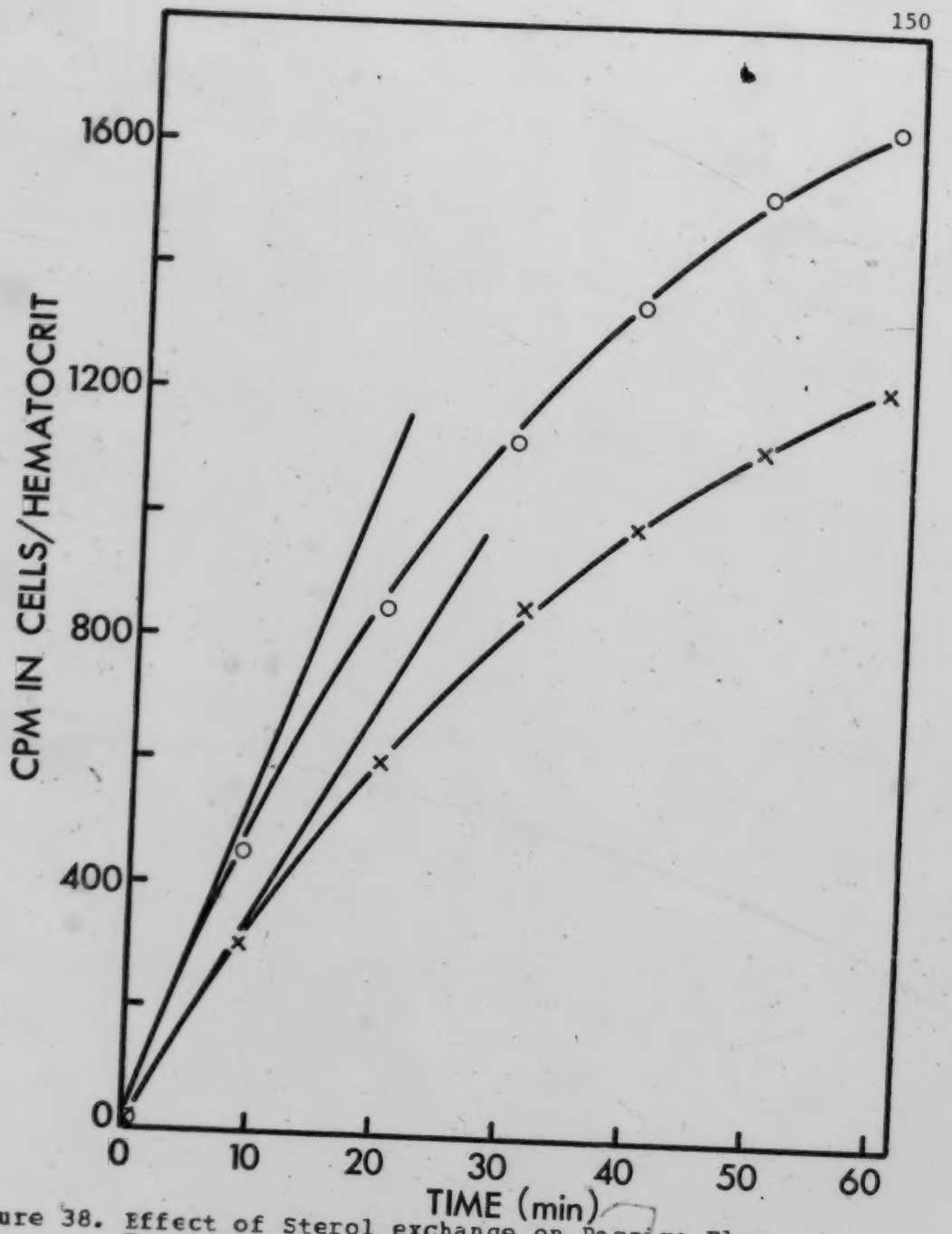

Figure 38. Effect of Sterol exchange on Passive Flux. Erythrocytes were incubated for 2 hr at 37°C with sonicated dispersions or 12 mg cholesterol plus lecithin or cholesterol and 12 mg cholest-4-en-3-one plus lecithin and rates of uptake of uridine at 37°C were determined in the presence of 0.05mM HTG.

x–x, cholesterol; o–o, 12 mg cholesterol plus 20 mg cholest-4-en-3-one'

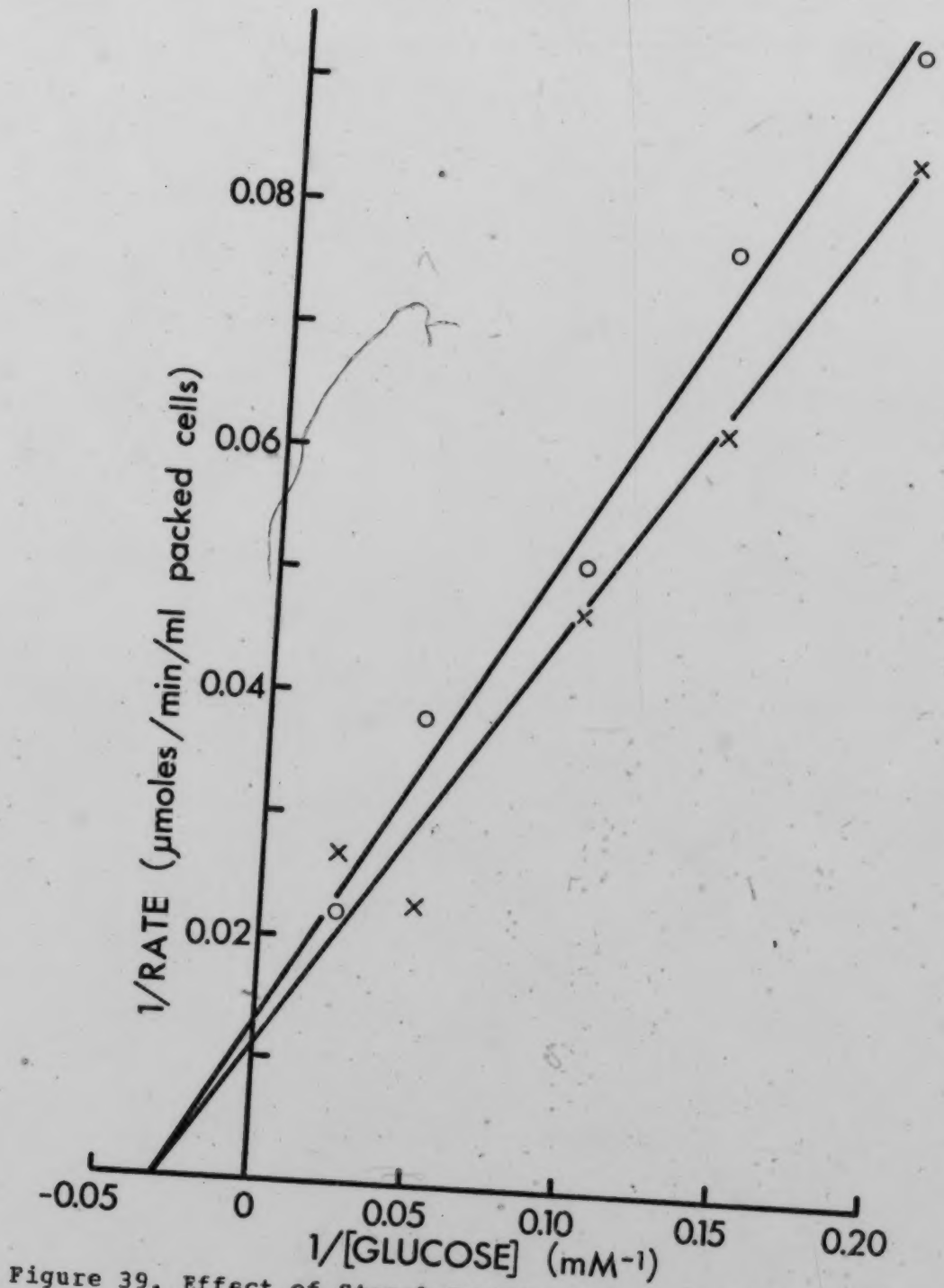

Figure 39. Effect of Sterol Exchange on Glucose Efflux. Rates of equilibrium exchange efflux of D-glucose from the same sterol-exchanged erythrocytes as shown in figure 38 were determined at 15°C. x–x, cholesterol; o–o, cholest-4-en-3-one.

Figures 40 and 41 show the effects on uridine passive flux, and on uridine equilibrium exchange efflux, of incubation of erythrocytes for 4 hr at 37°C with cholesterol plus lecithin, or cholesterol and cholest-4-en-3-one plus lecithin. Also included in these data are a control using cells which have not been incubated with sterol-lecithin mixtures. Analysis of membrane sterols of cells used in this experiment showed that approximately 13% of the cholesterol of the membrane was exchanged for cholest-4-en-3-one under the conditions used. It is seen in figure 40 that incubation of the erythrocytes with cholesterol decreases their passive permeability, and that cholest-4-en-3-one increases passive permeability, with respect to untreated cells. The behavior shown in figure 41, a Lineweaver-Burk plot of uridine efflux rates, is slightly more complex. The effects of incubation with sterols are summarized in Table VIII. The Km is increased by incubation with cholesterol, but not significantly affected by incubation with cholest-4-en-3-one. The Vm is decreased by incubation with both sterols, with cholesterol alone causing a smaller decrease than in the presence of both sterols.

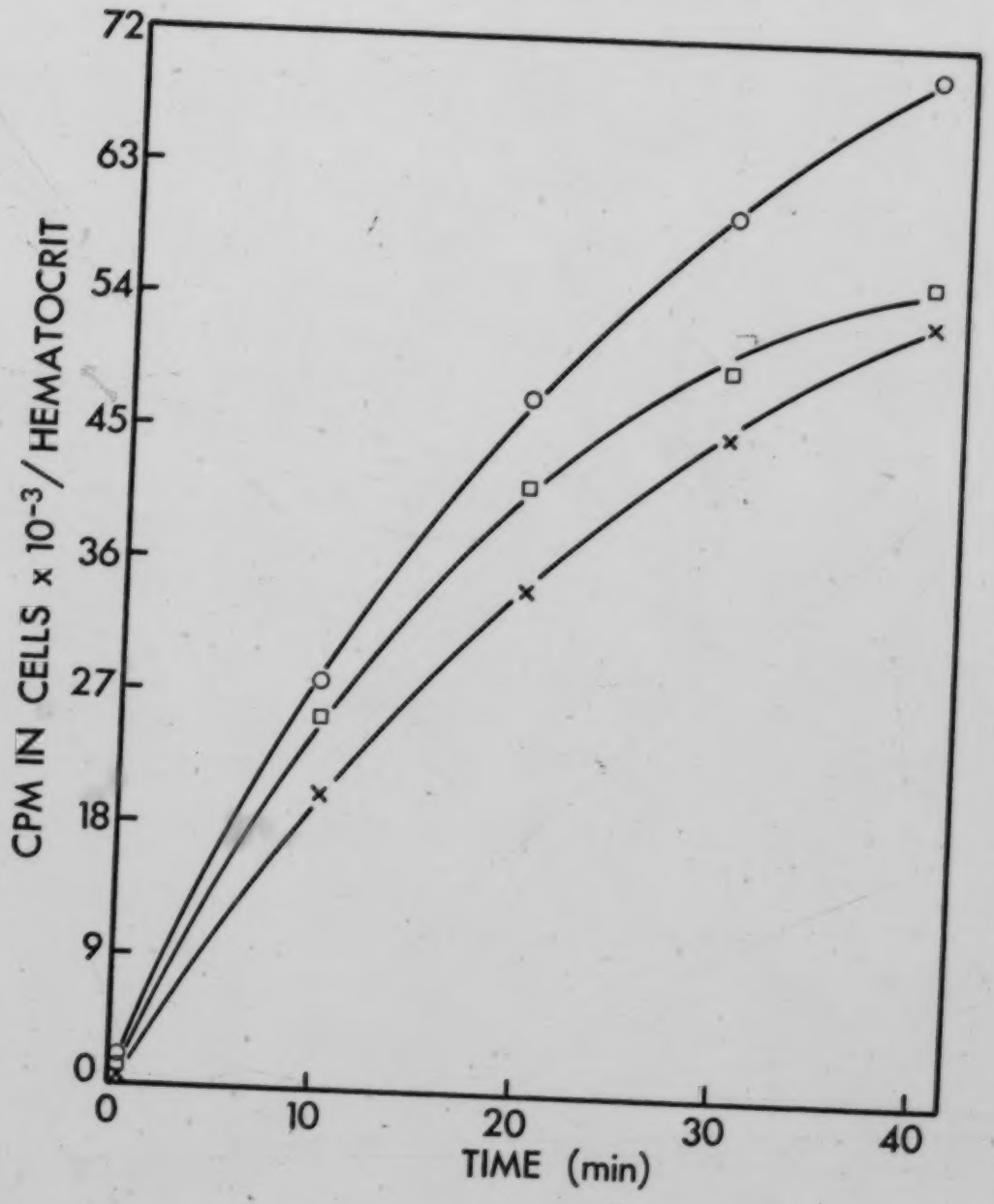

Figure 40. Effect of Sterol Exchange on Passive Uridine Flux. After exchanging membrane cholesterol at 37°C for 4 hr with sterols bound to egg lecithin, cells were incubated at 37°C with [^{14}C]-uridine in the presence of 0.05mM HTG.
x–x, cholesterol; □–□, control; o–o, cholest-4-en-3-cne.

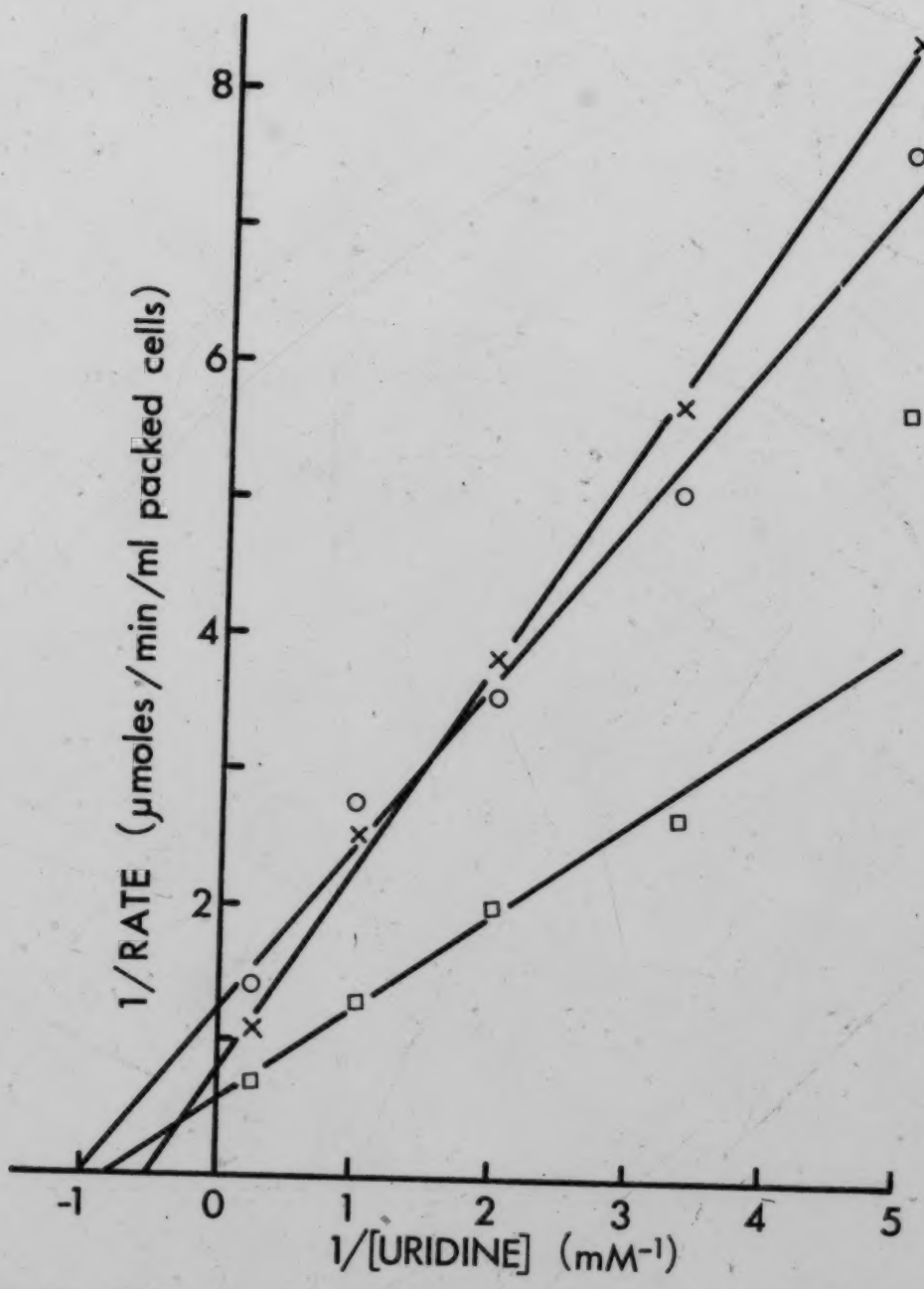

Figure 41. Effect of Sterol Exchange on Uridine Equilibrium Exchange Efflux. Lineweaver-Burk Plot.
After exchanging membrane cholesterol for sterols bound to egg lecithin, the rate of [^{14}C]-uridine efflux at 15°C was determined at various uridine concentrations.
x–x, cholesterol; □–□, control; o–o, cholest-4-en-3-one.

TABLE VIII

EFFECTS OF INCUBATION WITH STEROLS ON Km AND Vm OF URIDINE EQUILIBRIUM EXCHANGE EFFLUX

Sterol exchanged	Km (mM)	Vm (µmole/min/ml)
Control	1.1	3.6
Cholesterol	2.0	2.6
Cholest-4-en-3-one	1.0	1.7

IV Discussion

The data in this chapter suggest that facilitated diffusion of uridine and D-glucose in human erythrocytes is not directly dependent on membrane lipid fluidity, as increasing the fluidity by adding anesthetics or by exchanging cholest-4-en-3-one for cholesterol does not seem to increase Vm of these processes. This statement, however, must be qualified. The anesthetic, procaine-HCl, is strongly inhibitory to the facilitated diffusion of both permeants, so no information on the effect of fluidity on facilitated diffusion could be obtained using it. Ether causes a small decrease in Vm for glucose flux, and no detectable change in Vm for uridine flux. It is possible, however, that these facilitated diffusion rates are dependent on the lipid fluidity, but that the increase in rate with ether caused by enhanced fluidity is compensated for by a partial inhibition by ether acting directly on the transport protein. The fact that ether does not appear to change the values of Km significantly argues against an inhibitory effect, but is by no means conclusive, particularly in view of the fact that the quality of the data does not allow a precise determination of Km. It would be a rather unusual coincidence, however, if the inhibition of both transport proteins by ether exactly balanced the enhancement of flux due to increased lipid fluidity. The most reasonable interpretation seems to be that these processes are not

dependent on lipid fluidity and that ether does not strongly inhibit them. This finding is not in agreement with the postulated generalization that anesthetics invariably inhibit facilitated diffusion (165).

When erythrocytes were incubated with sterols to exchange them with membrane cholesterol, cholesterol-loaded membranes had only 65% as great a passive permeability as did cholest-4-en-3-one-loaded membranes, but the Kms for glucose flux were the same and Vm was slightly lower in the cells with higher passive permeabilities. The difficulty in the interpretation of this finding is that passive permeabilities were measured at 37°C, but facilitated diffusion was at 15°C. The effect of cholesterol is to decrease lipid fluidity at temperatures above Tc, but to increase fluidity below Tc, so the effect on fluidity may be minimal at the transition temperature (191,192). It has been found that a change in slope of the Arrhenius plot of exchange transport of D-glucose by human erythrocytes occurs at about 20°C (193). A non-linearity is also seen in plots of viscosity of human erythrocyte membrane suspensions vs reciprocal temperature at 18-19°C (194). This has been interpreted as being due to a phase transition in the membrane lipids. It is not clear why a phase transition should be seen in erythrocyte membranes, having 40 mole% of their lipid as cholesterol, since this amount of cholesterol is sufficient to abolish the phase transitions in pure

phospholipids, as detected by DSC (5,21,195), by NMR (20), or by fluorescence polarization (84). If, however, the postulate that a phase transition of erythrocyte membrane lipids occurs near 20°C is accepted, then it seems likely that changes in membrane sterol composition which cause marked alterations in fluidity at 37°C may have little or no effect on fluidity at 15°C.

The results obtained for uridine transport are subject to the same qualification. In addition, the possibility of some type of direct interaction of the transport protein with sterols is suggested. Incubation of the erythrocytes with cholesterol-lecithin mixtures increased the Km for uridine flux. The same effect of cholesterol loading on Km for glucose transport was seen by Masiak and LeFevre, and they attributed it to steric hindrance or otherwise altered accesibility (196). They found that the removal of about 8% of the membrane cholesterol increased glucose transport rates, but as more cholesterol was removed inhibition resulted. This inhibition could be relieved by substituting some other sterols for cholesterol, but 3-ketosteroids were ineffective. My results with uridine transport show a decrease in Vm caused by incubation with either sterol, although cholesterol inhibits passive flux at 37°C, while the two sterols together stimulate it. It is possible to that the decrease in Vm on incubation with cholesterol is due to a decreased fluidity resulting from cholesterol

loading, while the decrease on incubation with cholesterol and cholest-4-en-3-cne together is due to depletion of cholesterol, which is replaced by the 3-ketosteroid cholest-4-en-3-one, resulting in some specific effect on the transport protein. In this regard, the results obtained by Noguchi and Freed with membrane Na^+,K^+-ATPase from rat brain establish a precedent for a specific requirement for cholesterol tc activate membrane enzymes (197). They extracted all the lipid from this enzyme with organic solvents at -75°C, then fractionated the lipids and added various fractions back to the enzyme. Only cholesterol was able to restore the activity of the lipid-depleted enzyme as effectively as the total lipid; recovery with any other fraction was less than 25%.

In summary, the results in this chapter suggest that rates of facilitated diffusion of uridine and D-glucose are not affected by alteration of membrane lipid fluidity. This apparent insensitivity to fluidity could be questioned, however, on the basis of lack of alteration of fluidity by sterol exchange at the assay temperature, and specific effects on the transport proteins of the fluidity-perturbing agents.

CHAPTER V

URIDINE AND 3-O-METHYL GLUCOSE TRANSPORT IN RAT ERYTHROCYTES

I Introduction

Another possible approach to varying the lipid fluidity of erythrocyte membranes is the dietary manipulation of fatty acid composition. It has been shown that the fatty acid composition of total lipids from rat erythrocyte membranes can be altered by varying the amount of the essential fatty acid, linoleic acid (18:2cc), supplied in the diet (198-200). The most significant alterations seen by Walker and Kummerow (198,199) were in oleic (18:1) and eicosatrienoic (20:3) acids, which were increased with restricted lincleic acid intake, and in linoleic (18:2) and arachidonic (20:4) acids, which were decreased. Similar effects were seen by Jager and Houtsmuller (198), except that they reported little change in the arachidonic acid content. Both groups saw slight increases in lauric (12:0), myristic (14:0), and palmitoleic (16:1c) acids with restricted lincleic acid intake. The effects of these alterations on passive permeabilities, or lipid fluidity, are not straightforward. Essential fatty acid deficiency was seen by Walker and Kummerow to be associated with a more rapid hemolysis in isotonic glycerol, thiourea, or triethylene glycol (199). They have interpreted this as indicating an enhanced permeability of the erythrocytes from

this group, and have suggested that 5,8,11-eicosatrienoic acid, which is found only in essential fatty acid-deficient rat erythrocytes, may have a greater fluidizing effect than arachidonic acid (5,8,11,14-eicosatetraenoic) because of a greater cross-sectional area when incorporated into phospholipids arranged in a bilayer.

Jager and Houtsmuller also found a faster hemolysis in isotonic thiourea for erythrocytes from essential fatty acid-deficient rats (198). They note, however, that the curve of optical density vs time in the hemolyzing solution is divided into two phases. In the first part of the process, during which hemolysis takes place, the change in optical density is due to the osmotic swelling of the erythrocytes, and is truly a measure of permeability. No differences between different groups of rats were found in this region of the curves, thus permeabilities seem to be unaltered. The variations seen in actual hemolysis times may be due to differences in membrane fragility or critical hemolytic volume. In this regard, it has been shown by other investigators that hemolysis times, while related to the permeability of the substance in which hemolysis is carried out, also are dependent on other factors (201-203).

Chen and co-workers formed multilammelar bilayer vesicles in the presence of 300mM D-glucose from lecithins extracted from membranes of internal organs from normal and essential fatty acid-deficient rats (130). Using a

spectrophotometric assay, which coupled NADP reduction to oxidation of glucose-6-phosphate formed from extravesicular glucose, they measured the glucose efflux from these vesicles. The permeability of vesicles from normal rats was significantly higher than essential fatty acid-deficient rats. The applicability of this finding to the present problem, however, is questionable because only lecithin was used, and because other cell types than erythrocytes were used.

The experiments to be reported in this chapter involved the alteration of fatty acid composition of rat erythrocyte membranes by feeding with defined diets containing either trilinolein or a saturated triglyceride, and the determination of the effects on transport parameters of these alterations. Facilitated diffusion was investigated using the uridine and 3-O-methyl glucose systems, and passive diffusion was assessed by the glucose permeability of liposomes, measured by the assay procedure used by Chen et al. and Demel et al. (30).

II Methods

Diet formulation

A defined diet, designed to meet the NRC requirements for the rat (204), contained the following per kilogram of food:

220 g Casein, 470 g glucose, 48 g celluflour, 60 g salt mixture, 6.6 g vitamin mixture, 200 g fat (tripalmitin, tristearin, or safflower oil), 5 ml choline chloride solution (120 g/l) and 1.25 ml vitamin B12 solution (20 mg/l).

The specified composition of the safflower oil was 70-76% linoleic acid (18:2), 16-23% oleic acid (18:1), 0-0.3% linolenic acid (18:3) and 6.5-7% saturated fatty acids.

The vitamin mixture was made up as follows: 100 mg thiamine HCl, 100 mg riboflavin, 500 mg niacin, 400 mg calcium pantothenate, 50 mg pyridoxine HCl, 2 mg biotin, 10 mg vitamin K, 20 g vitamin A (10,000 IU/g), 85 g vitamin D (750,000 IU/lb), 20 g vitamin E (20,000 IU/lb) and 5 g ethoxyquin.

The salt mixture contained 341 g KH_2PO_4, 250 g iodized NaCl, 48.8 g $MgSO_4$, 6 g $FeCl_2 \cdot 4H_2O$, 1.57 g $CuSO_4 \cdot 5H_2O$, 1.2 g $MnSO_4 \cdot H_2O$, 0.12 g ZnO, 0.03 g $(NH_4)_6Mo_7O_{24} \cdot 4H_2O$ and 300 g $CaCO_3$.

This diet was formulated with the advice of Dr. R. Renner, Dept. of Household Economics, University of Alberta, who also supplied some of the constituents.

Metabolism of permeants

To verify that the permeants used were not metabolized in rat erythrocytes, cells were incubated at 37°C for 30 min with [^{14}C]-uridine or 3-O-methyl glucose, then the chemical distribution of radioactivity inside the cells was analyzed by paper chromatography. The same buffers and quench solutions as described in Chapter IV for human erythrocytes were used for investigating metabolism and measuring transport.

For analysis of metabolic products of [^{14}C]-uridine, 0.1 ml of cell suspension at a hematocrit of about 35% was incubated with 2 microCuries of uridine. After 30 min at 37°C, 1 ml of 11% TCA was added and the mixture was placed in a boiling water bath for 2 min. After freeze-thawing three times, the tube was centrifuged at 12,000Xg for 15 min. The clear supernatant was removed and extracted four times with 3 ml of diethyl ether to remove TCA. After evaporating the last traces of ether from the extract in a warm water bath, it was lyophylized to dryness and the residue taken up in 0.1 ml of water. Duplicate 0.02 ml aliquots of this extract were spotted onto Whatman No. 1

paper and chromatographed with standard compounds using solvent 28 (1N ammonium acetate, pH=5.0:95% ethanol 3:7 (v:v)) or solvent 30 (n-butanol:water 6:1 (v:v)) (205).

Metabolism of 3-O-methyl glucose was investigated by incubating 0.2 ml of a cell suspension having a hematocrit of about 25% with 0.14 micro-Curies of [^{14}C]-3-O-methyl glucose at a final concentration of 0.13mM at 37°C. After 30 min, the cells were washed three times in 3 ml of ice cold quench solution, then radioactivity extracted from the pellet by vortexing with 1.5 ml of distilled water. Protein was precipitated by adding 0.15 ml of 0.15M barium hydroxide, then 0.15 ml of 5% zinc sulfate and centrifuging in the clinical centrifuge at top speed for 10 min (206). The supernatant was removed and solvent evaporated as an azeotrope with 3 volumes of 2-propanol and the residue taken up in 0.1 ml of water (207). An aliquot of 0.08 ml of this was spotted on Whatman No. 1 paper, along with standards, and chromatographed using solvent 28.

Transport measurements

3-O-Methyl glucose uptake: The rate of uptake of 3-O-methyl glucose was measured by incubating cell suspensions at hematocrits of about 40% in isotonic buffer (page 122) containing inosine, with 0.5 to 50mM [^{14}C]-3-O-methyl glucose, at 37°C. Aliquots of 0.2 ml were taken at 15-30 sec

intervals up to 2.5 min and added to 3 ml of ice cold quench solution, then washed three times by centrifuging and resuspending the pellets in ice cold quench solution (0.1mM phloretin, 0.001mM HgCl2, 1.25mM KI in buffer) (page 122). Zero time samples were obtained by adding cells and label solution directly to the quench solution without prior mixing. Radioactive material was extracted by adding 1.5 ml of distilled water to the pellets and vortexing. Protein was precipitated by the addition of 0.15M barium hydroxide, then 5% zinc sulfate and centrifuging for 5 min at top speed on the clinical centrifuge. One ml aliquots of supernatant were counted for radioactivity in Aquasol. The final concentrations of 3-O-methyl glucose in the reaction mixtures are calculated from the initial concentrations of label and the hematocrits by considering the label to be diluted into the extracellular space (1-hematocrit plus the pellet interstitial volume).

Uridine equilibrium exchange efflux: Cells washed in isotonic buffer containing glucose were equilibrated with 0.2mM, 0.5mM, 1.0mM, or 2.0mM uridine in the same buffer by incubation at 37°C for 45 min with 8 ml of these solutions. After repeating this procedure three times, cell suspensions having hematocrits of about 30% were preloaded by incubation for 1 hr at 37°C with an analytically insignificant amount of dry [^{14}C]-uridine. The preloaded cells were concentrated by centrifuging and removing the supernatants, then efflux

was initiated by rapidly adding 2 ml of the appropriate uridine solution to 0.15 ml of preloaded cells in tubes in a 37°C water bath, while mixing with a magnetic stirrer. Aliquots of 0.2 ml of the reaction mixture were taken into 3 ml of ice cold quench solution (0.05mM HTG in buffer) (page 122), layered over 6 ml of dibutyl phthalate at 30 sec intervals and immediatly centrifuged. One ml aliquots of the supernatants were counted for radioactivity in Aquasol. Initial rates were calculated using the integrated form of the first-order rate equation as described for human erythrocytes in Chapter IV and Appendix 2.

Swelling rates in glycerol

The rate of change of the reciprocal of absorbance at 824nm was measured at 37°C as described for A. laidlawii in Chapter III, under conditions similar to those used by Bruckdorfer et al. (171). Erythrocytes were washed and suspended in 140mM (280mosM) NaCl in 20mM Tris-HCl, pH=7.2. The solution used for the swelling measurement contained 168mM (168mosM) glycerol, and 56mM (112mosM) NaCl in 20mM tris-HCl, pH=7.2.

Analytical procedures

The preparation of ghosts and the extraction and GLC analysis of membrane lipids were carried out as described in Chapters II and IV. Extra- and intra-cellular volumes of

erythrocyte suspensions were calculated from the [^{14}C]-sucrose and 3-O-methyl glucose spaces as described in Chapter IV. The preparation of D-glucose-loaded liposomes and the measurement of rate of glucose efflux from them is described in Chapter IV.

III Results

Metabolism of permeants

The chromatographic patterns which are obtained from extracts of rat erythrocytes incubated with [^{14}C]-uridine or 3-O-methyl glucose are shown in figures 42 and 43. It is seen in figure 42 that metabolic alteration of uridine is extremely slow in these cells, if it occurs at all. While cleavage to uracil could not be completely discounted because of lack of resolution of these two compounds, it seems that most of the radioactivity is still present as uridine after 1 hr at 37°C.

Figure 43 shows a lack of metabolism of 3-O-methyl glucose under the same conditions. The early peak, which constitutes less than 5% of the radioactive material inside the cells, could indicate a slight amount of phosphorylation, but it could also be due to contamination of the labelled 3-O-methyl glucose with a compound having this Rf, or with some other metabolizable substance such as

Figure 42. Metabolism of [^{14}C]-Uridine by Rat Erythrocytes. After 30 min incubation of rat erythrocytes with [^{14}C]-uridine, counts were extracted and chromatographed with solvent 30 (a), or solvent 28 (b). The positions of standards are indicated by the brackets. UMP and UDP remained at the origin in solvent 30.

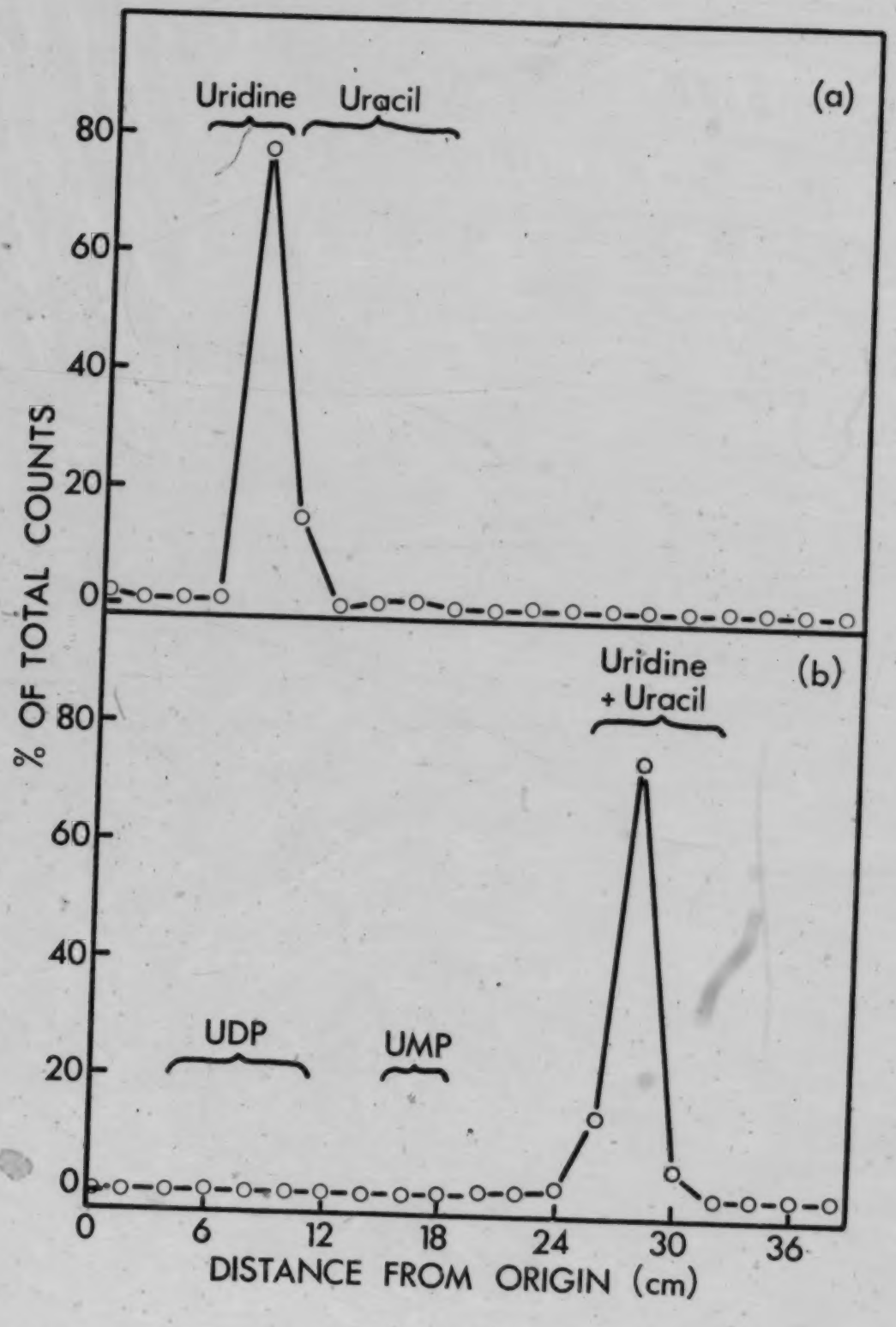
Uridine
Uracil
(a)
80
60
40
20
0
% OF TOTAL COUNTS
Uridine
+ Uracil
(b)
80
60
40
20
0
UDP
UMP
0
6
12
18
24
30
36
DISTANCE FROM ORIGIN (cm)

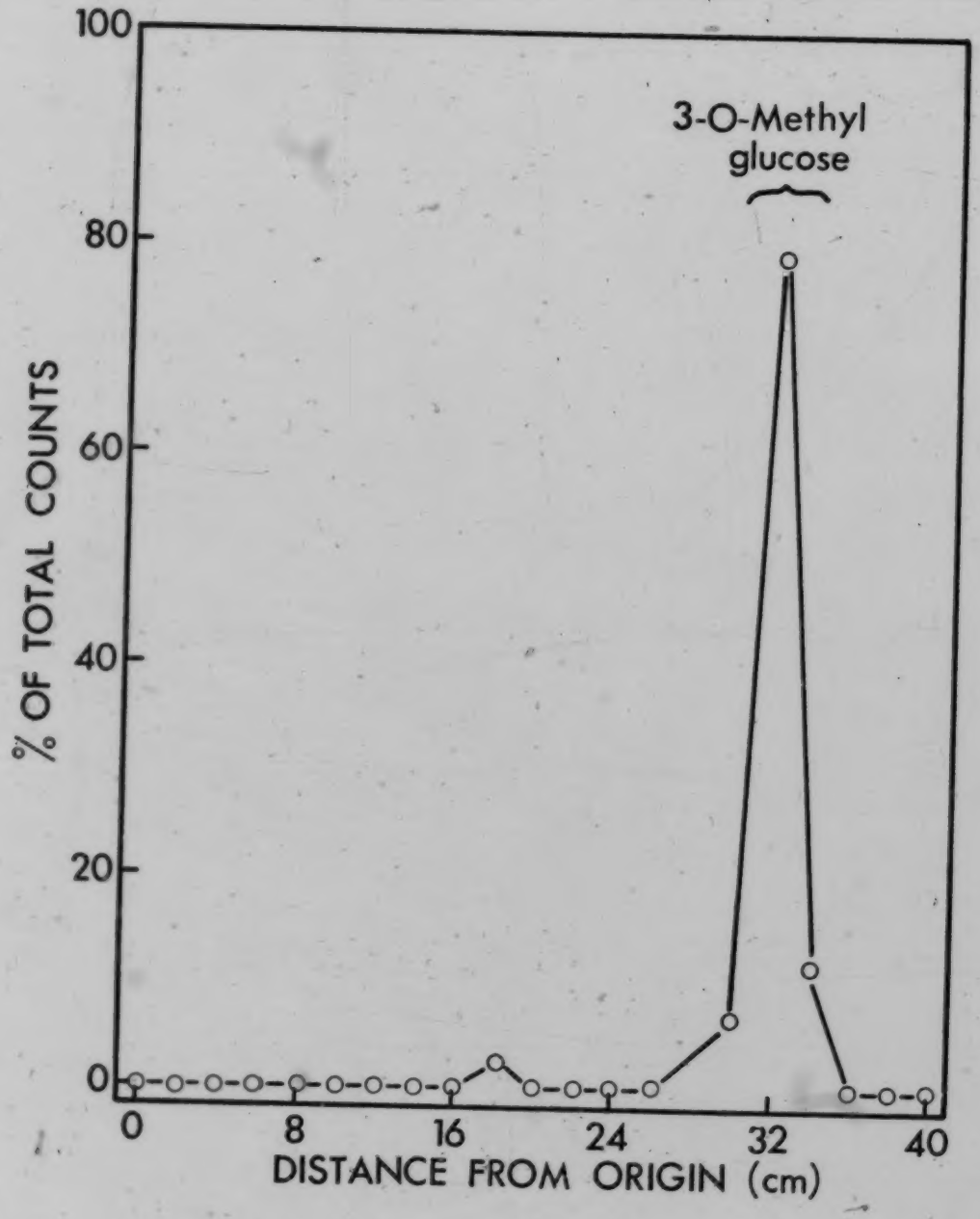

Figure 43. Metabolism of [^{14}C]-3-O-Methyl glucose by Rat Erythrocytes.
After 30 min incubation of rat erythrocytes with [^{14}C]-3-O-methyl glucose, cells were washed and counts extracted and chromatographed using solvent 28. The bracket indicates the position of standard 3-O-methyl glucose.

D-glucose.

Effects of diet on lipid fatty acid compositions

The fatty acid compositions of erythrocyte membrane lipids of two littermate rats, which were fed tripalmitin- or safflower oil (trilinolein)-supplemented diets for 13 months, are shown in Table IX. In general, these results confirm those reported by Walker and Kummerow (197,198) on the effect of diet on erythrocyte fatty acid composition. Restriction of the amount of linoleate present in the diet leads to significantly elevated levels of 18:1c, 16:1, and 20:3, and to depressed levels of 18:2 and 20:4. A slight elevation of 12:0 and of 14:0 is also seen, but the level of 16:0 is nearly the same in both groups.

The average fatty acid chain length is exactly the same in the two rats, and the average number of double bonds per fatty acid molecule does not differ significantly. This suggests that there must be compensatory metabolic mechanisms which prevent changes in erythrocyte membrane lipid fluidity in the rat.

Efflux of glucose from liposomes

Figure 44 shows the rates of efflux of D-glucose at 50°C from liposomes prepared from erythrocyte membrane lipids of rats fed safflower oil- and tristearin-

TABLE IX

FATTY ACID COMPOSITION OF RAT ERYTHROCYTE MEMBRANES

Retention Time (sec)	Probable Identity	Rat 1 (16:0) Wt %	Rat 1 (16:0) Mole %	Rat 2 (18:2) Wt %	Rat 2 (18:2) Mole %
66	12:0	2.0	2.7	1.7	2.3
79	12:1	2.6	3.6	1.9	2.6
122	14:0	10.4	12.5	7.2	8.8
198	16:0	23.9	26.0	23.3	25.4
227	16:1	6.4	17.0	---	---
330	18:0	8.3	8.2	15.0	14.8
376	18:1	17.0	16.8	9.0	8.9
460	18:2	1.0	---	10.0	10.0
832	20:3	8.2	7.5	---	---
1013	20:4	9.4	8.7	17.8	16.5
1182	20:5	6.1	5.7	3.7	3.4
1499	24:0	---	---	2.4	1.8
1605	22:5	0.9	---	1.9	1.6
1819	22:6	0.5	---	0.2	---
2126	?	1.6	---	---	---
3319	?	---	---	3.2	---

Average chain length: Rat 1=16.7 Rat 2=16.7

Average double bonds/f.a. molecule: Rat 1=1.13 Rat 2=1.15

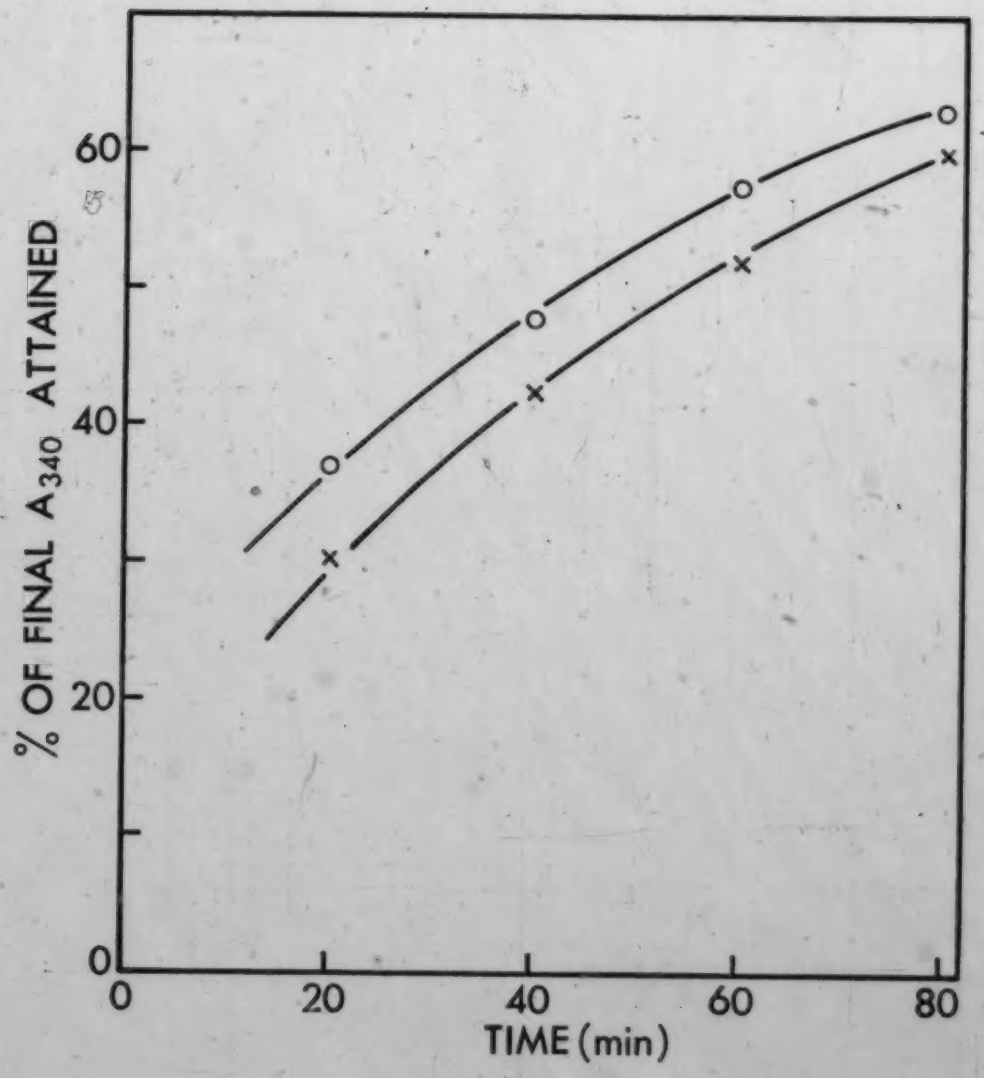

Figure 44. Efflux of Glucose from Rat Erythrocyte Liposomes. Lipcsomes were prepared from erythrocyte membrane lipids and efflux of glucose at 50°C measured by coupling glucose-6-phosphate oxidation to NADP reduction.
o–o, Rat fed 18:2; x–x, Rat fed 18:.

supplemented diets. There is no significant difference between the slopes of these two curves, which supports the suggestion from the fatty acid analysis that the erythrocyte compensates metabolically for dietary alterations to maintain a constant membrane lipid fluidity.

Swelling rates in glycerol

When rat erythrocytes were incubated at 37°C in glycerol-saline solutions, the tracings obtained of 1/absorbance *vs* time were biphasic. A short, initial period with a slow change in absorbance, due to swelling, was followed by a rapid change due to lysis. Because of the short duration of the initial phase, reliable estimates of the slope could not be obtained. The slopes from the steepest part of the curves confirm the observations of Walker and Kummerow (199), and of Jager and Houtsmuller (200), that erythrocytes from essential fatty acid-deficient rats undergo faster hemolysis. The rates seen are 4.77 ± 0.28 $hsec^{-1}$ for 16:0-fed rats and 2.12 ± 0.17 $hsec^{-1}$ for 18:2-fed rats.

Facilitated diffusion rates

Figures 45 and 46 are Lineweaver-Burk plots of the rates of 3-O-methyl glucose uptake and of uridine equilibrium exchange efflux in erythrocytes from rats fed trilinolein-supplemented and essential fatty acid-deficient

diets. Figure 45, showing 3-O-methyl glucose uptake in two littermates fed diets with defined lipid compositions for 13 months, shows no significant difference in transport between the two rats. The values obtained for Km and Vm are 20.8mM and 0.90 micro-moles/min/ml packed cells for the essential fatty acid-deficient (16:0) rat, and 25.6mM and 0.86 micro-moles/min/ml packed cells for the control (18:2) rat. Figure 46 shows that there is also no perceptible difference in uridine equilibrium exchange efflux between the two rats. The lines drawn on this plot give values for Km and Vm of 0.96mM and 0.23 micro-moles/min/ml packed cells for the essential fatty acid-deficient rat, and 0.77mM and 0.21 micro-moles/min/ml packed cells for the control.

Effect of HTG on uridine uptake

Figure 47 shows the uptake of radioactive uridine at 0.15mM in the presence of 0.05mM 6-[(2-hydroxy-5-nitrobenzyl)thio]guanosine (HTG), with and without added unlabelled uridine to a concentration of 6.7mM, and in the absence of HTG with 4.7mM unlabelled uridine present. The results in the presence and absence of HTG are not strictly comparable because the erythrocytes used were from different rats and the labelled solutions and detailed experimental conditions were not identical. For this figure, however, the results have been normalized to account for different label specific activities, different reaction mixture and sampling

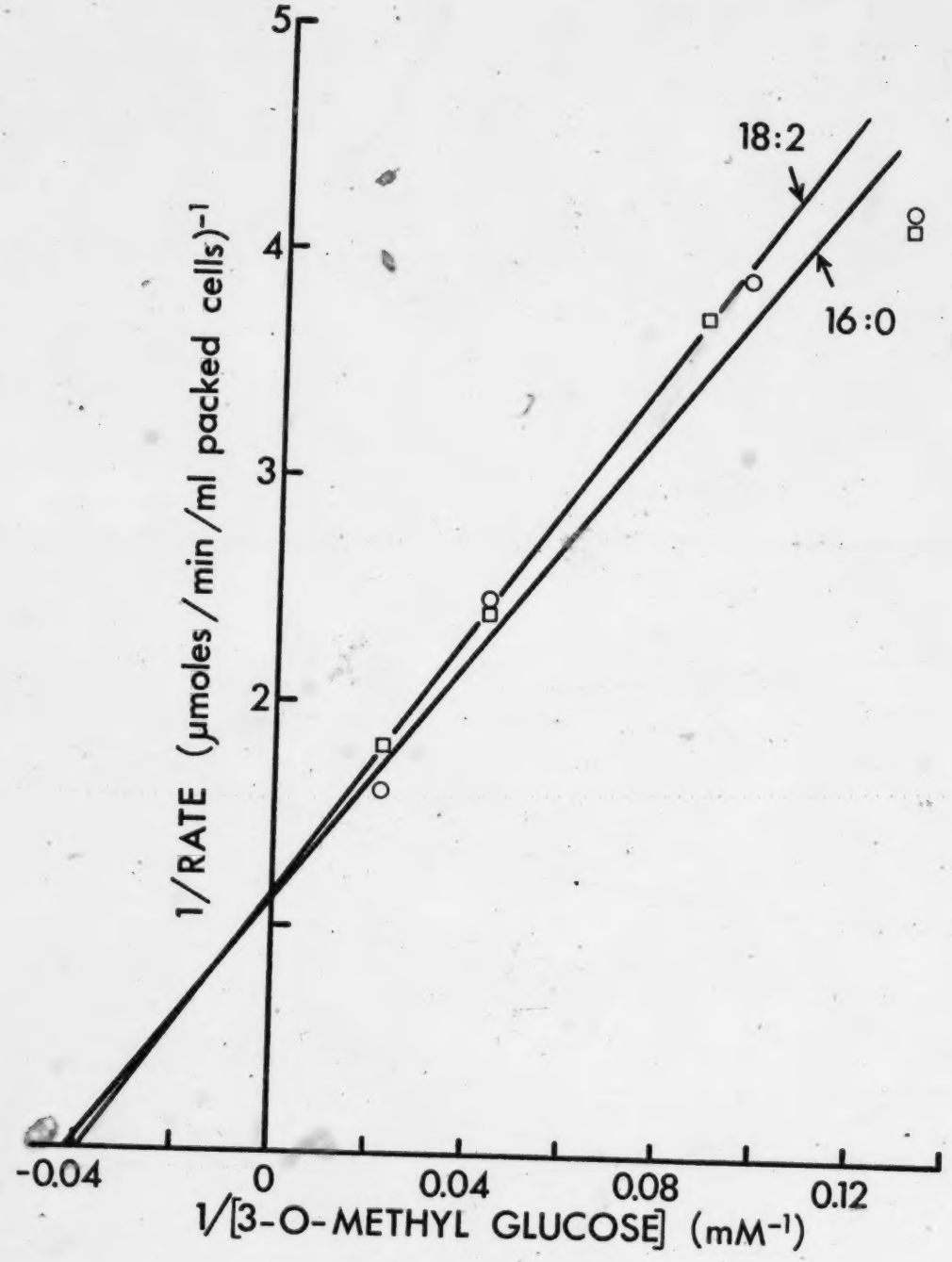

Figure 45. 3-O-Methyl Glucose Uptake by Rat Erythrocytes. Cells were incubated at 37°C with [^{14}C]-3-O-methyl glucose at various concentrations and the uptake stopped at 30 sec intervals by taking aliquots into ice cold quench solution. o–o, 16:0-fed; □–□, 18:2-fed.

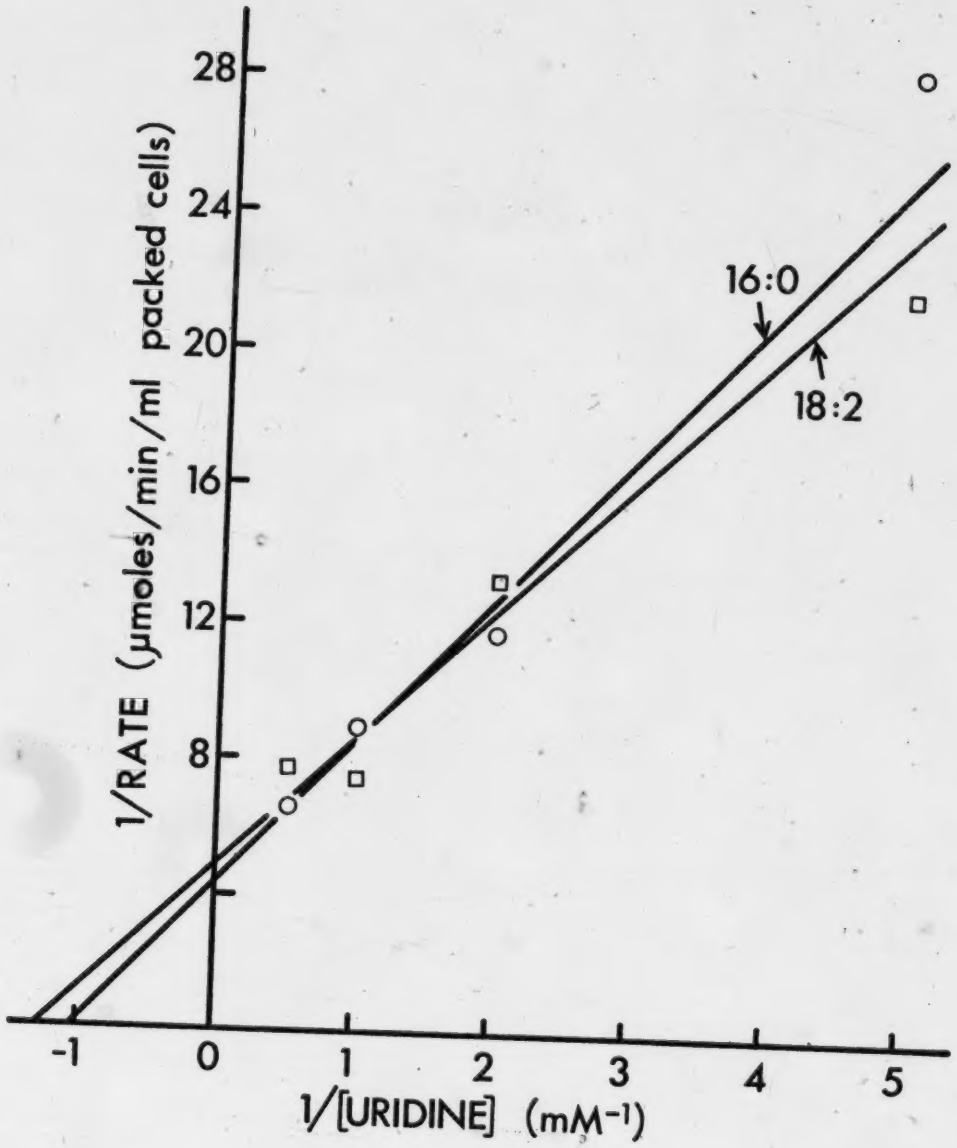

Figure 46. Uridine Exchange Efflux from Rat Erythrocytes. [^{14}C]-Uridine-preloaded cells were incubated at 37°C with unlabelled uridine solutions. Efflux was stopped at 30 sec intervals by taking aliquots into ice cold quench solution. o–o, 16:0-fed; □–□, 18:2-fed.

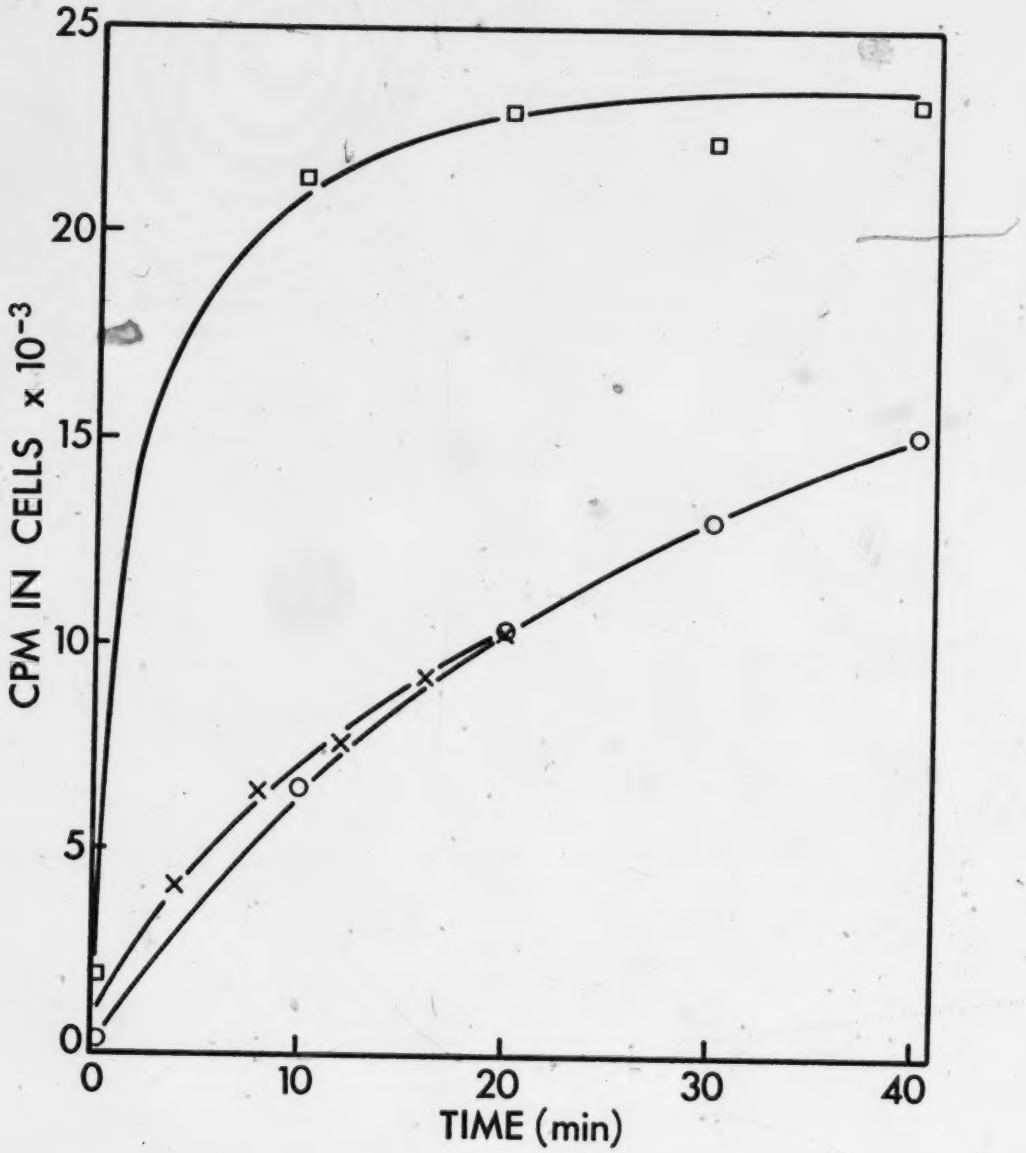

Figure 47. Effect of HTG on Uridine Flux in Rat Erythrocytes. After incubation at 37°C with a fixed amount of [^{14}C]-uridine, the uptake was stopped by taking portions into ice cold quench solution and cells were washed and counts extracted.
□–□, 0.05mM HTG; o–o, 0.05mM HTG + 6.7mM uridine
x–x, 4.7mM uridine

volumes, and different hematocrits of the cell suspensions. It is obvious that, contrary to the case with human erythrocytes, PTG at 0.05mM does not significantly inhibit uridine flux or remove the saturability seen in rat erythrocytes.

IV Discussion

From the results of the efflux of glucose from liposomes, it appears that alteration of the fatty acid species present in the diet failed to produce a difference in erythrocyte membrane lipid fluidity. In view of this, the lack of effect of diet on the kinetic parameters of uridine or 3-O-methyl glucose facilitated diffusion is what would be expected, and so this section gives no information about the effect of fluidity on facilitated diffusion. In spite of the lack of alteration of membrane fluidity, erythrocytes from essential fatty acid-deficient rats are lysed much more rapidly in glycerol solutions than those from controls. This seems to be due to changes in membrane fragility and critical hemolytic volume, rather than permeability.

The mechanism used to compensate for essential fatty acid deficiency involves desaturation of palmitic and stearic acids to replace the linoleic acid. The unsaturated fatty acids can be divided into four families, according to the number of carbon atoms between the terminal methyl group

and the nearest double bond (208). The biosynthetic relationships between the various fatty acids are shown in figure 48. The precursors can be converted to other unsaturated fatty acids in the family by desaturation and by 2-carbon elongations as shown. Of these families, two of the precursors, palmitoleic acid and oleic acid, can be formed from the 16 and 18 carbon saturated fatty acids by desaturation in the 9–10 position by a specific oxygenase. The other two, linoleic acid and linolenic acid, must be supplied in the diet.

The predominant unsaturated fatty acids present in normal rat erythrocyte membranes are oleic acid and members of the linoleic family, particularily linoleic and arachidonic acids. The major response to restriction of linoleic acid intake is an increased biosynthesis of members of the oleic acid family, primarily oleic and eicosatrienoic acids, and the production of some palmitoleic acid.

Certain species differences are seen between the 3–O-methyl glucose and uridine transport systems in human and rat erythrocytes. Although the values for Km are similar in both species (about 1mM for uridine and 20-40mM for glucose or 3–O-methyl glucose), Vm in the rat is about 100-fold lower for uridine than in the human (0.9 vs 90 micromoles/min/ml packed cells) and 10-fold lower for 3–O-methyl glucose than for glucose in the human (3 vs 0.2 micromoles/min/ml packed cells). Although 3–O-methyl glucose

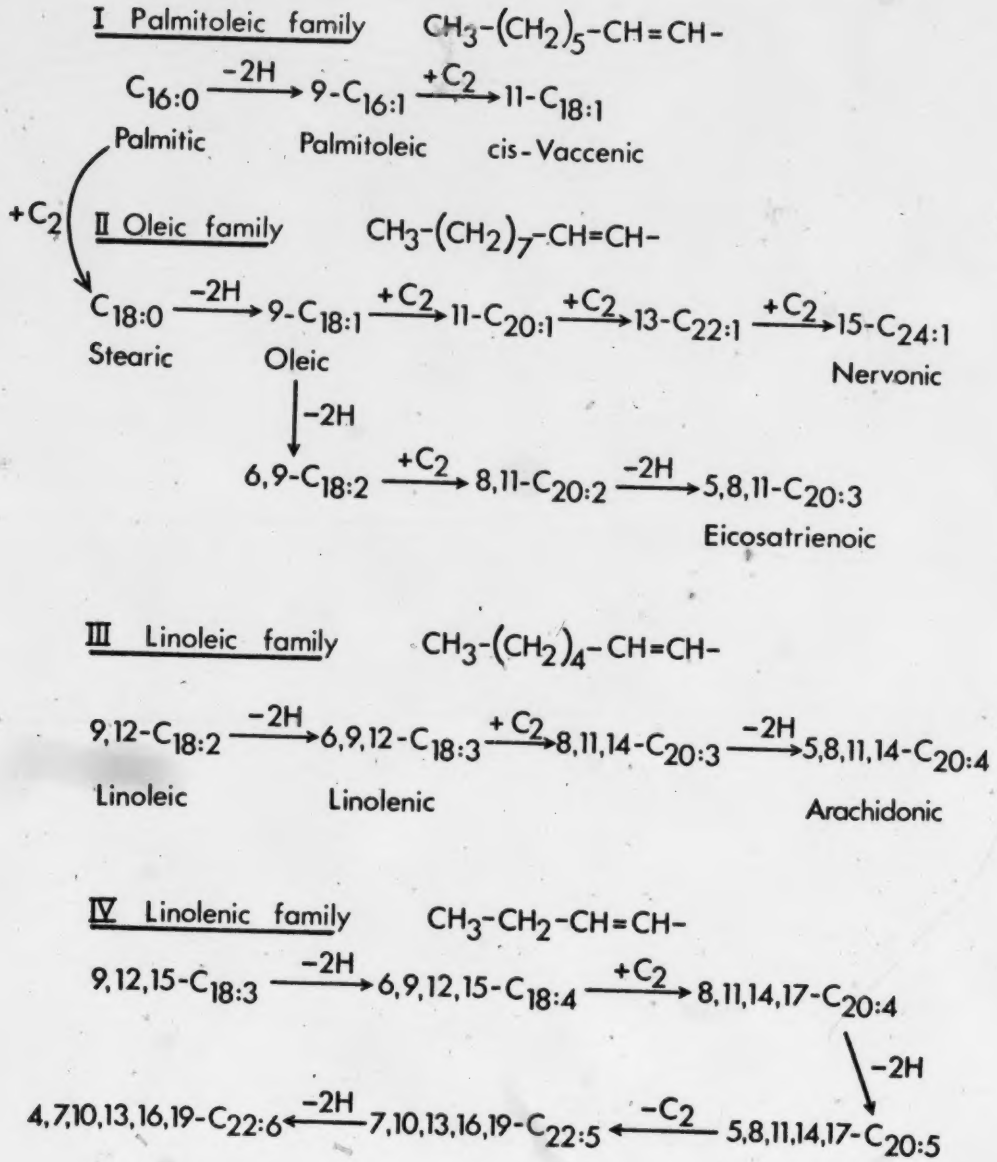

Figure 48. Biosynthetic Relationships Between Unsaturated Fatty Acids.

uptake in the rat was measured by a zero-*trans* experiment, while D-glucose efflux in human erythrocytes was measured by equilibrium exchange, this difference in techniques has been reported to result in a maximum difference in Vm of 2-fold only, and so can not account for the 10-fold difference observed (156).

CHAPTER VI

CONCLUSION

I Discussion of Results

The objective of this project was to determine whether or not facilitated diffusion rates are dependent on the membrane lipid fluidity. Although the answer obtained is not completely definitive and unambiguous, the results suggest that the maximum rates of facilitated diffusion of glucose and uridine in human erythrocytes are not directly related to the fluidity of the lipid region of the membrane. This is shown by the failure of 100 mM ether, or of substitution of cholest-4-en-3-one for membrane cholesterol, to increase the values of Vm for these processes. It appeared that dietary manipulation of rat erythrocyte membrane fatty acid compositions did not alter the membrane lipid fluidity, so this approach was unsuccessful.

With *Achcleplasma laidlawii*, the rate of glucose permeation was shown to increase with increasing lipid fluidity, and to show a discontinuity in the slope of the Arrhenius plot within the phase transition region. It was not established, however, whether the uptake of glucose by this organism occurs by active transport or facilitated diffusion.

The finding that mediated glucose permeation of *A. laidlawii* is influenced by physical properties of the lipid

region of the membrane extends the observations of this phenomenon which were made for the beta-glucoside and beta-galactoside transport systems of E. coli after this study was begun (81,82,93,209). These studies by other workers have characterized the influence of lipid physical properties on transport by relating the temperatures of occurrence of discontinuities in the slopes of the Arrhenius plots of transport to the lipid composition and phase state behavior of the membrane lipids. As many as three discontinuities were sometimes seen, and their positions were dependent on the membrane lipid fatty acid composition such that membranes having higher lipid transition temperatures also showed the discontinuities at higher temperatures (81-83,92,209). An alternative approach, which has been employed in this thesis, is to look at the effect of membrane lipid properties on the rate of transport under fixed conditions. The result obtained with A. laidlawii, that glucose flux rate increased with increasing membrane lipid fluidity, is consistent with a direct association of the transport protein with the membrane lipid, and with the occurrence of some type of motion of this protein in a rate-limiting step in the transport process. This result would support models for the transport process which feature either a movement of a shuttle-type carrier protein through the bilayer, or a conformational change in a transport protein intimately associated with the bilayer. Transport through fixed channels or at a specialized site which is

isolated from the bulk lipid region would seem to be excluded.

The uptake of beta-galactosides in E. coli (91), and possibly beta-glucosides in E. coli (210) and D-glucose in A. laidlawii, occurs by metabolic energy-dependent active transport systems. The efflux of thiomethyl-galactoside from E. coli occurs via the beta-galactoside transport system, but is not energy-dependent. Although this efflux was shown to be influenced by the fluidity of membrane lipids, this phenomenon has not been clearly demonstrated in a well-defined facilitated diffusion system (211). In fact, some observations have been reported which suggest a lack of correspondence of flux rates to lipid fluidity in certain facilitated diffusion systems. When the glycerol permeabilities of erythrocytes from several mammalian species were determined, the species examined fell into two groups (203,212). One group showed a low glycerol permeability and a high temperature dependence of permeation. Within this group, the sequence of increasing mean fatty acid chain length and decreasing mean number of double bonds (i.e., decreasing lipid fluidity) coincided with the sequence of increasing glycerol permeability. No such correspondence was seen in the other group, which had higher permeabilities with lower temperature dependencies. It was postulated that glycerol permeation occurs by passive diffusion in the first group, but by facilitated diffusion

in the second group. This observation is not, however, a convincing demonstration of a lack of effect of lipid fluidity on facilitated diffusion, since species differences in the transport systems could obscure the lipid fluidity effect. As examples of such species differences, glucose and 3-O-methyl glucose transport in beef erythrocytes were shown to have a Km 100-fold lower and a Vm at least 1000-fold lower than in human erythrocytes (146), and rat erythrocytes were shown in the present work to transport 3-O-methyl glucose with a 10-fold lower Vm and uridine with a 100-fold lower Vm than human erythrocytes.

The results reported here indicate a lack of correlation of the values of Vm for uridine and glucose fluxes in human erythrocytes with lipid fluidity. The interpretation of such a result is either that the portion of the transport system undergoing movement during the permeation process is not in direct contact with the bulk lipid region, or else that no such movement occurs. It is possible to envision several types of models having these characteristics.

A model proposed by Naftalin for glucose facilitated diffusion features a fixed aqueous channel at the transport site, lined on the inside surface with permeant binding sites (157). While this model is certainly compatible with the lack of influence of lipid fluidity seen on transport rates, particularily in light of the analogy with the

channel-forming antibiotic, gramicidin (95), there are certain objections to it on the basis of other kinetic data (156). Specifically, it cannot account for the fact that the Km for glucose transport measured by the infinite-*cis* procedure is an order of magnitude lower than that measured by equilibrium exchange.

The concept of a mobile carrier-type transport protein which shuttles from one side of the membrane to the other seems difficult to reconcile with the results reported here, but there are several ways to accomodate a protein which translocates the permeant by a conformational change, without having it interact with the bulk lipid of the membrane during this process. The protein could have a rather rigid shell, with the movement occurring at its interior without disturbing the surrounding lipid or changing the overall shape of the protein appreciably. It could also be in the center of an aggregate of other proteins, which shield it from the lipid region. Alternatively, it may have lipid of some specific class, which is not fluidized by anesthetics or by sterol exchange, bound to its surface. If this were the case, the overall passive permeability of the membrane could be increased due to an increase in the fluidity of certain regions of the lipid, while the fluidity of the lipid immediately surrounding the transport site was unaltered.

In addition to the qualified answer which was obtained

to the question posed, several interesting miscellaneous observations came to light in this work.

Although a complete characterization of the glucose transport system in A. laidlawii was not achieved, it was shown that it is specific for D-glucose and 2-deoxyglucose, but not 3-O-methyl glucose, and that the accumulation of radioactivity seen probably represents a steady-state labelling of metabolic pools, unless uptake is measured at very early times. This means that the conditions employed by other workers to measure this phenomenon were probably not appropriate to this system (118,120), presuming that the strain used by them did not differ significantly from ours with respect to glucose uptake and metabolism.

The failure of methylarsine oxide to inhibit maltase in this organism seems to indicate a difference between this enzyme and the maltase studied by Rona et al. (origin not specified) (148). The inhibition of binding of phloretin to A. laidlawii, which is apparently not due to competition at a specific binding site, is an interesting phenomenon. This inhibition seems to indicate a change in the partitioning of phloretin into the membranes elicited by glucose, and may be related to the energetic state of the cell.

Species differences in the Vms of 3-O-methyl glucose and uridine transport have been noted between human and rat erythrocytes, as well as a difference in the effect of HTG

on uridine transport.

The alteration in hemolysis rates of rat erythrocytes in glycerol reported by Walker and Kummerow (199) and by Jager and Houtsmuller (200), as a result of essential fatty acid deficient-diets, were confirmed. However, it was also noted that alterations of the dietary essential fatty acids supplied did not elicit changes in the mean fatty acid chain length or mean double bond index, nor did it change the passive permeability of liposomes formed from membrane lipids.

Procaine-HCl at 50mM inhibited facilitated diffusion of both D-glucose and uridine in human erythrocytes. Ether, however, did not inhibit either system when present at 100mM. This disagrees with the generalization that all anesthetics inhibit facilitated diffusion (165), and also with the statement that therapeutic concentrations of ether inhibit glucose penetration into erythrocytes (213). (A therapeutic concentration of ether is of the order of 10mM (186)).

II Suggestions for Further Research

A number of suggestions come to mind for the extention and clarification of this work. It would obviously be desirable to characterize more rigorously the transport systems studied in A. laidlawii. In order to do this it is

necessary to determine the actual flux of the permeant, rather than an apparent uptake which is influenced in an unknown way by metabolism of the permeant. One approach would be to use some non-metabolizable substance which is transported by the system being investigated. Although 2-deoxyglucose and 3-O-methyl glucose were not suitable under the conditions employed in this study, there are other compounds which could be tested as non-metabolizable substrates for the glucose transport system in this organism. 6-Deoxyglucose might be promising, as it has no 6-hydroxyl group to be phosphorylated. 5-Thio-D-glucopyranose has the oxygen atom in the pyranose ring replaced by a sulfur atom, and is the nearest available structural analog to normal D-glucose (214). This substitution seems to cause no change in affinity for the transport carrier in rabbit kidney cortex (214), but does decrease the affinity for binding to isolated human erythrocyte membranes (215). Another possible glucose analog for the transport system in A. laidlawii is alpha-methyl-D-glucopyranoside. This compound has been reported to be a substrate for the glucose transport system of Salmonella typhimurium (216).

It has been reported that, in some organisms, 2-deoxyglucose is phosphorylated, but not further metabolized (131,136-139). If this can be verified to also occur in A. laidlawii, then 2-deoxyglucose may be an ideal glucose analog for studying the transport system, since it has been

demonstrated here that this compound competes with glucose for uptake, and since the intracellular sugar would be trapped by phosphorylation. The phosphorylation of 2-deoxyglucose causes depletion of cellular ATP, so it would be necessary to provide the cells with an energy source. One possibility for this role is maltose, provided that it can be demonstrated that maltose doesn't compete with glucose or 2-deoxyglucose for uptake.

An attempt to find a non-metabolizable analog of maltose which uses the maltose transport system in A. laidlawii might also prove to be fruitful. Since the first step in the metabolism of maltose is its hydrolysis to glucose by a specific maltase, any modification which stabilizes the bond between the two glucose moieties should prevent its metabolism (120). It seems likely that many other groups on the maltose molecule are involved in binding to the transport carrier, so the glucosyl linkage could probably be stabilized to the maltase without preventing transport. The replacement of this ether oxygen by a sulfur atom or by a methylene group are two obvious possibilities.

Another approach to measuring the rate of uptake of glucose or maltose would be to account for all the radioactivity lost from the cells due to metabolism in order to obtain an estimate of the actual uptake rate. This strategy was used by Renner et al. to measure the uptake of D-glucose by cultured rat tumor cells (131). They found that

a significant proportion of the glucose taken up was not found in the intracellular compartment, but rather appeared as CO_2 given off or as lactate dissolved in the medium. *A. laidlawii*, strain B, converts [^{14}C]-glucose to CO_2, acetate, pyruvate and lactate, so it would be necessary to add the amount of radioactivity in the extra-cellular space present as these compounds to the intracellular radioactivity in order to determine the total amount of [^{14}C]-glucose or maltose which has permeated the cells (113).

The attempts made to inhibit glucose metabolism have not been exhaustive. Any other metabolic inhibitor used will present the same problem as did IAA; one can not be certain what effect, if any, it has on the transport protein. Nevertheless, if two or more inhibitors are found which completely prevent glucose metabolism, and if the rates of uptake of label in their presence are similar, it would seem likely that the actual transport step is unaffected. It might also be possible to inhibit metabolism by feedback and mass-action effects simply by carrying out the assay in the presence of high concentrations of metabolic end products, such as acetate or lactate. If cells could be completely depleted of ATP, perhaps by pre-treatment at 37°C with 2-deoxyglucose, then they may not be able to initiate the metabolism of glucose which is subsequently added, since the first step in glucose metabolism requires ATP. This procedure might also reveal whether or not glucose uptake by

these cells requires energy.

Although Rottem et al. reported that osmotic lysis of A. laidlawii cells led to the formation of leaky structures, the possibility of forming sealed vesicles which are free of cytoplasm should not be completely discounted (114). By varying the temperature, the pH and salt concentration of the lysing solution, or other conditions, it may be possible to obtain vesicles which would be suitable for transport measurements.

One problem in the interpretation of the results obtained with human erythrocytes was the uncertainty regarding the effect of sterol exchange on membrane lipid fluidity at the transport assay temperature. Carrying out the transport measurements at 37°C, rather than at 15°C, would eliminate this problem, if this measurement could be achieved. Since the fluxes of uridine and of glucose are rapid, it may be difficult to measure them accurately at the higher temperature. Another approach would be to carry out differential thermal analysis of erythrocyte membrane lipids to determine where the phase transition actually occurs. If it is at a temperature significantly below 15°C, then the validity of the conclusions obtained from the results with sterol exchange would be vindicated. It would be necessary to seperate cholesterol from the rest of the erythrocyte lipids for the thermal analysis, since the presence of cholesterol destroys the cooperativity of the phase

transition. In a preliminary experiment, we have determined that this seperation can readily be achieved by chromatography on silicic acid, using chloroform to elute the cholesterol, and methanol to elute all other lipids.

A final suggestion is to extend this type of study to other organisms. The fatty acid composition and phase transition temperature of mitochondrial membranes from the yeast Saccharomyces cerevisiae are profoundly affected by the growth conditions (217). Anaerobic growth results in a much smaller proportion of unsaturated fatty acids in the membrane, and the occurrence of discontinuities in the Arrhenius plots of activities of membrane enzymes at higher temperatures. This yeast, and the unsaturated fatty acid auxotrophs of E. coli are examples of organisms whose membrane lipid fluidity can be experimentally manipulated; there may be others as well. It would certainly be worth while to look at the effect of fluidity in such systems on various transport processes to see how general the phenomenon of dependence of transport rates on lipid fluidity is.

BIBLIOGRAPHY

1. Gorter, E., and Grendel, F.: J. Exptl. Med., 439-443 (1925).

2. Danielli, J. F., and Davson, H.: J. Cell. Comp. Physiol., 5, 495-508 (1935).

3. Hendler, R. W.: Physiological Rev., 51, 66-97 (1971).

4. Ladbrooke, B. D., and Chapman, D.: Chem. Phys. Lipids, 3, 304-367 (1969).

5. Phillips, M. C., Williams, R. M., and Chapman, D.: Chem. Phys. Lipids, 3, 234-244 (1969).

6. Razin, S., Tourtellotte, M. E., McElhaney, R. N., and Pollack, J. D.: J. Bacteriol., 91, 609-616 (1966).

7. Steim, J. M., Tourtellotte, M. E., Reinert, J. C., McElhaney, R. N., and Rader, R. L.: Proc. Nat. Acad. Sci., 63, 104-109 (1969).

8. Ladbrooke, B. D., Williams, R. M., and Chapman, D.: Biochim. Biophys. Acta, 150, 333-340 (1968).

9. Phillips, M. C., Ladbrooke, B. D., and Chapman, D.: Biochim. Biophys. Acta, 196, 35-44 (1970).

10. McElhaney, R. N.: J. Mol. Biol., 84, 145-157 (1974).

11. Ashe, G. B., and Steim, J. M.: Biochim. Biophys. Acta, 233, 810-814 (1971).

12. Blazyk, J. F., and Steim, J. M.: Biochim. Biophys. Acta, 266, 737-741 (1972).

13. Engelman, D. M.: J. Mol. Biol., 58, 153-165 (1971).

14. Chang, R.: "Basic Principles of Spectroscopy", McGraw-Hill, New York (1971).

15. McLaughlan, K. A.: "Magnetic Resonance" (Atkins, P. W., Holker, J. S. E., and Holliday, A. K., Eds.) Clarendon Press, Oxford (1972).

16. Chapman, D., and Salsbury, N. J.: Trans. Faraday Soc., 62, 2607-2621 (1966).

17. Veksli, Z., Salsbury, N. J., and Chapman, D.: Biochim. Biophys. Acta, 183, 434-446 (1969).

18. Chapman, D.: Ann. N. Y. Acad. Sci., 195, 179-206 (1972).

19. Oldfield, E., Chapman, D., and Derbyshire, W.: FEBS. Lett., 16, 102-104 (1971).

20. Finer, E. G.: Chem. Phys. Lipids, 8, 327-332 (1972).

21. Oldfield, E., and Chapman, D.: FEBS. Lett., 21, 303-306 (1972).

22. Godici, P. E., and Landsberger, F. R.: Biochemistry, 13, 362-368 (1974).

23. Jenkinson, T. J., Kamat, V. B., and Chapman, D.: Biochim. Biophys Acta, 183, 427-433 (1969).

24. Davis, D. G., and Inesi, G.: Biochim. Biophys. Acta, 241, 1-8 (1971).

25. Oldfield, E., Chapman, D., and Derbyshire, W.: Chem. Phys. Lipids, 9, 69-81 (1972).

26. Hsia, J. C., Schneider, H., and Smith, I. C. P.: Can. J. Biochem., 49, 614-622 (1971).

27. Long, R. A., Hruska, F. E., Gesser, H. D., and Hsia, J. C.: Biochem. Biophys. Res. Comm., 45, 167-173 (1971).

28. Landsberger, F. R., Lenard, J., Paxton, J., and Compans, R. W.: Proc. Nat. Acad. Sci., 68, 2579-2583 (1971).

29. Jost, P., Libertini, L. J., Herbert, V. C., and Griffith, O. H.: J. Mol. Biol., 59, 77-98 (1971).

30. Esser, A. F., and Lanyi, J. K.: Biochemistry, 12, 1933-1939 (1973).

31. Rottem, S., and Samuni, A.: Biochim. Biophys. Acta, 298, 32-38 (1973).

32. Eletr, S., and Keith, A. D.: Proc. Nat. Acad. Sci., 69, 1353-1357 (1972).

33. Raison, J. K., Lyons, J. M., Mehlhorn, R. J., and Keith, A. D.: J. Biol. Chem., 246, 4036-4040 (1971).

34. Baldassare, J. J., McAfee, A. G., and Ho, C.: Biochem. Biophys. Res. Comm., 53, 617-623 (1973).

35. Grisham, C. M., and Barnett, R. E.: Biochemistry, 12, 2635-2637 (1973).

36. Stier, A., and Sackman, E.: Biochim. Biophys. Acta, 311, 400-408 (1973).

37. Oldfield, E., and Chapman, D.: Biochem. Biophys. Res. Comm., 43, 610-615 (1971).

38. Kroes, J., Ostwald, R., and Keith, A.: Biochim. Biophys. Acta, 274, 71-74 (1972).

39. Landsberger, F. R., Compans, R. W., Choppin, P. W., and Lenard, J.: Biochemistry, 12, 4498-4502 (1973).

40. Jost, P., Griffith, O. H., Capaldi, R. A., and Vanderkooi, G.: Biochim. Biophys. Acta, 311, 141-152 (1973).

41. Jost, P., Griffith, O. H., Capaldi, R. A., and Vanderkooi, G.: Proc. Nat. Acad. Sci., 70, 480-484 (1973).

42. Jost, P., Capaldi, R. A., Vanderkooi, G., and Griffith, O. H.: J. Supra. Struct., 1, 269-280 (1973).

43. Kornberg, R. D., and McConnell, H. M.: Biochemistry, 10, 1111-1120 (1971).

44. Scandella, C. J., Devaux, P., and McConnell, H. M.: Proc. Nat. Acad. Sci., 70, 1238-1240 (1973).

45. Grant, C. W. M., and McConnell, H. M.: Proc. Nat. Acad. Sci., 70, 1238-1240 (1973).

46. McConnell, H. M., Wright, K. L., and McFarland, B. G.: Biochem. Biophys. Res. Comm., 47, 273-281 (1972).

47. Linden, C. D., Wright, K. L., McConnell, H. M., and Fox, C. F.: Proc. Nat. Acad. Sci., 70, 2271-2275 (1973).

48. Henry, S. A., and Keith, A. D.: Chem. Phys. Lipids, 7, 245-265 (1971).

49. Mehlhorn, R., Snipes, W., and Keith, A.: Biophys. J., 13, 1223-1231 (1973).

50. Moor, H., and Muhlethaler, K.: J. Cell Biol., 17, 609-628 (1963).

51. Branton, D.: Proc. Nat. Acad. Sci., 55, 1048-1056 (1966).

52. daSilva, P. P., and Branton, D.: J. Cell Biol., 45, 598-605 (1970).

53. Tillack, T. W., and Marchesi, V.: J. Cell Biol., 45, 649-653 (1970).

54. Marchesi, V. T., Tillack, T. W., Jackson, R. L., Segrest, J. P., and Scott, R. E.: Proc. Nat. Acad. Sci., 69, 1445-1449 (1972).

55. daSilva, P. P.: J. Cell Biol., 53, 777-787, (1972).

56. Speth, V., and Wunderlich, F.: Biochim. Biophys. Acta, 291, 621-628 (1973).

57. Verkleij, A. J., Ververgaert, P. H. J., Van Deenen, L. L. M., and Elbers, P. F.: Biochim. Biophys. Acta, 288, 326-332 (1972).

58. Tourtellotte, M. E., and Zupnik, J. S.: Science, 179, 84-86 (1972).

59. Branton, D.: Phil. Trans. Roy. Soc. London, Ser. B, 261, 133-138 (1971).

60. Bender, W. W., Garan, H., and Berg, H. C.: J. Mol. Biol., 58, 783-797 (1971).

61. Bretscher, M. S.: Nature New Biol., 231, 229-232 (1971).

62. Phillips, D. R., and Morrison, M.: Biochem. Biophys. Res. Comm., 45, 1103-1107 (1971).

63. Triplett, R. B., and Carraway, K. L.: Biochemistry, 11, 2897-2903 (1972).

64. Steck, T. L., Fairbanks, G., and Wallach, D. F. H.: Biochemistry, 10, 2617-2623 (1971).

65. Phillips, D. R., and Morrison, M.: Biochemistry, 10, 1766-1771 (1971).

66. Carraway, K. L., Kobylka, D., and Triplett, R. B.: Biochim. Biophys. Acta, 241, 934-940 (1971).

67. Morrison, M., Mueller, T. J., and Huber, C. T.: J. Biol. Chem., 249, 2658-2660 (1974).

68. Frye, L. D., and Edidin, M.: J. Cell Sci., 7, 319-335 (1970).

69. Singer, S. J., and Nicolson, G. L.: Am. J. of Pathology, 65, 427-435 (1971).

70. Singer, S. J., and Nicolson, G. L.: Science, 175, 720-731 (1972).

71. De Gier, J., Mandersloot, J. G., Hupkes, J. V., McElhaney, R. N., and Van Beek, W. P.: Biochim. Biophys. Acta, 233, 610-618 (1971).

72. McElhaney, R. N., De Gier, J., and Van Der Neut-Kok, E. C. M.: Biochim. Biophys. Acta, 298, 500-512 (1973).

73. Raison, J. K., Lyons, J. M., and Thomson, W. W.: Arch. Biochem. Biophys., 142, 83-90 (1971).

74. Mavis, R. D., and Vagelos, P. R.: J. Biol. Chem., 247, 652-659 (1972).

75. Ainsworth, P. J., Tustanoff, E. R., and Ball, A. J. S.: Biochem. Biophys. Res. Comm., 47, 1299-1305 (1972).

76. Jauki, R. M., Aithal, H. N., McMurray, W. C., and Tustanoff, E. R.: Biochem. Biophys. Res. Comm., 56, 1078-1085 (1974).

77. DeKruyff, B., Van Dijck, P. W. M., Goldbach, R. W., Demel, R. A., and Van Deenen, L. L. M.: Biochim. Biophys. Acta, 330, 269-282 (1973).

78. Bloj, B., Morero, R. D., Farias, R. N., and Trucco, R. E.: Biochim. Biophys. Acta, 311, 67-69 (1973).

79. Farias, R. N., Londero, L., and Trucco, R. E.: J. Bacteriol., 109, 471-473 (1972).

80. Overath, P., and Trauble, H.: Biochemistry, 12, 2625-2634 (1973).

81. Linden, C. D., Wright, K. L., McConnell, H. M., and Fox, C. F.: Proc. Nat. Acad. Sci., 70, 2271-2275 (1973).

82. Linden, C. D., Keith, A. D., and Fox, C. F.: J. Supra. Struct., 1, 519-534 (1973).

83. Linden, C. D., and Fox, C. F.: J. Supra. Struct., 1, 535-543 (1973).

84. Papahadjopoulos, D., Jacobson, K., Nir, S., and Isac, T.: Biochim. Biophys. Acta, 311, 330-348 (1973).

85. Petit, V. A., and Edidin, M.: Science, 184, 1183-1185 (1974).

86. Ray, P. H., White, D. C., and Brock, T. D.: J. Bacteriol., 106, 25-30 (1971).

87. Sinensky, M.: J. Bacteriol., 106, 449-455 (1971).

88. McMurrough, I., and Rose, A. H.: J. Bacteriol., 107, 753-758 (1971).

89. Adams, B. L., McMahon, V., and Seckbach, J.: Biochem. Biophys. Res. Comm., 42, 359-365 (1971).

90. Esfahni, M., Ioneda, T., and Wakil, S. J.: J. Biol. Chem., 246, 50-56 (1971).

91. Kaback, H. R.: Biochim. Biophys. Acta, 265, 367-416 (1972).

92. Schairer, H. U., and Overath, P.: J. Mol. Biol., 44, 209-214 (1969).

93. Wilson, G., Rose, S. P., and Fox, C. F.: Biochem. Biophys. Res. Comm., 38, 617-623 (1970).

94. Naftalin, R. J.: Biochim. Biophys. Acta, 211, 65-78 (1970).

95. Krasne, S., Eisenman, G., and Szabo, G.: Science, 174, 412-415 (1971).

96. Urry, D. W., Goodall, M. C., Glickson, J. D., and Mayers, D. F.: Proc. Nat. Acad. Sci., 68, 1907-1911 (1971).

97. Ciani, S., Eisenman, G., and Szabo, G.: J. Mem. Biol., 1, 1-36 (1969).

98. Eisenman, G., Ciani, S., and Szabo, G.: J. Mem. Biol., 1, 294-345 (1969).

99. Szabo, G., Eisenman, G., and Ciani, S.: J. Mem. Biol., 1, 346-382 (1969).

100. Van Der Neut-Kok, E. C. M., De Gier, J., Middelbeek, E. J., and Van Deenen, L. L. M.: Biochim. Biophys. Acta, 332, 97-103 (1974).

101. Sen, A. K., and Widdas, W. F.: J. Physiol., 160, 392-403 (1962).

102. Mawe, R. C., and Hempling, H. G.: J. Cell. Comp. Physiol., 66, 95-104 (1965).

103. Miller, D. M.: Biophys. J., 11, 915-923 (1971).

104. Stein, W. D.: Ann. N. Y. Acad. Sci., 195, 412-428 (1972).

105. Oliver, J. M., and Paterson, A. R. P.: Can. J. Biochem., 49, 262-270 (1971).

106. Cass, C. E., and Paterson, A. R. P.: J. Biol. Chem., 247, 3314-3320 (1972).

107. Cass, C. E., and Paterson, A. R. P.: Biochim. Biophys. Acta, 291, 734-736 (1973).

108. Bligh, E. G., and Dyer, W. J.: Can. J. Biochem. Physiol., 37, 911-930 (1959).

109. Block, R. J., Durrum, E. L., and Zweig, G.: "A Manual of Paper Chromatography and Paper Electrophoresis", Academic Press, New York (1958).

110. Englund, P. T., Huberman, J. A., Jovin, T. M., and Kornberg, A.: J. Biol. Chem., 244, 3038-3044 (1969).

111. Razin, S.: Ann. Rev. Microbiol., 23, 317-356 (1969).

112. DeKruyff, B., Demel, R. A., and Van Deenen, L. L. M.: Biochim. Biophys. Acta, 255, 331-347 (1972).

113. Smith, P. F.: "The Biology of Mycoplasmas" (Buetow, D. E., Cameron, I. L., and Padilla, G. M., Eds.) Academic Press, New York (1971).

114. Rottem, S., Stein, O., and Razin, S.: Arch. Biochem. Biophys., 125, 46-56 (1968).

115. Cho, H. W., and Morowitz, H. J.: Biochim. Biophys. Acta, 183, 295-303 (1969).

116. Cho, H. W., and Morowitz, H. J.: Biochim. Biophys. Acta, 274, 105-110 (1972).

117. Cirillo, V. P., and Razin, S.: J. Bacteriol., 113, 212-217 (1973).

118. Tarshis, M. A., Panchenko, L. F., Migoushina, V. L., and Bourd, G. I.: Biokhimiya, 37, 930-935 (1972).

119. Tarshis, M. A., Migoushina, V. L., and Panchenko, L. F.: FEBS. Lett., 31, 111-113 (1973).

120. Tarshis, M. A., Migoushina, V. L., Panchenko, L. F., Fedotov, N. S., and Bourd, H. I.: Eur. J. Biochem., 40, 171-175 (1973).

121. McElhaney, R. N., and Tourtellotte, M. E.: Biochim. Biophys. Acta, 202, 120-128 (1970).

122. De Gier, J., Mandersloot, J. G., and Van Deenen, L. L. M.: Biochim. Biophys. Acta, 150, 666-675 (1968).

123. Rottem, S., and Razin, S.: J. Bacteriol., 97, 787-792 (1969).

124. Koch, A. L., and Putnam, S. L.: Analyt. Biochem., 44, 239-245 (1971).

125. Chen, P. S., Jr., Toribara, T. Y., and Warner, H.: Analyt. Chem., 28, 1756-1758 (1956).

126. Sacket, G. E.: J. Biol. Chem., 64, 203-205 (1925).

127. Scatchard, G.: Ann. N. Y. Acad. Sci., 51, 660-672 (1949).

128. Maniloff, J.: Microbios, 2, 125-135 (1969).

129. Papahadjopolous, D., Nir, S., and Ohki, S.: Biochim. Biophys. Acta, 266, 561-583 (1971).

130. Chen. L. F., Lund, D. B., and Richardson, T.: Biochim. Biophys. Acta, 225, 89-95 (1971).

131. Renner, E. D., Plagemann, G. W., and Bernlohr, R.: J. Biol. Chem., 247, 5765-5776 (1972).

132. Maxwell, W. A., and Spoerl, E.: J. Bacteriol., 105, 753-758 (1971).

133. Manno, J. A., and Schacter, D.: J. Biol. Chem., 245, 1217-1223 (1970).

134. King, M. J., and Diwan, J. J.: Arch. Biochem. Biophys., 152, 670-676 (1972).

135. Jung, C. Y., Carlson, L. M., and Whaley, D. A.: Biochim. Biophys. Acta, 241, 613-627 (1971).

136. Komor, E., and Tanner, W.: Biochim. Biophys Acta, 241, 170-179 (1971).

137. Czech, M. P., Lynn, D. G., and Lynn, W. S.: J. Biol. Chem., 248, 3636-3641 (1973).

138. Mizel, S. B., and Wilson, L.: J. Biol. Chem., 247, 4102-4105 (1972).

139. Weber, M. J.: J. Biol. Chem., 248, 2978-2983 (1973).

140. Eagon, R. G.: Can. J. Biochem. 49, 606-613 (1971).

141. LeFevre, P. G., and Marshall, J. K.: Am. J. Physiol., 194, 333-337 (1958).

142. Carter, J. R., Jr., Avruch, J., and Martin, D. B.: Biochim. Biophys. Acta, 291, 506-518 (1973).

143. Hellman, B., Sehlin, J., and Taljedal, I. B.: Biochim. Biophys. Acta, 241, 147-154 (1971).

144. Carter, J. R., Jr., Avruch, J., and Martin, D. B.: J. Biol. Chem., 247, 2682-2688 (1972).

145. Hopfer, U., Nelson, K., Perrotto, J., and Isselbacher, K. J.: J. Biol. Chem., 248, 25-32 (1973).

146. Hoos, R. T., Tarpley, H. L., and Regen, D. M.: Biochim. Biophys. Acta, 266, 174-181 (1972).

147. Peters, J. H., and Hausen, P.: Eur. J. Biochem., 19, 509-513 (1971).

148. Rona, P., Airila, Y., and Lasnitzki, A.: Biochem. Z., 130, 582-591 (1922).

149. Sen, A. K., and Widdas, W. F.: J. Physiol., 160, 404-416 (1962).

150. Batt, E., and Schacter, D.: Biochim. Biophys. Acta, 233, 189-200 (1971).

151. Kohn, P. G., and Clausen, T.: Biochim. Biophys. Acta, 225, 277-290 (1971).

152. Giacombino, J. P., and Favarger, P.: Life Sciences, 11, 763-771 (1972).

153. Colombo, V. E., and Semenza, G.: Biochim. Biophys. Acta, 288, 145-152 (1972).

154. Benes, I., Kolinska, J., and Kotyk, A.: J. Mem. Biol., 8, 303-309 (1972).

155. Stein, W. D.: "The Movement of Molecules Across Cell Membranes" (Danielli, J. F., Ed.) Academic Press, New York, Chapter 4 (1967).

156. Lieb, W. R., and Stein, W. D.: Biochim. Biophys. Acta, 265, 187-207 (1972).

157. Naftalin, R. J.: Biochim. Biophys. Acta, 233, 635-643 (1971).

158. Baker, G. F., and Widdas, W. F.: J. Physiol., 231, 143-165 (1973).

159. Widdas, W. F.: J. Physiol., 125, 163-180 (1954).

160. Taverna, R. D., and Langdon, R. C.: Biochim. Biophys. Acta, 298, 412-421 (1973).

161. Karlish, S. J. D., Lieb, W. R., Ram, D., and Stein, W. D.: Biochim. Biophys. Acta, 255, 126-132 (1972).

162. Levine, M., and Stein, W. D.: Biochim. Biophys. Acta, 127, 179-193 (1966).

163. Cass, C. E., Gaudette, L. A., and Paterson, A. R. P.: Biochim. Biophys. Acta, 345, 1-10 (1974).

164. Picard, M. A., Brown, R. R., Paul, B., and Paterson, A. R. P.: Can. J. Biochem, 51, 666-672 (1973).

165. Seeman, P.: Pharmacological Rev., 24, 583-655 (1972).

166. Metcalfe, J. C., Seeman, P., and Burgen, A. S. V.: Mol. Pharmacol., 4, 87-95 (1968).

167. Spero, L., and Roth, S.: Fed. Proc., 29, 474Abs (1970).

168. Hubbell, W. L., and McConnell, H. M.: Proc. Nat. Acad. Sci., 63, 16-22 (1969).

169. Weed, R. I., LaCelle, P. L., and Udkow, M.: in "The Human Red Cell *in vitro*" (Greenwalt, T. J., and Jamieson, G. A., Eds.) Grune and Stratton, Inc., New York, Chapter 4 (1974).

170. Bruckdorfer, K. R., Demel, R. A., De Gier, J., and Van Deenen, L. L. M.: Biochim. Biophys. Acta, 183, 334-345 (1969).

171. Robins, S. J., and Miller, A.: J. Lab. Clin. Chem., 83, 436-443 (1974).

172. Rottem, S., Yashouv, J., Ne'Eman, Z., and Razin, S.: Biochim. Biophys. Acta, 323, 495-508 (1973).

173. Rottem, S., Cirillo, V. P., DeKruyff, B., Shinitzky, M., and Razin, S.: Biochim. Biophys. Acta, 323, 509-519 (1973).

174. Vanderkooi, J., Fischkoff, S., Chance, B., and Cooper, R. A.: Biochemistry, 13, 1589-1595 (1974).

175. Kroes, J., and Ostwald, R.: Biochim. Biophys. Acta, 249, 647-650 (1971).

176. Deuticke, B., and Zollner, Chr.: Biochim. Biophys. Acta, 266, 726-731 (1972).

177. Grunze, M., and Deuticke, B.: Biochim. Biophys. Acta, 356, 125-130 (1974).

178. Smith, R. J. M., and Green, C.: FEBS. Lett., 42, 108-110 (1974).

179. Bartlett, G. R.: in "Hemoglobin and Red Cell Structure and Function" (Brewer, J. G., Ed.) Plenum Publishing Corp., New York, 479-493 (1972).

180. Bartlett, G. R.: in "VI Internationales Symposium uber Struktur und Funktion der Erythrocyten", Akademie-Verlag, Berlin, 355-362 (1972).

181. Bartlett, G. R.: in "Erythrocytes Thrombocytes Leukocytes; Recent Advances in Membrane and Metabolic Research" (Gerlach, E., Moser, K., Deutsch, E., and Wilmanns, W., Eds.) Georg Thieme, Stuttgard, 139-143 (1973).

182. Lea, C. H., Rhodes, D. N., and Stoll, R. D.: Biochem. J., 60, 353-363 (1955).

183. White, B. J., Tipton, C. L., and Dressel, M.: J. Chem. Education, 51, 533-536 (1974).

184. Skipski, V. P., and Barclay, M.: in "Methods in Enzymology, XIV" (Lowenstein, J. M., Ed.) Academic Press, New York, 543-544 (1969).

185. Bolis, L., and Gomperts, B. D.: in "Transport and Accumulation in Biological Systems" (Harris, E. J., Ed.) Butterworth and Co. Ltd., London, and University Park Press, Baltimore, 110-111 (1972).

186. Roth, S., and Seeman, P.: Nature New Biol., 231, 284-285 (1971).

187. Demel, R. A., Kinsky, S. C., Kinsky, C. B., and Van Deenen, L. L. M.: Biochim. Biophys. Acta, 150, 655-665 (1968).

188. Dodge, J. T., Mitchell, C., and Hanahan, D. J.: Arch. Biochem. Biophys., 100, 119-130 (1963).

189. Dodge, J. T., and Phillips, G. B.: J. Lipid Res., 7, 387-395 (1966).

190. Bruchovsky, N.: Endochrinology, 89, 1212-1221 (1971).

191. Oldfield, E., and Chapman, D.: FEBS. Lett., 23, 285-297 (1972).

192. De Gier, J., Mandersloot, J. G., and Van Deenen, L. L. M.: Biochim. Biophys. Acta, 173, 143-145 (1969).

193. Lacko, L., Wittke, B., and Geck, P.: J. Cell. Physiol., 82, 213-218 (1973).

194. Zimmer, G., and Schirmer, H.: Biochim. Biophys. Acta, 345, 314-320 (1974).

195. Hinz, H. J., and Sturtevant, J. M.: J. Biol. Chem., 247, 3697-3700 (1972).

196. Masiak, S. J., and LeFevre, P. G.: Arch Biochem. Biophys., 162, 442-447 (1974).

197. Noguchi, T., and Freed, S.: Nature New Biol., 230, 148-150 (1971).

198. Walker, B. L., and Kummerow, F. A.: J. Nutrition, 82, 329-332 (1964).

199. Walker, B. L., and Kummerow, F. A.: Proc. Soc. Exptl. Biol., 115, 1099-1103 (1964).

200. Jager, F. C., and Houtsmuller, U. M. T.: Nutr. Metabol., 12, 3-12 (1970).

201. Wessels, J. M. C., Pals, D. T. F., and Veerkamp, J. H.: Biochim. Biophys. Acta, 291, 165-177 (1973).

202. Wessels, J. M. C., and Veerkamp, J. H.: Biochim. Biophys. Acta, 291, 178-189 (1973).

203. Wessels, J. M. C., and Veerkamp, J. H.: Biochim. Biophys. Acta, 291, 190-196 (1973).

204. "Nutrient Requirements of Laboratory Animals", Publication 990, National Academy of Sciences, National Research Council, Washington D. C. 20025, National Research Council Subcommittee on Animal Nutrition (1962).

205. Plagemann, P. G. W.: J. Cell. Physiol., 77, 213-240 (1971).

206. Lacko, L., Wittke, B., and Kromphardt, H.: Eur. J. Biochem., 25, 447-454 (1972).

207. Fischer, W., Heinz, E., and Zeus, M.: Hoppe-Seyler's Z. Physiol. Chem., 354, 1115-1123 (1973).

208. Lehninger, A. L.: "Biochemistry. The Molecular Basis of Cell Structure and Function", Worth Publishers, Inc., New York, Chapter 23 (1972).

209. Wilson, G., and Fox, C. F.: J. Mol. Biol., 55, 49-60 (1971).

210. Schaefler, S.: J. Bacteriol., 93, 254-263 (1967).

211. Overath, P., Schairer, H. U., and Stoffel, W.: Proc. Nat. Acad. Sci., 67, 606-612 (1970).

212. De Gier, J., Van Deenen, L. L. M., and Van Senden, K. G.: Experientia, XXII, 20-21 (1965).

213. Baker, G. F., and Rogers, H. J.: Biochemical Pharmacol., 21, 1871-1878 (1972).

214. Whistler, R. L., and Lake, W. C.: Biochem. J., 130, 919-925 (1972).

215. Kahlenberg, A., and Dolansky, D.: Can. J. Biochem., 50, 638-643 (1972).

216. Pierson, M. D., and Ordal, Z. J.: Biochem. Biophys. Res. Comm., 43, 378-383 (1971).

217. Watson, K., Bertoli, E., and Griffiths, D. E.: FEBS. Lett., 30, 120-124 (1973).

218. Myers, O. E., and Prestwood, R. J.: in "Radioactivity Applied to Chemistry" (Wahl, A. C., and Bonner, N. A., Eds.) Wiley, New York, 6-10 (1951).

Appendix 1. An Evaluation of the Description of Sugar Transport Systems in Acholeplasma laidlawii Given by Tarshis et al.

Tarshis and co-workers have described transport systems for glucose, maltose and fructose in A. laidlawii (118-120). While some of their data agree with mine, there are also some differences, and their interpretations of the data are different from those I have made. Two criticisms can be made of Tarshis' work: some of the calculations seem to show internal inconsistencies; and some of the interpretations are based on false assumptions about the nature of the phenomenon which is being observed.

These workers quote values of 0.13 to 0.48mM for the Km for glucose uptake and 0.5 nmoles/min/mg cell protein for Vm (119,120). The basis for their calculation is the assumption that transport is rate-limiting for the accumulation of counts, and they support this contention by showing that glucose phosphorylation by cell-free extracts occurs with a Km similar to that for accumulation, but an 11-fold higher Vm (119). It is clear, however, that the quoted value for Vm of uptake is not consistent with figure 3 of reference 120, since rates significantly higher than the supposed Vm are plotted on this figure. The value obtained by measuring the intercept of the inset Lineweaver-Burk plot is approximately 17 nmoles/min/mg cell protein. The calculation of Vm, rather than the axis of the figure, is probably incorrect, as the

points plotted in figure 3 are consistent with rates derived from data plotted on figure 1 of the same reference (120).

Apart from the apparent error in calculating Vm for glucose uptake, this comparison between rates of phosphorylation and accumulation is not really valid anyway because 10mM ATP was added to the reaction mixture in assaying phosphorylation by cell-free extracts. If the availability of ATP was partially rate-limiting for phosphorylation in intact cells, then a comparison of the two rates is not meaningful unless the amount of ATP present was the same in both cases. That ATP availability is rate-limiting *in vivo* is suggested by the acceleration of label accumulation seen in the presence of added unlabelled glucose under certain conditions (Chapter III: figures 25 and 26), and by the earlier attainment of the peak value of intracellular radioactivity seen in the presence of ATP or of ADP plus PEP (Chapter III: figure 24). The fact that some radioactivity with the same Rf as glucose is found inside the cells at various times during the uptake assay also suggests that transport is not completely rate-limiting under the conditions of these assays (Chapter III: figures 15 and 27). In fact, the similarity in Km for uptake to that for phosphorylation noted by Tarshis *et al*. tends to suggest that the Km that they observe for uptake is actually due to the phosphorylation process. At 37°C and at 0.03mM D-glucose, Tarshis *et al*. give an uptake rate near 1

nmole/min/mg cell protein. Using cells grown in the presence of palmitate plus oleate, whose membrane lipids would be considerably more fluid than those of cells grown on unsupplemented medium, I obtained a rate of about 0.2 nmoles/min/mg cell protein, under the same assay conditions (Chapter III: figure 24). This lower value may reflect the increased loss of metabolic products by the more leaky cells. As shown in figure 28 (chapter III), however, rates of between 6 and 40 nmoles/min/mg cell protein, depending on the membrane lipid composition, are obtained with 0.1mM glucose at 25°C when the assay is performed at earlier times. This wide variation between the two types of assay indicates that, at times that were used by Tarshis for sampling, the rate of accumulation of radioactivity is dependent on metabolic processes and reflect loss as well as uptake of counts. The actual glucose flux rates are significantly higher than those calculated from uptake of counts when sampling is done at 5 min intervals.

It may not be valid to make a direct comparison of these results with mine, since the strain used by Tarshis et al. is not reported, and some of the variations in the results obtained could be due to strain differences. Nevertheless, the points made regarding their calculation of Vm and assignment of rate-limiting steps are not dependent on any information other than that contained in Tarshis' papers.

Appendix 2. Kinetics of Equilibrium Exchange Efflux

The derivation used by Myers and Prestwood in describing a simple homogeneous exchange reaction is followed, with the additional constraint that the two species involved in exchange (intracellular permeant and extracellular permeant) are present in different compartments having different volumes (218).

The following terms are defined:

R=flux rate in moles/sec

I=moles of permeant inside

E=moles of permeant outside

I'=moles of labelled permeant inside

E'=moles of labelled permeant outside

Si=Specific activity inside=I'/I

Se=Specific activity outside=E'/E

Vi=Volume of intracellular compartment (l)

Ve=Volume of extracellular compartment (l)

The following assumptions are made about the system:

(a) Concentration inside=concentration outside (the system is at equilibrium).

(b) No energy-requiring accumulation occurs.

F=fraction exchange=$(Si-Si_0)/(Si_\infty-Si_0)=(Se-Se_0)/(Se_\infty-Se_0)$

(1) $F=(I'-I'_0)/(I'_\infty-I'_0)=(E'-E'_0)/(E'_\infty-E'_0)$

Se=fraction of permeant outside that is radioactive.

(1-Si)=fraction inside that is not radioactive.

Only an exchange of external radioactive for internal unlabelled permeant increases E', therefore:

(2) $d(E'/Ve)/dt=(1/Ve)R\cdot Si(1-Se)-(1/Ve)R\cdot Se(1-Si)$

or $dE'/dt=R(Si-Se)$

(3) $dE'/dt=R[(I'E-E'I)/IE]=(R/IE)(I'E-E'I)$

(4) $E'+I'=E'_\infty+I'_\infty$, therefore $I'=E'_\infty+I'_\infty-E'$

(5) $I'_\infty=(Vi/Ve)E'_\infty$ (since concentrations inside and outside are equal)

Substitute (5) into (4), and result into (3) to get:

(6) $dE'/dt=R/(IE)[EE'_\infty+(EE'_\infty)(Vi/Ve)-EE'-E'I]$

But $E(Vi/Ve)=I$, therefore

(7) $dE'/dt=[R/(IE)]\cdot[EE'_\infty+IE'_\infty-EE'-IE']$

(8) $dE'/dt=[R/(IE)]\cdot(E'_\infty-E')(E+I)$

(9) $dE'/(E'_\infty-E')=\{[R(E+I)]/EI\}dt$

(10) $-\ln(E'_\infty-E')=[R/(EI)](E+I)t+\text{constant}$

(11) At $t=0$, $E'=E'$, therefore $\text{constant}=-\ln(E'_\infty-E'_0)$

(12) $-\ln(E'_\infty-E')=[R/(EI)](E+I)t-\ln(E'_\infty-E'_0)$

(13) $\ln[E'_\infty-E')/(E'_\infty-E'_0)]=-Rt[(E+I)/EI]$

$(E'_\infty-E')$ can be written as: $(E'_\infty-E'_0)-(E'-E'_0)$, therefore:

(14) $\ln\{[(E'_\infty-E'_0)-(E'-E'_0)]/(E'_\infty-E'_0)\}=-Rt[(E+I)/EI]$

(15) $\ln[1-(E'-E'_0)/(E'_\infty-E'_0)]=-Rt[(E+I)/EI]$

From (1) and (15):

(16) $\ln(1-F)=-Rt[(E+I)/EI]$ or $Rt=[(EI)/(E+I)]\ln(1-F)$

C=concentration of permeant inside=concentration of permeant outside, therefore:

(17) $E=C\cdot Ve$ and $I=C\cdot Vi$

(18) $(E+I)/EI=(CVe+CVi)/(CVe\cdot CVi)=(Ve+Vi)/CVeVi)$

Therefore, from (16) and (18):

(19) $Rt=-\{[(CVeVi)/(Ve+Vi)]\ln(1-F)\}$

(20) $-\log(1-F)=[(Ve+Vi)/(2.303CVeVi)]Rt$

Let N be cpm in a specified volume of the extracellular fluid at time=t:

(21) $(1-F)=-(N_\infty-N_t)/(N_\infty-N_o)$

Therefore, plot $\log[(N_\infty-N_t)/(N_\infty-N_o)]$ vs time in sec.

(22) $(slope)\cdot-[(2.303CVeVi)/(Ve+Vi)]=R$, where R is initial rate in moles/sec/l of extracellular water. Let Vi=intracellular volume/ml extracellular water in ml, so Ve=1; therefore:

(23) $slope\ X\ -[(2.303)CVi)/(1+Vi)]=R$

If C is expressed in mM, and Vi and Ve in ml, R is micro moles/sec/l extracellular water.

The hematocrit of the assay mixture is determined directly, and the intracellular and interstitial volumes per ml of packed cells are obtainable from the [^{14}C]-Sucrose and 3-O-Methyl glucose spaces of a cell suspension.

(24) $Vi=(Wh)/[1-h(1-Q)]$

where: W=intracellular volume/ml packed cells

h=hematocrit

Q=interstitial volume/ml packed cells

(25) $RATE=Slope\ X\ -[138.18CVi/(1+Vi)]\cdot[h^{-1}-1+Q]$

where RATE is expressed as μmoles/min/ml packed cells.

Appendix 3. Fatty Acid Nomenclature

In the shorthand nomenclature used for identifying fatty acids, the numbers before the colon designate the number of carbon atoms present, and that after it the number of double bonds. The letters "c" or "t" designate the *cis* or *trans* isomers.

Some of the fatty acids commonly encountered in biological systems are listed in Table X, along with their anhydrous melting points. Unless otherwise specified, double bonds are assumed to be in the *cis* configuration. The tendency for the melting temperature to increase with increasing chain length or saturation, and the lower melting temperatures seen with *cis*, as opposed to *trans* double bonds is evident in this table. While the hydrated phospholipids' transition temperatures are affected qualitatively in the same manner by these features as the melting points of the anhydrous fatty acids, there is not a direct correspondence between the two, and the transition temperatures for hydrated phospholipids are lower than anhydrous melting points. For example, the transition temperatures of hydrated distearyl, dipalmitoyl, dimyristoyl, and dielaidyl phosphatidylcholines are at 60°C, 41°C, 23°C, and -22°C respectively. These are about 10C°, 22C°, 31C°, and 35C° lower than the capillary melting points of the corresponding anhydrous fatty acids.

TABLE X

FATTY ACID NOMENCLATURE AND MELTING POINTS

SHORTHAND DESIGNATION	TRIVIAL NAME	SYSTEMATIC NAME	MELTING POINT
12:0	lauric	dodecanoic	44.8°
14:0	myristic	tetradecanoic	54.4°
16:0	palmitic	hexadecanoic	62.9°
18:0	stearic	octadecanoic	70.1°
18:1t	elaidic	octadecenoic	45.0°
18:1c	oleic	octadecenoic	10.5°
18:2cc	linoleic	octadecadienoic	-5°
20:2	---	eicosadienoic	---
20:3	---	eicosatrienoic	---
20:4	arachidonic	eicosatetraenoic	-49.5°
20:5	---	eicosapentaenoic	-54.4°